Detection Strategies for Bioassays Based on Liquid Chromatography, Fluorescence Spectroscopy and Mass Spectrometry

Christel Maria Hempen

Members of committee:

Chairman/secretary:	Prof. Dr. P. J. Gellings	University of Twente
Promotor:	Prof. Dr. U. Karst	University of Twente
Members:	Prof. Dr. W. Engewald	University of Leipzig
	Dr. U. Kunz	Boehringer Ingelheim
	Dr. B. J. Ravoo	University of Twente
	Prof. Dr. V. Subramaniam	University of Twente
	Prof. Dr. I. Vermes	University of Twente
	Prof. Dr. A. Zemann	University of Innsbruck

Print: Print Partners Ipskamp, P.O. Box 333, 7500 AH Enschede, The Netherlands

www.ppi.nl

ISBN 90-365-2225-0

Detection Strategies for Bioassays Based on Liquid Chromatography, Fluorescence Spectroscopy and Mass Spectrometry

DISSERTATION

To obtain

the doctor´s degree at the University of Twente,

on the authority of the rector magnificus,

prof. dr. W. H. M. Zijm,

on account of the decision of the graduation committee,

to be publicly defended

on Friday July 15th, 2005 at 13:15

by

Christel Maria Hempen

Born on December 1st, 1977

in Haren, Germany

The dissertation has been approved by the promotor:

Prof. Dr. Uwe Karst

Für meine Eltern

Contents

Abbreviations

Å	Ångström
ABTS	2,2'-azino-bis-(-3-ethylbenzothiazoline-6-sulfonic acid) diammonium salt
AcNi	acetonitrile
APCI	atmospheric pressure chemical ionization
acP	acid phosphatase
aP	alkaline phosphatase
BSA	bovine serum albumin
c	concentration
DAD	diode array detector
DMF	dimethyl formamide
EALL	enzyme-amplified lanthanide luminescence
EDC	N-ethyl-N'-(3-dimethylaminopropyl)-carbodiimide hydrochloride
ELISA	enzyme-linked immunosorbent assay
EIA	enzyme immunoassay
ESI	electrospray ionization
FIA	flow-injection analysis
5-FSA	5-fluorosalicylic acid
5-FSAP	5-fluorosalicylic phosphate
GOD	glucose oxidase
HAc	acetic acid
HMTD	hexamethylenetriperoxide diamine
HPLC	high-performance liquid chromatography

pHPAA	p-hydroxyphenylacetic acid
I	intensity
IgG	immunoglobulin G
IR	infrared
LC	liquid chromatography
LC/MS	liquid chromatography/mass spectrometry
LOD	limit of detection
LOQ	limit of quantification
MNBDA	4-(N-methylamino)-7-nitro-2,1,3-benzooxadiazole
MNBDH	4-(N-methylhydrazino)-7-nitro-2,1,3-benzooxadiazole
MP	microperoxidase
MRM	multiple reaction monitoring
MS	mass spectrometry
m/z	mass-to-charge ratio
NBDCl	4-chloro-7-nitrobenzofurazan
NHS	N-hydroxysuccinimide
NIR	near infrared
NMR	nuclear magnetic resonance
NPP	p-nitrophenyl phosphate
OPD	o-phenylenediamine
POD	horseradish peroxidase
p,p'-DDD	1,1-dichloro-2,2-bis-(4-chlorophenyl)ethane
p,p'-DDE	1,1-dichloro-2,2-bis(p-chlorophenyl)ethylene
p,p'-DTT	1,1,1-trichloro-2,2-bis(p-chloro-phenyl)ethane
QD	quantum dot

R^2	regression coefficient
RFU	relative fluorescence units
RIA	radioimmunoassay
RP	reversed phase
RSD	relative standard deviation
SD	standard deviation
SERS	surface-enhanced Raman scattering
S/N	signal to noise
SPE	solid phase extraction
TATP	triacetonetriperoxide
TFC	turbulent flow chromatography
TIC	total ion current
TMB	3,3',5,5'-tetramethylbenzidine
Tris	tris-(hydroxymethyl)aminomethane
u	unit
UV	ultraviolet
vis	visible
λ	wavelength
λ_{em}	emission wavelength
λ_{ex}	excitation wavelength

Chapter 1

Introduction and Scope

Bioassays find widespread application in clinical chemistry and various other fields as environmental or food analysis. Enzymatic assays and immunoassays have already been applied for several decades and are widely used in routine analysis. The most prominent features of these assays are high selectivity and sensitivity. Their ease of automation leads to frequent use in high-throughput instrumentation. However, the interest in enzymatic assays and immunoassays is still increasing and strong research effort has to be made to further improve the analytical figures of merit. The development of new approaches is required to improve the selectivity, e.g., by coupling bioassays to separation methods and to allow multianalyte measurements by using novel detection schemes such as mass spectrometry.

Chapter 2 reviews different labeling strategies for enzymatic assays and immunoassays. Besides, enzyme-labeled analytical techniques as enzyme-linked immunosorbent assays (ELISAs) and enzyme-catalyzed reaction schemes, which can be found throughout this thesis, direct labeling assays as radioimmunoassays, nanoparticle-based assays and methods for combining bioassays to chromatographic methods are introduced. The advantages and drawbacks of the different assay principles, also including their future perspectives, are discussed and compared.

A detection scheme for the simultaneous evaluation of two bioassays based on fluorescence spectroscopy is presented in **Chapter 3**. It is desirable to improve enzymatic assays with respect to throughput and limits of detection. In the case of fluorescence-based enzymatic assays, these aims can be

achieved by performing the determination of different analytes simultaneously. Prerequisites for these measurements are non-overlapping emission bands of the fluorescent products. Phosphatases catalyze the reaction of 5-fluorosalicyl phosphate (5-FSAP) to the fluorescing 5-fluorosalicylic acid (5-FSA). The non-fluorescent 4-(N-methylhydrazino)-7-nitro-2,1,3-benzooxadiazole (MNBDH) is converted into the fluorescent 4-(N-methylamino)-7-nitro-2,1,3-benzooxadiazole (MNBDA) by hydrogen peroxide-generating enzymes and/or peroxidases. As the emission spectra of the reaction products 5-FSA and MNBDA do not overlap, the respective enzymes can be determined in one single assay. Based on these reactions, a simple fluorescence detection scheme for two-analyte enzyme assays, carried out on microtiter plates with readily available instrumentation and without the use of chemometric tools, was developed and applied for the analysis of acid phosphatase and glucose oxidase in honey samples.

A comparative study on the method development for simultaneous enzymatic conversions with fluorescence and mass spectrometric detection is presented in **Chapter 4**. The possibility of MS detection as an alternative to fluorescence-based enzymatic assays was investigated by means of direct flow-injection measurements on a coupled fluorescence and mass spectrometric detection system for the simultaneous two-enzyme analysis. The alkaline phosphatase-catalyzed reaction under formation of the fluorescent 5-FSA and the microperoxidase 11-catalyzed reaction resulting in MNBDA were carried out at-line, generating time-resolved reaction profiles simultaneously for two analytes.

Liquid chromatographic/mass spectrometric investigations on the products in the peroxidase-catalyzed reaction of o-phenylenediamine, one of the most widely used peroxidase substrates, by hydrogen peroxide are described in **Chapter 5**. Although the reaction has been known since decades, literature data on the identity of the reaction product(s) are still strongly contradictory. In order to clarify these conflicting results described in literature, the assay was investigated under reaction conditions similar to the ELISA. The products were identified by means of LC/UV/APCI-MS and ESI-MS after LC fraction collection.

In **Chapter 6**, the proteolytic cleavage of different cytochromes was investigated. After enzymatic digestion of a cytochrome, possibly under formation of microperoxidases, the product mixture was separated by means of reversed-phase liquid chromatography. The activity of the separated microperoxidases was determined by employing a post-column derivatization set-up. In a reaction coil, the analytes were treated with hydrogen peroxide in the presence of MNBDH. During the enzymatic reaction, the strongly fluorescent MNBDA was generated and subsequently detected by means of fluorescence spectroscopy. The identity of the generated microperoxidases was confirmed by means of LC/ESI-MS.

The development of two new methods for the determination of telmisartan in human blood plasma is presented in **Chapter 7**. This drug against high blood pressure was determined by means of a competitive ELISA, for which a glucose oxidase (GOD) enzyme tracer was synthesized and by means of

LC/APCI-MS after on-line turbulent flow chromatography (TFC) sample clean-up procedure. In case of the ELISA, the quantification was performed by the reaction of GOD with glucose and a mixture of MNBDH and H_2O_2 yielding the fluorescent MNBDA. In case of LC/MS, telmisartan was determined using tandem-MS measurements with both external and internal calibration. The results of all measurements in the pharmacokinetic investigation of the telmisartan concentration were compared for four test persons.

Chapter 8 summarizes the results obtained in the different chapters of the thesis. General conclusions and remarks regarding the advantages and drawbacks as well as future perspectives of the approaches are presented.

Chapter 2

Labeling Strategies in Bioassays*

* C. Hempen, U. Karst, *Anal. Bioanal. Chem.*, accepted for publication

2.1 Abstract

Different labeling strategies for enzymatic assays and immunoassays are reviewed. Techniques, which make use of the direct detection of a label, e.g., radioimmunoassays are discussed as well as techniques, in which the label is associated with inherent signal amplification. Examples for the latter, e.g., enzyme-linked immunosorbent assays or nanoparticle-label based assays are presented. Coupling of the bioassays to chromatographic separations adds selectivity, but renders the assays more difficult to apply. The advantages and drawbacks of the different analytical principles, also including future perspectives, are discussed and compared. Selected applications from clinical and pharmaceutical analysis as well as environmental analysis are provided as examples.

2.2 Introduction

Bioassays are analytical techniques, in which selectivity and/or sensitivity are generated by a biomolecular interaction, e.g., an enzymatic amplification in metabolic assays (enzyme assays) or an antibody-antigen recognition in affinity assays (immunoassays). They find widespread application in several fields as clinical chemistry, drug analysis, food analysis, environmental chemistry and even in the analysis of explosives. Although the first bioassays have already been applied for decades, this field of analysis is still open for and applicable to new and interesting approaches and developments.

Immunoassays are based on the highly selective interaction/binding of antibodies to antigens, which can be read out by a label being attached either to the antigen or to the antibody. Although some techniques for direct and specific interaction monitoring between antibody and antigen have become available in recent years (e.g., surface plasmon resonance, SPR [1] or related techniques), most quantitative assays rely on indirect approaches, which are based on labeling strategies [2]. The term "labeling" describes a chemical reaction between the analyte and a suitable reagent under formation of a product, which allows and/or improves the detection of a (bio)molecule or a (bio)molecular interaction. This review focuses on different labeling strategies in enzyme and immunoassays.

It is possible to label a biomolecule in such a way that a direct detection is possible thereafter. This is achieved in case of radioimmunoassays (RIAs) and related techniques. On the other hand, labeling with enzymes requires a subsequent chemical amplification reaction under formation of a product, which may be detected by means of spectroscopic or electrochemical methods.

Enzymatic assays are based on the high selectivity of the enzymes. They react as biological catalysts and therefore increase the velocity of reactions typically by a factor between 10^6 and 10^{12}. Due to this large turnover, a strong improvement of the limit of detection based on the corresponding signal amplification is possible [2].

In general, the advantages of bioassays are, next to the high sensitivity and selectivity, comparably low costs of operation, simple and readily available instrumentation and low limits of detection. The extremely high sample throughput, which is possible based on massive assay automation with robotic systems, is an additional advantage.

This review shall provide a general overview on different labeling strategies applied in bioassays, including their advantages and disadvantages as well as their future perspectives. As demonstrated by thousands of original papers going along with numerous dedicated textbooks [2,3] and review articles [4,5], it is evident that this scientific area cannot be covered comprehensively. Rather, selected techniques and applications, which are considered to be of particularly high value, will be summarized and discussed.

2.3 Direct Labeling

2.3.1 Radioimmunoassays

Radioimmunoassays (RIAs) are based on the competition between radiolabeled (e.g., by means of ^{125}I, ^{3}H) and non-labeled antigens for limited antibody binding sites. The unknown amount of the analyte can be measured by increasing the concentration of “cold” (non-labeled) antigen, which causes a replacement of “hot” (labeled) antigen, and thus a decrease in measurable radioactivity. The displacement is calibrated by means of known antigen amounts so that unknown analyte concentrations can be determined by the

resulting anti-proportional calibration curve [2]. This kind of competitive immunoassay is one of the most sensitive methods for the determination of antigens (LOD ~ 0.5 pg/mL), including a high precision of the measurements. It therefore finds widespread application in several fields.

Rosalyn Yalow and Solomon Berson developed the first radioisotope immunoassay in 1960 [6]. They determined the concentration of insulin in plasma samples by using ^{131}I-labeled insulin as reference. This was possible due to the ability of human insulin to react strongly with the insulin-binding antibodies present in guinea pig antibeef insulin serum so that ^{131}I-labeled insulin could competitively be replaced. This method yielded quantitative and reproducible results, thus leading to an increase of the interest in this technique. In 1977, Rosalyn Yalow was awarded the Nobel Prize in Physiology or Medicine for the development of radioimmunoassays of peptide hormones.

The possibilities of RIAs are best demonstrated with two typical examples for applications in the field of clinical chemistry: In 1988, Coates et al. introduced a radioimmunoassay of salivary cyclosporine with use of ^{125}I-labeled cyclosporine [7]. Cyclosporine belongs to the group of pharmaceuticals as immunosuppressive agents. It is used to reduce the body's natural immunity in those patients who receive organ (for example, kidney, liver, or heart) transplants. When a patient receives an organ transplant, the body's white blood cells try to reject the transplanted organ. Cyclosporine works by hindering the white blood cells from doing this. In this case, cyclosporine was

determined in saliva samples of 38 kidney-transplant patients. The limit of quantification was 0.34 µg/L.

In 1996, Ma et al. developed a radioimmunoasssay for the determination of the protein hormone leptin in human plasma or serum samples [8]. They performed a competitive assay of the leptin samples (or calibrations) with ^{125}I-labeled leptin for antibody binding sites with a final precipitation of the antibody-antigen complex. Centrifugation and decantation of the supernatant with subsequent counting of the radioactivity in the pellets were carried out in order to determine remaining radioactivity. By means of this accurate and precise technique, they found out that leptin concentrations vary little due to short-term fasting, age or race and that leptin concentrations are gender specific.

Several reviews on radioimmunoassays, alone or in comparison with other (bio)analytical techniques are available. In 1993 for instance, Deridovich and Reunova reviewed the analysis of prostaglandins determined in different tissues by means of radioimmunoassays in comparison to other bioassays and HPLC techniques [4]. In 1996, Leveque and Jehl reviewed the clinical pharmacokinetics of the semisynthetic anticancer drug vinorelbine and compared the determination by means of HPLC methods to that using radioactive assays [9].

These examples show that radioimmunoassays have already successfully been used for a very long period. Nevertheless, the drawbacks of this type of

immunoassay have to be considered: One main problem is the radioactivity itself, which causes on the one hand a lack of shelf life of the radiolabeled antigens, and on the other hand the need for special safety precautions and dedicated laboratory equipment, thus resulting in high infrastructural costs. Therefore, other immunoassay principles, which allow achieving similarly low limits of detection, are becoming more and more popular.

2.3.2 Fluoroimmunoassay

The group of immunoassays based on direct labeling does also include fluoroimmunoassays. This technique works with antibodies, which are labeled with fluorescent markers. Therefore, the selectivity of antibody-binding interactions is combined with simple, sensitive, cheap and hazard-free fluorescence detection. Already in 1941, Coons found out that there is a possibility to couple antibodies to fluorescent dyes (e.g., rhodamines) without changing their specificity [10]. The development of powerful fluorescence immunoassay applications took until the 1980s. Two types of fluoroimmunoassays are distinguished: Homogeneous and heterogeneous assays. In case of heterogeneous fluoroimmunoassays, antigens or antibodies labeled with a fluorophore are used, which require the separation of bound from free tracer before fluorescence detection. In homogeneous assays, quantification is possible without performing separation procedures [2].

Again, an example is provided to demonstrate the use of this type of assay: In 1983, Bailey et al. described the use of lucifer yellow VS as label for

fluoroimmunoassays [11]. Lucifer yellow VS is a highly fluorescent vinyl sulphone dye, which binds under mild alkaline conditions to both amino and thiol groups in proteins. The large Stokes´ shift of 110 nm and the emission maximum at 540 nm provide advantages over the more commonly used labels (e.g., fluorescein). The use of the dye as a label has been demonstrated by developing a heterogeneous fluoroimmunoassay for human serum albumin by polyethylene precipitation of bound fluorophore and automated fluorometry on the supernatants. In later studies, Bailey and colleagues used lucifer yellow VS in case of homogeneous non-separation fluoroimmunoassays [12]. A homogeneous resonance energy transfer fluorescence (FRET) based immunoassay for plasma albumin was described, in which lucifer yellow VS was used to label albumin, and rhodamine B isothiocyanate was used to label anti-albumin antibodies. The assay showed good correlation with the dye-binding method for albumin and had sensitivity and precision, which favorably compete with similar assays using a fluorescein label.

Fluoroimmunoassay measurements combined with flow-injection techniques can often be found in literature [13-17]. Khokhar et al. [14], for instance, worked with immunoreactors containing immobilized protein G as solid phase. The set-up of the measurements is presented in Figure 2.1. Insulin, used as model analyte, was labeled with the pH-resistant and fluorescent rhodamine isothiocyanate. After incubation of the rhodamine-insulin conjugate with anti-insulin antibodies and the respective sample or standard solution, the mixture was injected into the system at pH 8.8. The antibody-bound insulin was

retained. By changing to pH 2.5, the protein G combined conjugates were eluted, so that the fluorescence could be determined.

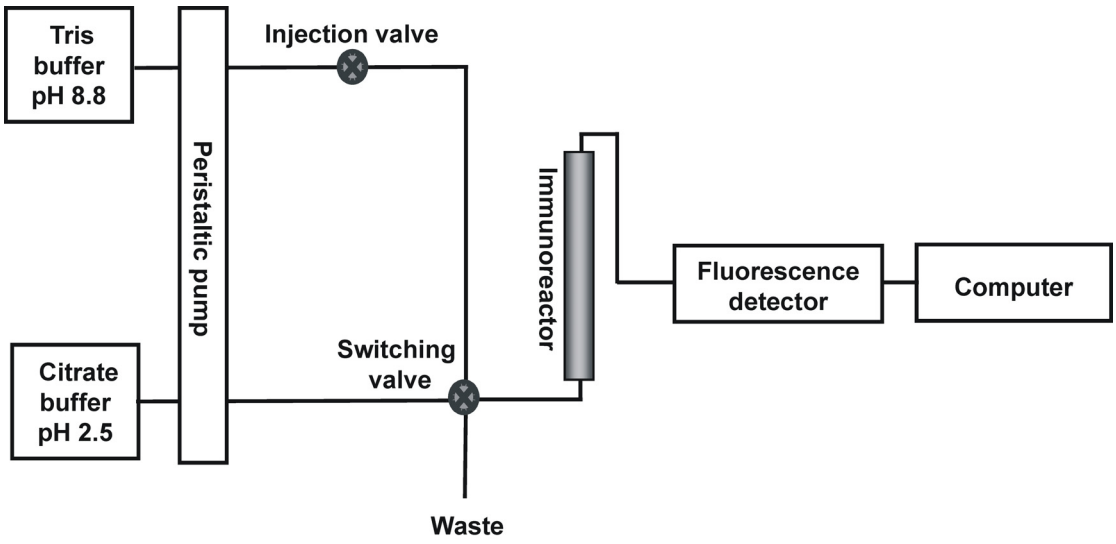

Figure 2.1: *Flow-injection manifold for heterogeneous fluorescence immunoassays.*

In general, detection limits tend to be high due to background fluorescence and quenching problems, especially in case of homogeneous assays. Therefore, the popularity of these fluoroimmunoassays is not as high as for radioimmunoassays. Heterogeneous immunoassays, especially in combination with flow-injection analysis, can overcome these problems. Considerable improvements have been achieved using time-resolved fluorescence techniques, which enable highly sensitive measurements with decreased background. Hemmilä and Webb [18] and, recently, Steinkamp and Karst [19] gave an overview on this technique. The use of fluorophores excited in the red or the near infrared (NIR) part (600 nm - 1000 nm) of the

electromagnetic spectrum is another successful approach to obtain less interferences from background signals [20-23]. Boyer et al. [20], for example, studied for the first time the use of NIR fluorescent dyes as quantitative labels for immunoassays. After an isocyanate-functionalized dye was conjugated to goat anti-human immunoglobulins, it was used in an immunoassay to detect and to quantify the respective analytes, human immunoglobulins, by means of laser diode-induced fluorescence spectroscopy. Although all of these more recent approaches are helpful in reducing the limits of detection, they are still inferior in this matter compared with RIAs. On the other hand, their easy handling and the fact that only readily available instrumentation is required, makes these assays attractive for applications, in which only moderate limits of detection have to be achieved.

2.4 Enzyme Labeling

Enzymatic assays and enzyme immunoassays play an important role in clinical chemistry and related fields. Enzymes react as biological catalysts by lowering the activation energy of chemical reactions, resulting in the acceleration of the reactions [2]. Many different enzymes are applied as labels for these types of assays. The advantages of working with enzymes are their high catalytic activity, selectivity and their sensitivity due to strong signal amplification.

2.4.1 Enzyme-catalyzed bioassays

Numerous enzyme-catalyzed reactions are known and currently applied in bioassays. They are combined with various detection schemes like UV/vis absorbance, fluorescence, chemiluminescence, electrochemical and, most recently, mass spectrometric detection. Enzymes, which are used in bioassays have to fulfil several quality demands: high selectivity, no contaminations with inhibitors or disturbing substances, a high stability, a pH optimum, which should fit to the assay conditions and reasonable costs. By means of enzymatic assays, it is not only possible to determine the concentration of substrates, but also the activity of the enzymes themselves. A list of some selected popular enzymes for bioassays, including frequently used substrates and applied detection schemes is provided in Table 2.1. Some examples are also provided within the text: The reaction of horseradish peroxidase (POD), for instance, with hydrogen peroxide and o-phenylenediamine (OPD) is already known since decades [34, 37-40] and is frequently applied for enzymatic and immunoassays. The concentration of the enzyme, hydrogen peroxide or a respective precursor (hydrogen peroxide-generating enzyme) is determined using the POD-catalyzed conversion of OPD to an orange-red reaction product, 2,3-diaminophenazine. This is most frequently detected by UV/vis absorbance using microplate readers in the wavelength range between 425 and 450 nm and after quenching with sulfuric acid at a wavelength of approximately 490 nm.

Table 2.1: *Enzymes used in Analytical Chemistry.*

Enzyme	EC No.	Origin	Mass (kDa)	pH Optimum	Detection	Substrate	Ref
alkaline phosphatase	EC 3.1.3.1	calf intestine	140	9.8	fluorescence, EALL	5-FSAP	[24,25]
					UV/vis	4-nitrophenyl-phosphate	[26]
					electrochemistry	1-naphtylphosphate	[27]
ß-D-galactosidase	EC 3.2.1.23	escherichia coli	465	8	fluorescence	4-methyl-umbelliferone- ß-D-galactoside	[26]
					UV/vis	2-nitrophenyl- ß-D-galactoside	[24]
ß-D-glucose oxidase	EC 1.1.3.4	aspergillus niger	160	5.5-6.5	fluorescence	4-(N-methylhydrazino)-7-nitro-2,1,3-benzooxadiazole (MNBDH)	[24,29]
					UV/vis	4-aminophenazone	[30]
luciferase	EC 1.13.12.7	photinus pyralis	100	7.5-7.8	bioluminescence	adenosine-triphosphate (ATP)	[31]
peroxidase	EC 1.11.1.7	horseradish	44	6.0-7.0	fluorescence	MNBDH	[29]
					fluorescence	p-hydroxyphenyl propionic acid (pHPPA)	[32]
					UV/vis	TMB	[33]
					UV/vis	OPD	[34]
					UV/vis	2,2'-azino-bis-(-3-ethylbenzothiazoline-6-sulfonic acid) diammonium salt (ABTS)	[35]
xanthine oxidase	EC 1.1.3.22	bovine milk	283	8.5-9.0	UV/vis	hypoxanthine	[36]

Phosphatases are another important group of enzymes with applications in bioassays: Acid phosphatase (acP), for instance, reacts with p-nitrophenyl phosphate (NPP) to a dye, which can be detected photometrically [41]. Evangelista et al. developed a method for the determination of alkaline phosphatase (aP) with the use of 5-fluorosalicylic phosphate (5-FSAP), which reacts to the fluorescent 5-fluorosalicylic acid (5-FSA). For their investigations, a second reaction step was introduced, during which 5-FSA formed a complex with Tb(III)/EDTA, so that time-resolved measurements were enabled [25]. The reaction scheme is shown in Figure 2.2. These so-called enzyme-amplified lanthanide luminescence (EALL) assays have recently been reviewed as well [19]. Due to the combination of enzymatic amplification and time-resolved measurements, the limits of detection of EALL assays may be very low under optimized conditions.

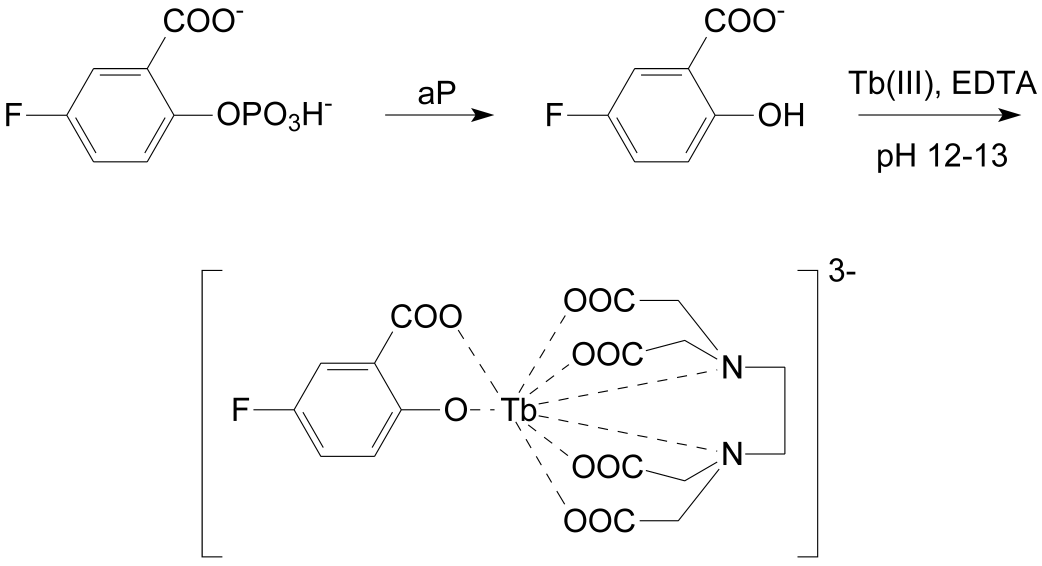

Figure 2.2: *Reaction scheme of the aP-catalyzed cleavage of 5-FSAP to 5-FSA with subsequent complexation with Tb(III)/EDTA.*

Today, mass spectrometric detection schemes gain more and more interest with respect to enzymatic assays. The first approach was published in 1989 by Henion and co-workers [42]. They coupled a closed reaction vessel to an electrospray ionization (ESI) interface of a triple quadrupole mass spectrometer and monitored on-going reactions in continuous-flow experiments. A few years later, the same group introduced an off-line LC/ESI-MS approach for the determination of the kinetic parameters for ribonuclease A and β-galactosidase [43]. Liesener and Karst have recently published a review on the monitoring of enzymatic conversions by mass spectrometry [44]. The advantage of MS-based detection schemes is that multiplexing reactions can be monitored without any interference of one reaction with respect to the other. It is even possible to determine the decrease of educt and the increase of product simultaneously by means of on-line or at-line measurements. In case of photometric detection schemes, simultaneous measurements are extremely difficult. Enzymatic assays yielding fluorescence detection do in principle allow simultaneous measurements for a limited number of fluorophores, provided that the emission bands of the fluorescent products do not overlap [24]. Therefore, mass spectrometric detection is likely to dominate the field of simultaneous multianalyte bioassays in the future. Its major drawbacks, however, are expensive instrumentation and limited sample throughput.

2.4.2 Enzyme-linked immunosorbent assays (ELISAs)

At the beginning of the 1970s, enzymes were introduced as alternatives to radioisotopes as labels in immunoassays [45, 46]. Since that time, they have

evolved to become the most versatile and popular class of labels for immunoassays. Their application will probably increase further due to the fact that no radioactive substances are necessary and that the sensitivity of enzyme immunoassays (EIAs) is, nowadays, comparable to that of RIAs and (time-resolved) fluorescence immunoassays. Prerequisites for enzyme-based immunoassays are the possibility of coupling an enzyme to an antibody/antigen without loss of enzyme activity and with no or only limited change in specificity of the immunological component. In the last reaction step of an ELISA, the enzyme label catalyzes the conversion of a substrate into a colored or fluorescent product. Although electrochemical detection schemes [47] have been applied for this purpose as well, the two earlier techniques are predominantly used in routine analysis.

Two different types of heterogeneous enzyme immunoassays are schematically presented in Figure 2.3: The competitive (A) and the non-competitive (B) (sandwich) ELISA. In case of a competitive assay, unlabeled (analyte) and labeled antigens compete for the binding sites of an antibody, which is bound to a solid phase. Therefore, a high signal in the subsequent detection scheme indicates the presence of a low analyte concentration and vice versa. In the sandwich ELISA, the bound antibody first reacts with the analyte of unknown concentration. Then, an enzyme-labeled antibody is added, which couples to a second binding site of the analyte. The subsequent enzyme-catalyzed reaction leads to a proportional relation between signal and analyte concentration.

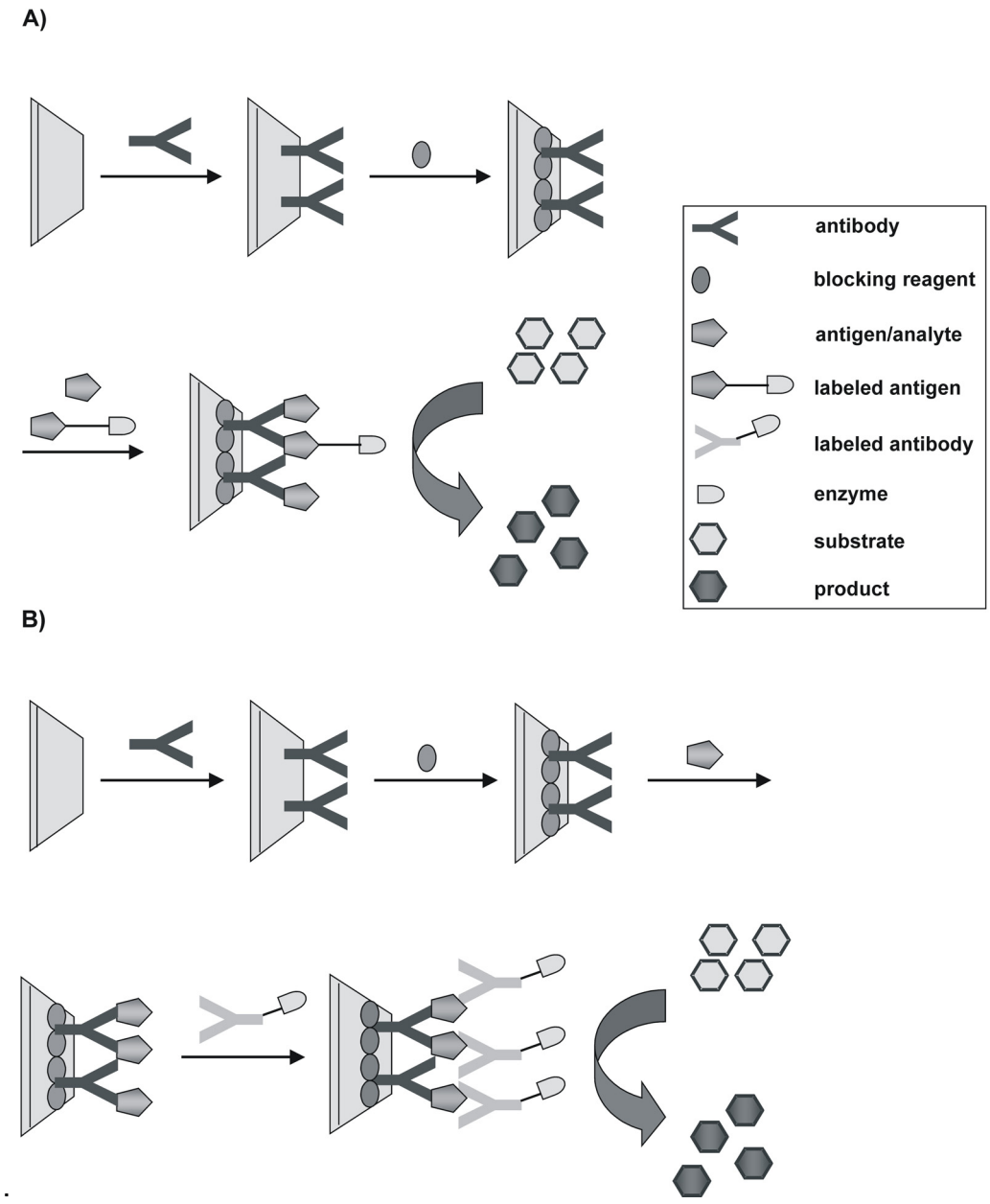

Figure 2.3: *A) Competitive ELISA scheme. B) Non-competitive (Sandwich) ELISA scheme.*

In case of both techniques, the adding of a blocking reagent is important with respect to the reduction of non-specific binding sites at the (microplate) surfaces. However, frequent washing steps between the different immunological reactions are also required for both methods and lead to long

and laborious assay protocols. Automation has, on the other hand, reduced the level of manual work to a minimum and is a major prerequisite for the predominance of ELISAs in the clinical laboratory.

Two examples demonstrate the broad applicability of ELISAs in environmental and biomedical analysis: In 1997, Winklmair et al. have developed a highly sensitive competitive immunoassay for the determination of triazine herbicides in water samples of different origins using a monoclonal antibody [48]. The peroxidase-labeled triazine tracer reacted in the last step with 3,3',5,5'-tetramethylbenzidine (TMB), one of the most commonly used chromogenic substrates, thus enabling a photometric detection. The obtained results showed good correlation to additionally performed comparative gas chromatographic measurements.

Ikemoto et al. have developed a sandwich-immunoassay system for the measurement of human liver type arginase, which could be useful in the diagnosis of various hepatic disorders as well as for the follow-up of post-operative conditions of patients [49]. The serum samples and calibration solutions, respectively, reacted first with the absorbed anti-human liver type arginase antibody and afterwards with the POD-labeled second antibody. Finally, UV/vis detection was performed after the POD-catalyzed oxidation of OPD. They found out that the arginase concentration in serum increases markedly and temporally at the time of surgical operation or later injury to the liver.

EIAs based on other detection methods, as fluorescence, chemiluminescence or electrochemistry have been developed as well. Evangelista et al. [25] combined an immunoassay for rat IgG with the time-resolved fluorescence detection for aP based on Tb(III) described above. In 1997, Dou et al. developed an enzyme immunoassay with surface-enhanced Raman scattering (SERS) detection of the reaction product [50]. The performance of this sandwich assay is based on a linkage between an anti-mouse IgG, a mouse immunoglobulin G (IgG) (anti-insulin) and an anti-mouse IgG labeled with POD. Finally, the OPD reaction was performed; an aliquot of the reaction mixture was taken, added to a silver colloid solution and put into a cylindrical cell. A SERS spectrum of the reaction product was measured by excitation with an Ar ion laser at a wavelength of 514.5 nm.

A chemiluminescence enzyme immunoassay with aP as marker, using cortisol-21-phosphate as substrate and lucigenin as chemiluminescence reagent was presented by Kokado and co-workers in 1997 [51]. By means of this method, human chorionic gonadotropin (HCG), human growth hormone, α-fetoprotein and estradiol could by determined in human serum or urine samples. The respective antibodies for each analyte were used. A scheme of the aP-catalyzed reaction and the chemiluminescence detection is presented in Figure 2.4. In the first step, cortisol is generated, which reduces lucigenin to the chemiluminescent product in the subsequent reaction step.

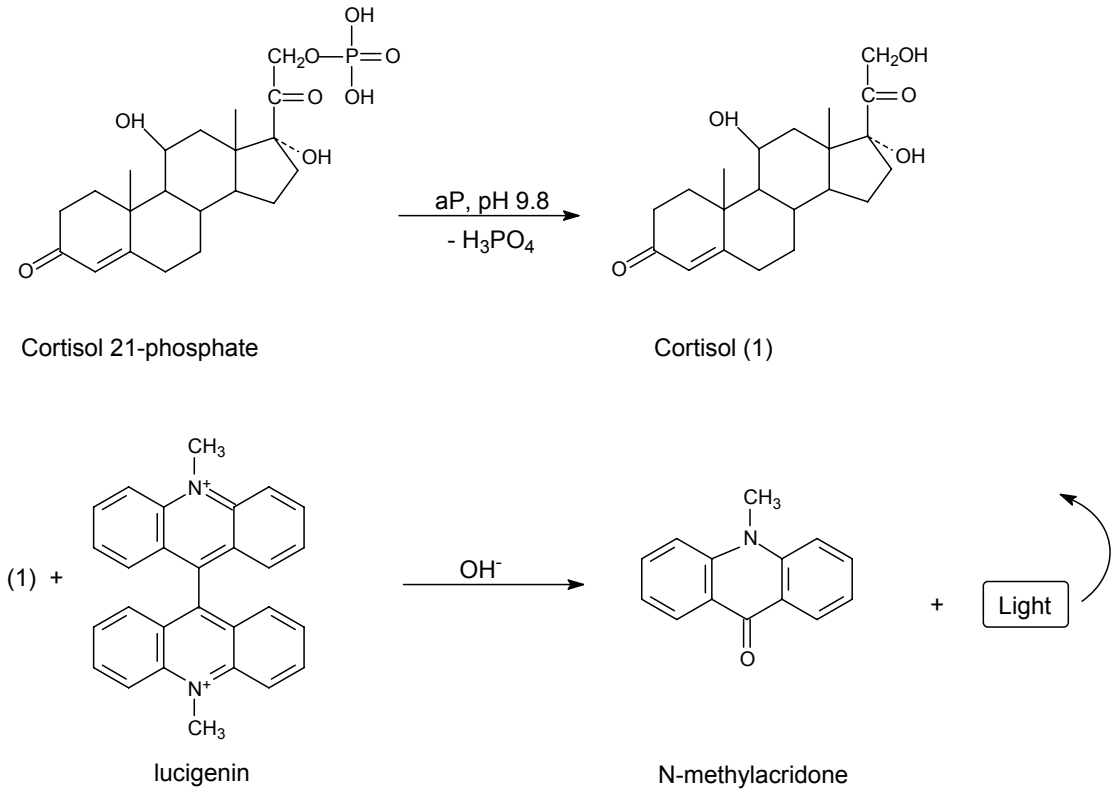

Figure 2.4: *The principle of the chemiluminescence assay for aP using lucigenin.*

Valentini et al. developed an ELISA with electrochemical detection for the screening of the pesticide 1,1,1-trichloro-2,2-bis(p-chlorophenyl)ethane (p,p'-DTT) and its metabolites 1,1-dichloro-2,2-bis(p-chlorophenyl)ethylene (p,p'-DDE) and 1,1-dichloro-2,2-bis-(4-chlorophenyl)ethane (p,p'-DDD) in waste waters [52]. The activity of the label enzyme POD was determined using TMB as substrate. The detection was performed by injecting the reaction mixture into a flow-injection analysis system with a thin-layer transducer cell (glassy carbon working electrode, Ag/AgCl reference, stainless steel auxiliary electrode).

To summarize, it can be concluded that the interest in enzyme immunoassays is very high and is likely to further remain on a high level. This is indicated by the large number of current scientific publications and overview articles [5, 26, 53] on this topic. Major advantages are a combination of very low limits of detection with a very high degree of automation, thus enabling an extremely high sample throughput. Another advantage is the applicability in several different fields of research as clinical, environmental or food chemistry.

2.5 Nanoparticles as Labels

Especially in the last few years, the interest in the bioanalytical use of nanoparticles has increased enormously. Mainly, fluorescent particles of nanometric dimensions are applied because of several important advantages in comparison with molecular fluorescent dyes. Due to the presence of a large number of fluorescent centers in one single nanoparticle, the obtained signals are much larger compared with individual molecules. Depending on the nature of the nanoparticle, there may also be advantages with respect to narrow-banded emission characteristics, which may allow improved simultaneous multianalyte determination. Meanwhile, nanoparticles with anchor groups to be linked to biomolecules are commercially available. These particles are often modified in such a way that functional groups (-COOH, -NH_2) are attached to the surface of the particles, which enable linkage to peptides/proteins. However, other coupling principles, as the cyanogen

bromide (CNBr) method for a covalent particle-biomolecule linkage are also established [54].

Different kinds of nanoparticles can be applied: Semiconductor quantum dots (QDs), which contain hundreds or thousands of atoms are often used [55]. The radius of these particles, generated of II-VI or III-V group elements (e.g., CdSe-ZnS), is usually between 1 and 10 nm. Their properties are caused by the size: The larger the size of the QD, the longer the maximum fluorescence emission wavelength. Another type of nanoparticles is based on embedding a large number of conventional fluorophores into a protecting polymer [56,57] or silica [58]. The nanoparticles encapsulate thousands of fluorescent dye molecules (fluorescein, rhodamine), providing a highly amplified and reproducible signal for fluorescence-based bioanalysis.

He et al. presented a method for cell recognition of system lupus erythematosus patients that uses photostable luminescent nanoparticles as biological labels [59]. They worked with silica particles, which were doped with the luminescent tris(2,2'-bipyridyl)dichlororuthenium(II)hexahydrate ($Ru(II)(bpy)_3^{2+}$). These particles were covalently immobilized with goat anti-human IgG according to the CNBr method. The reaction was based on a recognition principle of a surface membrane IgG (SmIgG) from the circulating blood of the test persons and the luminescent nanoparticle-labeled IgG. Comparative measurements with organic dye (fluorescein isothiocyanate) labeled IgGs showed a fast and significant decrease of fluorescence intensity with time, whereas the intensity of the nanoparticles was almost constant.

Two years later, the same group published a similar approach with fluorescein isothiocyanate doped silica particles for the recognition of HepG liver cancer cells [60].

A rapid bioconjugated nanoparticle-based bioassay for the quantification of pathogenic bacteria (e.g., escherichia coli) in spiked ground beef samples was presented by Zhao et al. in 2004 [61]. For coupling of the $Ru(II)(bpy)_3^{2+}$-particles to the antibody against escherichia coli, the particle surface was functionalized with amino groups. The spectrofluorometric results of the immunoassay applying the nanoparticles correlated well with flow cytometry measurements of the antibody-conjugated nanoparticles bound to single bacterial cells. The possibility of performing the immunoassay on microtiter plates enabled the high throughput detection of multiple samples.

Chan and Nie have developed luminescent semiconductor CdSe-ZnS quantum dot bioconjugates for ultrasensitive non-isotopic detection [62]. These nanoconjugates are biocompatible and are suitable for use in cell biology and immunoassays. The solubility of the QDs in aqueous media was achieved by using mercaptoacetic acid, which bound to the Zn atoms of the particle. The polar carboxylic acid group rendered the QDs water-soluble and enabled the protein (here: transferrin) coupling. The schematic structure of these QD bioconjugates is shown in Figure 2.5. The biocompability could be demonstrated in vitro and for living cells by means of fluorescence images.

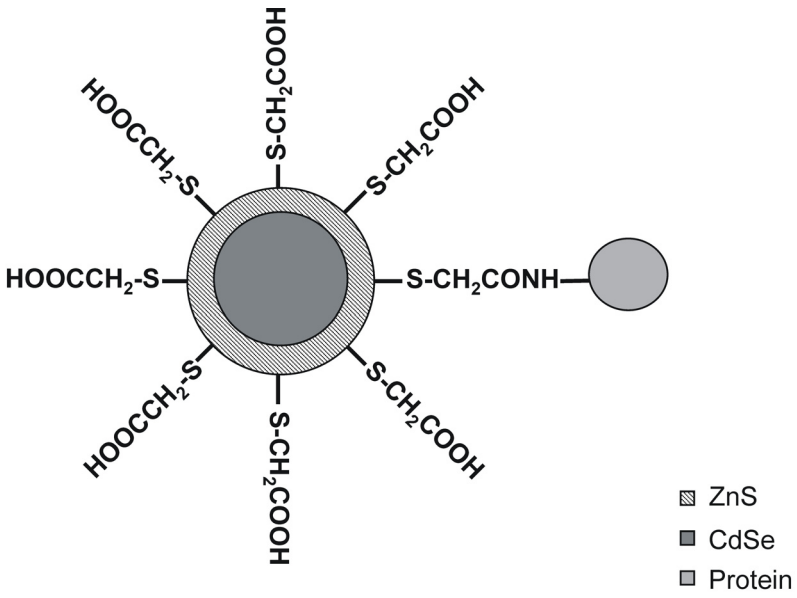

Figure 2.5: *Scheme of a ZnS-capped CdSe quantum dot that is covalently bound to a protein by mercaptoacetic acid.*

Another approach for the coupling of luminescent semiconductor CdSe-ZnS QDs to biomolecules was presented by Goldman et al. in 2002 [63]. In this case, the surface of the QDs was modified by dihydrolipoic acid. The positively charged protein avidin was used as bridge between the bioinorganic nanoparticles and biotinylated antibodies. These particles were successfully applied in sandwich-fluoroimmunoassays on microtiter plates for the determination of protein toxins (e.g., cholera toxin). First results of the simultaneous analysis on the determination of two protein toxins were also presented.

Taylor et al. reported a class of luminescent latex nanobeads that were covalently linked to DNA binding proteins, which allowed the study of specific sequences on single DNA molecules [64]. The latex particles, which

contained about 100-200 molecules of an embedded dye that is protected from the outside environment, conjugated to proteins through amide bond formation. It has been demonstrated that the site-specific restriction enzyme EcoRI can be conjugated to 20-nm fluorescent nanoparticles and that the resulting nanoconjugates display DNA binding and cleavage activities of the native enzyme. The feasibility of mapping sequence-specific sites on genomic DNA molecules was shown.

The increasing number of reviews on nanoparticles applied in bioassays shows the growing importance and the possibilities of these approaches [19,65-68]. Compared with conventional immunoassays, the number of fluorophore molecules, which is attached to an antibody, is significantly increased due to embedding of many dye molecules into the nanoparticle. This amplification, reduced photobleaching effects, the safe handling in comparison with radioisotopes, the reduction of one reaction step in comparison to ELISAs and the possibility of performing multiplexing assays due to the narrow emission bands of the fluorescent nanoparticles are advantages, which will be used more and more in the future.

2.6 Coupling to Separation Techniques

2.6.1 Enzymatic assays

The combination of enzymatic assays with chromatographic separation techniques is found frequently in literature. On the one hand, enzymes are

separated on the HPLC column and subsequently reacted with an enzymatic substrate. On the other hand, substrates may be separated and react in a post-column derivatization with the enzyme to the respective product. In both cases, the post-column reaction enables the detection so that either the substrate or, in the latter case, the enzyme acts as label. In case of enzyme separation, wide-pore LC columns are normally used due to the large dimensions of the proteins and due to strong adsorption of the enzymes to the stationary phase. However, in case of enzymes or analogues with lower molecular masses, as for instance microperoxidases MPs, a separation on standard columns used for small molecule separation is possible. The following examples show the applicability of enzymatic assays for separation techniques and for several different fields of applications. Heinmöller et al. presented a sensitive HPLC method for the analysis of n-alkyl hydroperoxides [69]. A series the analytes was separated by HPLC and detected by means of a post-column reaction with POD and p-hydroxyphenylacetic acid (pHPAA) and subsequent fluorescence detection. It was possible to separate seven n-alkyl hydroperoxides from C-4 to C-18 on a RP-18 ODS-Hypersil column and to perform the subsequent derivatization with only minimally reduced efficiency at greater alkyl chain lengths.

The application of POD for post-column reactions was presented by Schulte-Ladbeck et al. for the trace analysis of peroxide-based explosives [70]. A RP-HPLC method with post-column UV irradiation and fluorescence detection for the analysis of triacetonetriperoxide (TATP) and hexamethylenetriperoxide diamine (HMTD) was developed. After separation, the analytes were

photochemically degraded to H_2O_2, which was subsequently oxidized in a POD-catalyzed reaction with p-hydroxyphenylacetic acid. The resulting fluorescent dimer of pHPAA was then detected. The set-up of this method is presented in Figure 2.6. It allows to analyze post-explosion sites and to track residues of either HMTD or TATP.

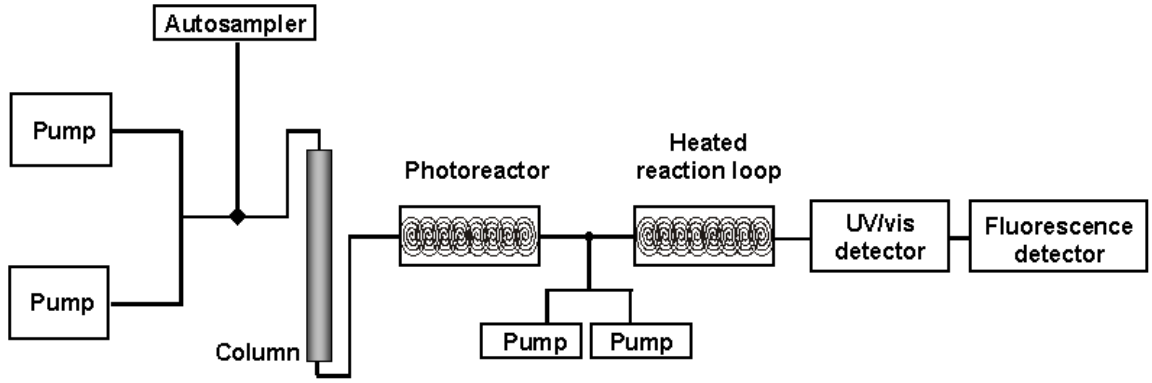

Figure 2.6: HPLC set-up for the analysis of the explosives TATP and HMTD including photoreactor and post-column reaction apparatus for enzymatic conversion.

Irth and co-workers developed an approach for the on-line coupling of HPLC to a continuous-flow enzymatic assay with subsequent ESI-MS detection [71]. By means of the set-up presented in Figure 2.7, natural products, as e.g., an extracted fungi sample, were separated and reacted with added enzyme in a knitted reaction coil. As long as no bioactive compounds were eluting from the RP-18 column, the enzyme continuously converted added substrate into products (equation 2). Bioactive compounds eluting from the column reacted

as enzyme inhibitors (equation 1), which resulted in a decrease of product formation (equation 3).

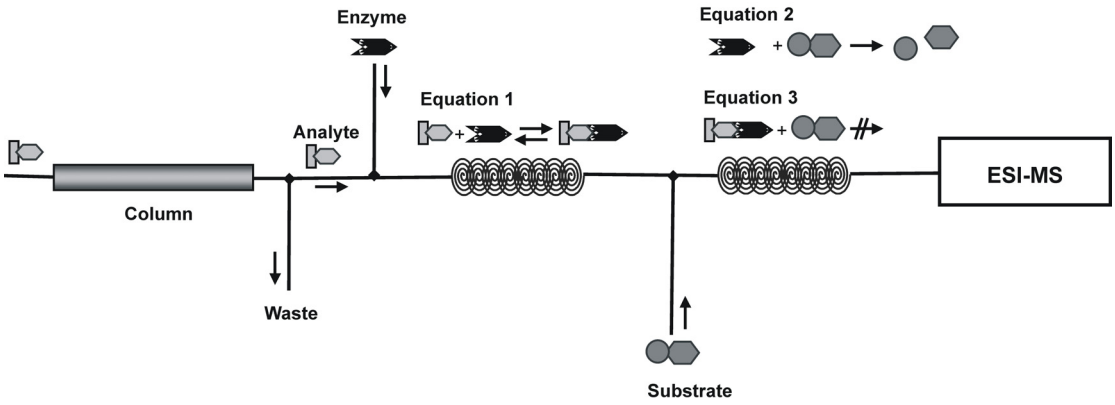

Figure 2.7: *Scheme of the on-line continuous-flow system.*

2.6.2 Chromatographic immunoassays

Several reviews give an overview on the broad topic of chromatographic immunoassays [72-74]. Shahdeo and Karnes [73] present pre- and post-column/capillary immunoassay possibilities for the combination with chromatographic and electrophoretic separation techniques. Hage and Nelson [74] describe the variety of formats and labels and the sensitivity of chromatographic immunoassays. The examples presented here show various approaches in this field.

Different measurement techniques for chromatographic immunoassays have been developed. It is possible to carry out the assays on-line or off-line, prior to and subsequent to separation. The on-line post separation technique is

often favored, due to the possibility for high throughput measurements, which is especially important in case of routine analysis.

In 1988, Stone and Soldin presented an HPLC method coupled to off-line immunoassay measurements for the determination of digoxin in serum [75]. By means of this method, they could improve the accuracy of the digoxin determination, which is usually interfered by metabolites and endogeneous digoxin-like factors, so that overestimation of the digoxin content frequently occurs. The serum samples were extracted, injected into the HPLC system, separated on a RP18 column, and the different fractions were collected separately from each other. The calibration was performed by means of an added internal standard. The results from 49 samples of different patients, taking digoxin, were successfully compared with a fluorescence polarization immunoassay.

Irth and co-workers published an overview on strategies for the on-line coupling of immunoassays to HPLC using either labeled antibodies or labeled antigens [76] (see also Figure 2.8). In the first case, they worked with fluorescein-labeled antibodies to monitor the presence of antigenic analytes, as digoxin and metabolites in human plasma samples, which were separated by a LC column. In the first assay step, a post-column reaction between the effluent and added labeled antibodies took place. Then, a separation step was carried out by means of an immobilized antigen support packed in a short column. Free antibodies were trapped by the support and the fluorescent antibody-antigen complexes passed through and were detected by a

fluorescence detector. The high selectivity of this method was shown by a limit of detection for digoxin and two metabolites of $2 \cdot 10^{-10}$ mol L^{-1}. The second possibility, the use of labeled antigens, was also presented by Irth et al.:The first step of this assay scheme is similar to the first step of the previously described assay: The eluting analytes reacted with (in this case unlabeled) antibodies. Then, fluorescein-labeled antigens were added and reacted with unlabeled antibodies.

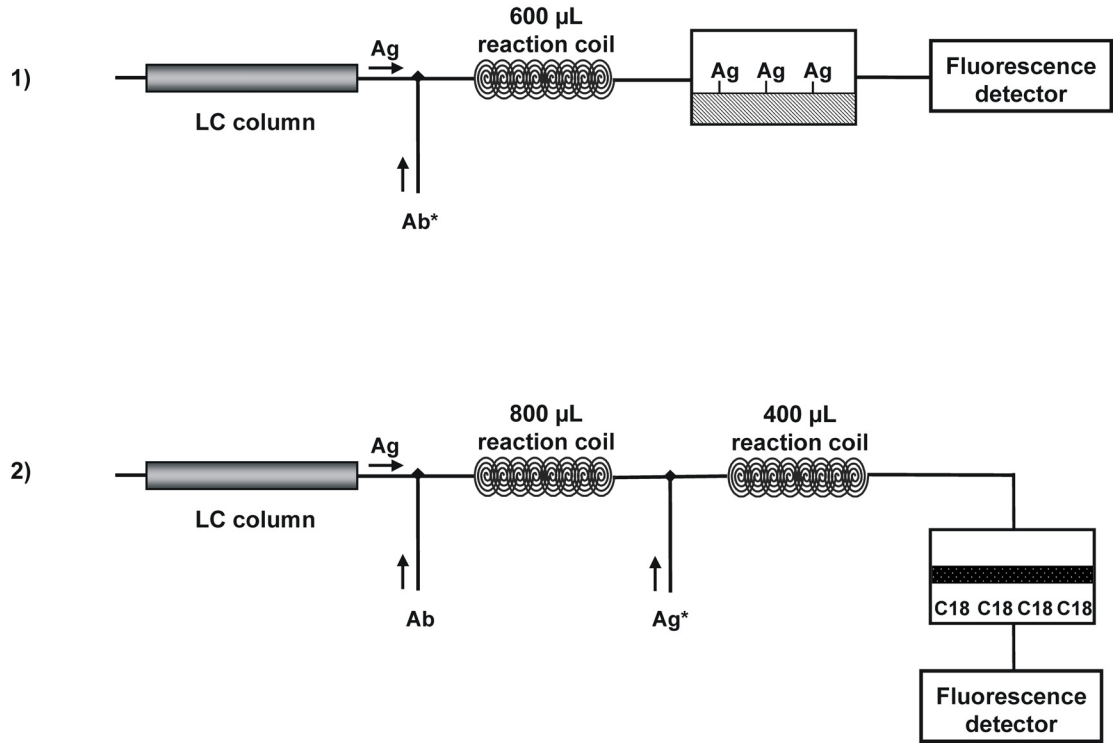

Figure 2.8: *1) Set-up of the on-line detection system using labeled antibodies (Ab*). 2) Scheme of the on-line coupling of RP-HPLC to immunochemical detection using fluorescein-labeled antigens (Ag*). (Ab: antibody, Ag: antigen)*

Prior to detection of the generated labeled complexes, they were separated from free fluorescein-labeled antigens by means of an inserted column containing a restricted-access chromatographic support. Low molecular mass compounds, as labeled antigens, were retained in the pores of the hydrophobic surface, whereas high molecular mass compounds, as the labeled antigen-antibody complex, passed through and could be detected by fluorescence spectroscopy. They applied this technique to avidin-biotin as model system using fluorescein-biotin as labeled antigen.

Oates et al. developed and optimized a HPLC-based one-site immunometric assay working with post-column chemiluminescence detection of the analyte L-thyroxine (T_4) [77]. Anti-T_4 antibody Fab fragments were conjugated with chemiluminescent acridinium ester labels through lysine residues or terminal amine groups, combined in excess with the analyte, incubated and afterwards injected onto a column that contained T_4. Unbound Fab fragments were retained on the column, whereas T_4-bound antibodies passed directly through. The detection could either be done by post-column derivatization of the non-retained T_4-bound antibodies or by reaction of the retained and later eluted non-T_4-bound antibodies with H_2O_2 under alkaline conditions. The chemiluminescence of the generated N-methylacridone was measured. The results could be provided 1.5 minutes after sample injection so that many samples could be analyzed between column elution steps within a short time.

These examples demonstrate the wide range of possibilities for sensitive and selective results by combining immunoassay techniques with

chromatographic methods. However, one drawback, especially of using a solid phase to separate antibody bound and free fractions, is the requirement of regeneration of the stationary phase following each injection. This makes it more difficult to apply these methods in a high-throughput environment.

2.7 Conclusions

Current labeling strategies for metabolic (enzyme) and affinity (antibody-based) bioassays were summarized and discussed. It is evident that, despite the achievements in the fields of label-free bioassays, labeling techniques will continue to play a leading role in the field of bioassays. It can be expected that labeling techniques based on radioactive isotopes will significantly decrease in importance due to stability, safety and handling considerations. Enzyme labels, on the other hand, are most likely to hold the leading role for the next years. However, extremely strong competition arises from fluorescent nanoparticle labels owing to easy handling, robustness and compatibility with existing (microplate) spectroscopic instrumentation. It can be expected that the current rapid progress will lead to an even faster implementation of fluorescent nanoparticles into new detection schemes. On the long term, there might be a significant replacement of ELISAs by nanoparticle-based assays. The bioassays based on a combination of liquid-phase separation and labeling are likely to further play an important role for solving analytical problems, in which selectivity is most important. On the other hand, they are laborious and still require well-trained personnel for routine applications.

2.8 References

[1] R. J. Green, R. A. Frazier, K. M. Shakesheff, M. C. Davies, C. J. Roberts, S. J. B. Tendler, Biomaterials 21 (2000) 1823-1835.

[2[C. P. Price, D. J. Newman, Principles and practice of immunoassay, New York, Stockton Press, 1997.

[3] E. P. Diamandis, T. K. Christopoulos, Immunoassay, San Diego, Academic Press, 1996.

[4] I. I. Deridovich, O. V. Reunova, Comp. Biochem. Physiol. 104 (1993) 23-27.

[5] G. B. Wisdom, Clin. Chem. 22 (1976) 1243-1255.

[6] R. S. Yalow, S. A. Berson, J. Clin. Invest. 39 (1960) 1157-1175.

[7] J. E. Coates, S. F. Lam, W. T. McGaw, Clin. Chem. 34 (1988) 1545-1551.

[8] Z. Ma, R. L. Gingerich, J. V. Santiago, S. Klein, C. H. Smith, M. Landt, Clin. Chem. 42 (1996) 942-946.

[9] D. Leveque, F. Jehl, Clin. Pharmacokinet. 31 (1996) 184-197.

[10] A. B. Coons, H. J. Creech, R. N. Jones, Proc. Soc. Exp. Biol. Med. 47 (1941) 200-202.

[11] M. P. Bailey, B. F. Rocks, C. Riley, Ann. Clin. Biochem. 20 (1983) 213-216.

[12] M. P. Bailey, B. F. Rocks, C. Riley, Ann. Clin. Biochem. 21 (1984) 59-64.

[13] D. A. Palmer, M. Evans, J. N. Miller, Analyst 119 (1994) 943-947.

[14] M. Y. Khokhar, J. N. Miller, N. J. Seare, Anal. Chim. Acta 290 (1994) 154-158.

[15] T. K. Lim, N. Nakamura, T. Matsunaga, Anal. Chim. Acta 354 (1997) 29-34.

[16] A. Bereczki, V. Horvath, Anal. Chim. Acta 391 (1999) 9-17.

[17] H. H. Yang, Q. Z. Zhu, H. Y. Qu, X. L. Chen, M. T. Ding, J. G. Xu, Anal. Biochem. 308 (2002) 71-76.

[18] I. A. Hemmilä, S. Webb, Drug Discovery Today 2 (1997) 373-381.

[19] T. Steinkamp, U. Karst, Anal. Bioanal. Chem. 380 (2004) 24-30.

[20] A. E. Boyer, M. Lipowska, J. M. Zen, G. Patonay, V. C. W. Tsang, Anal. Lett. 25 (1992) 415-428.

[21] M. I. Daneshvar, J. M. Peralta, G. A. Casay, N. Narayanan, L. Evans, G. Patonay, L. Strekowski J. Immunol. Meth. 226 (1999) 119-128.

[22] J. Sowell, R. Parihar, G. Patonay, J. Chromatogr. B 752 (2001) 1-8.

[23] X. Zhao, S. A. Shippy, Anal. Chem. 76 (2004) 1871-1876.

[24] C. Hempen, U. Karst, Anal. Chim. Acta 521 (2004) 117-122.

[25] R. A. Evangelista, A. Pollak, E. F. Gudgin Templeton, Anal. Biochem. 197 (1991) 213-224.

[26] E. Ishikawa, Clin. Biochem. 20 (1987) 375-385.

[27] D. Athey, M. Ball, C. J. McNeill, Ann. Clin. Biochem. 30 (1993) 570-577.

[28] K. Suzuki, Meth. Enzymol. 50 (1978) 456-488.

[29] J. Meyer, A. Büldt, M. Vogel, U. Karst, Angew. Chem. Int. Ed. 39 (2000) 1453-1455.

[30] J. Raba, S. F. Li, H. A. Mottola, Anal. Chim. Acta 300 (1995) 299-305.

[31] M. Maeda, J. Pharmaceut. Biomed. Anal. 30 (2003) 1725-1734.

[32] G. G. Guilbault, P. J. Brignac, M. Juneau, Anal. Chem. 40 (1968) 1256-1263.

[33] L. A. Marquez, H. B. Dunford, Biochem. 36 (1997) 9349-9355.

[34] P. J. Tarcha, V. P. Chu, D. Whittern, Anal. Biochem. 165 (1987) 230-233.

[35] K. K. Mäkinen, J. Tenovuo, Anal. Biochem. 126 (1982) 100-108.

[36] B. Hernandez, F. J. Luque, M. Orozco, J. Organ. Chem. 61 (1996) 5964-5971.

[37] K. Zhang, R. Cai, D. Chen, L. Mao, Anal. Chim. Acta 413 (2000) 109-113.

[38] P. Griess, J. Prakt. Chem. 3 (1871) 143-144.

[39] E. Knoevenagel, J. Prakt. Chem. 89 (1914) 25-75.

[40] S. Y. Niu, S. S. Zhang, L. B. Ma, K. Jiao, Bull. Korean. Chem. Soc. 25 (2004) 829-832.

[41] H. U. Bergmeyer, Methoden der enzymatischen Analyse, VCH: Weinheim, 1974.

[42] E. D. Lee, W. Mück, J. D. Henion, T. R. Covey, J. Am. Chem. Soc. 111 (1989) 4600-4604.

[43] F. Y. L. Hsieh, X. Tong, T. Wachs, B. Ganem, J. Henion, Anal. Biochem. 229 (1995) 20-25.

[44] A. Liesener, U. Karst, Monitoring enzymatic conversions by mass spectrometry – A critical review, submitted to Anal. Bioanal. Chem. 2005.

[45] B. K. van Weeman, A. H. W. M. Schuurs, FEBS Lett. 15 (1971) 232-236.

[46] E. Engvall, P. Perlmann, Immunochem. 8 (1971) 871-874.

[47] R. Q. Thompson, G. C. Barone, H. B. Halsall, W. R. Heineman, Anal. Biochem. 192 (1991) 90-95.

[48] M. Winklmair, M. G. Weller, J. Mangler, B. Schlosshauer, R. Niessner, Fresenius J. Anal. Chem. 358 (1997) 614-622.

[49] M. Ikemoto, A. Ishida, S. Tsunekawa, K. Ozawa, Y. Kasai, M Totani, K. Ueda, Clin. Chem. 39 (1993) 794-799.

[50] X. Dou, T. Takama, Y. Yamaguchi, H. Yamamoto, Anal. Chem. 69 (1997) 1492-1495.

[51] A. Kokado, A. Tsuji, M. Maeda, Anal. Chim. Acta 337 (1997) 335-340.

[52] F. Valentini, D. Compagnone, G. Giraudi, G. Palleschi, Anal. Chim. Acta 487 (2003) 83-90.

[53] V. S. Morozova, A. I. Levashova, S. A. Eremin, J. Anal. Chem. 60 (2005) 202-217.

[54] C. A. Schall, J. M. Wiencenk, Biotechnol. Bioeng. 53 (1997) 41-48.

[55] C. J. Murphy, J. L. Coffer, Appl. Spec. 56 (2002) 16A-27A.

[56] P. K. Sahoo, R. Mohapatra, Eur. Polymer J. 39 (2003) 1839-1846.

[57] M. T. Charreyre, O. Tcherkasskaya, M. A. Winnik, Langmuir 13 (1997) 3103-3110.

[58] M. Qhobosheane, S. Santra, P. Zhang, W. Tan, Analyst 126 (2001) 1274-1278.

[59] X. He, K. Wang, W. Tan, J. Li, X. Yang, S. Huang, D. Li, D. Xiao, J. Nanosci. Nanotech. 2 (2002) 317-320.

[60] X. He, J. Duan, K. Wang, W. Tan, X. Lin, C. He, J. Nanosci. Nanotech. 4 (2004) 585-589.

[61] X. Zhao, L. R. Hilliard, S. J. Mechery, Y. Wang, R. P. Bagwe, S. Jin, W. Tan, PNAS 101 (2004) 15027-15032.

[62] W. C. W. Chan, S. Nie, Science 281 (1998) 2016-2018.

[63] E. R. Goldman, E. D. Balighian, H. Mattoussi, M. K. Kuno,J. M. Mauro, P. T. Tran, G. P. Anderson, J. Am. Chem. Soc. 124 (2002) 6378-6382.

[64] J. R. Taylor, M. M. Fang, S. Nie, Anal. Chem. 72 (2000) 1979-1986.

[65] S. G. Penn, L. He, M. J. Natan, Current Op. Chem. Biol. 7 (2003) 609-615.

[66] M. Ozkan, Drug Discovery Today 9 (2004) 1065-1071.

[67] A. K. Gupta, M. Gupta, Biomaterials 26 (2005) 3995-4021.

[68] A. J. Haes, D. A. Stuart, S. Nie, R. P. van Duyne, J. Fluorescence 14 (2004) 355-367.

[69] P. Heinmöller, H. H. Kurth, R. Rabong, W. V. Turner, A. Kettrup, S. Gäb, Anal. Chem. 70 (1998) 1437-1439.

[70] R. Schulte-Ladbeck, P. Kolla, U. Karst, Anal. Chem. 75 (2003) 731-735.

[71] A. R. de Boer, T. Letzel, D. A. van Elswijk, H. Lingeman, W. M. A. Niessen, H. Irth, Anal. Chem. 76 (2004) 3155-3161.

[72] D. S. Hage, J. Chromatogr. B 715 (1998) 3-28.

[73] K. Shahdeo, H. T. Karnes, Mikrochim. Acta 129 (1998) 19-27.

[74] D. S. Hage, M. A. Nelson, Anal. Chem. 73 (2001) 198A-205A.

[75] J. A. Stone, S. J. Soldin, Clin. Chem. 34 (1988) 2547-2551.

[76] H. Irth, A. J. Oosterkamp, U. R. Tjaden, J. van der Greef, Trends Anal. Chem. 14 (1995) 355-361.

[77] M. R. Oates, W. Clarke, A. Zimlich, D. S. Hage, Anal. Chim. Acta 470 (2002) 37-50.

Chapter 3

A Dual Fluorophore System for Simultaneous Bioassays*

* C. Hempen, U. Karst, *Anal. Chim. Acta* **2004,** 521, 117-122.

3.1 Abstract

A detection scheme for the simultaneous evaluation of two bioassays based on fluorescence spectroscopy is presented. For the determination of either hydrogen peroxide-generating enzymes or peroxidases, the non-fluorescent 4-(N-methylhydrazino)-7-nitro-2,1,3-benzooxadiazole (MNBDH) is converted into the strongly fluorescent 4-(N-methylamino)-7-nitro-2,1,3-benzooxadiazole (MNBDA). Phosphatases are detected based on the cleavage of the non-fluorescent 5-fluorosalicyl phosphate (5-FSAP) under formation of the fluorescent 5-fluorosalicylic acid (5-FSA). While excitation of the fluorophores may be carried out at the same wavelength, their emission spectra differ significantly. This allows the read-out of both assays using commercially available microplate readers without additional chemometric tools. Compared with individual assays, limits of detection are similar, and linearity of the calibration functions for both enzymes is observed over 2-3 concentration decades starting at the limit of quantification. The simultaneous determination of glucose oxidase and acid phosphatase in honey is presented as an example for the application of the detection scheme.

3.2 Introduction

In bioanalysis, the determination of various enzymatic activities is one of the most important tasks [1] (see also Chapter 2). Natural products are screened with respect to the presence of biocatalysts [2] and enzymes are also used as markers for signal amplification in several types of bioassays, including enzyme-linked immunosorbent assays (ELISA) [3]. In this field, they have partly replaced other sensitive detection schemes, for example radioimunoassays (RIAs) [4]. Large series of synthetic substrates have been introduced for the most important enzymes, and in most cases, they are chromogenic or fluorogenic [5-11]. While chromogenic substrates are popular because only readily available instrumentation is required, fluorogenic substrates typically allow to obtain lower limits of detection [9]. To achieve higher sample throughput, it is desirable to miniaturize assay formats, to increase the speed of analysis and to obtain more information within a single assay.

Simultaneous bioassays are a possibility to increase the degree of analytical information that can be gathered from a sample within a short time. Important aspects are low limits of detection, easy handling and readily available instrumentation. Currently, several different approaches to achieve this goal are described or are under development. Chelates of europium(III), terbium(III), dysprosium(III) and samarium(III), all of which are characterized by intense long-lived fluorescence, have been proposed as markers for immunoassays, in which up to four analytes can be determined

simultaneously [12]. However, as the quantum yield varies strongly between these complexes, time-resolved fluorescence should be used to fully exploit the potential of this method and the determination of enzymatic activity is difficult. Although the enzyme-amplified lanthanide luminescence (EALL) [13], a detection scheme in which a substrate is converted into a product that can transfer excitation energy to the lanthanide cations, has been described in recent years, a simultaneous enzymatic activity determination based on this approach has not been introduced yet and will be difficult to achieve due to the special requirements of these methods. Luminescent nanoparticles either based on semiconductor materials ("quantum dots") [14-17] or on dyes entrapped in polymer materials [18, 19] have also been proposed as biolabels with multiple colors for affinity assays [17, 20], thus resulting in the possibility of multianalyte measurements. However, there is currently no means to change their fluorescent properties by an enzymatic conversion, so that they cannot be used in enzyme assays.

Therefore, a simple fluorescence-based detection scheme for two-analyte enzyme assays has been set up, which should be carried out with readily available instrumentation and without the use of chemometric tools.

3.3 Experimental

Chemicals

All chemicals were purchased from Aldrich (Steinheim, Germany), Merck (Darmstadt, Germany) and Fluka (Neu-Ulm, Germany). The enzymes glucose oxidase GOD (E.C 1.1.3.4), alkaline phosphatase aP (E.C. 3.1.3.1), acid phosphatase acP (E.C. 3.1.3.2) and horseradish peroxidase POD (E.C. 1.11.1.7) as well as microperoxidase MP-11 (from equine heart cytochrome c) were purchased from Sigma (Deisenhofen, Germany).

Synthesis of 4-(N-methylhydrazino)-7-nitro-2,1,3-benzooxadiazole (MNBDH) [21]

Methylhydrazine (5 mmol, 280 μL) in 25 mL of methanol was added dropwise to a solution of 1.25 mmol 4-chloro-7-nitrobenzofurazan (NBDCl) in 20 mL of chloroform. The mixture was allowed to react for 2 h. After precipitation of the product, it was filtered off, washed with methanol and dried in vacuo. The yield of the product depends on the intensity of washing and was typically 20%. The product was characterized spectroscopically and by reversed-phase HPLC using conditions described in [21]. MNBDH has recently become commercially available by Molecular Probes (Eugene, OR, U.S.A.).

Synthesis of 5-fluorosalicyl phosphate (5-FSAP) [22]

Initially, 5-fluorosalicylic acid (5-FSA) was dried in vacuo over KOH pellets. For the reaction, 7 mmol of 5-FSA were stirred with 1.33 g PCl_5 and a few milliliter of toluene in oven-dried glassware fitted with a $CaCl_2$-tube. The

mixture was stirred for 2 h and subsequently cooled in an ice bath, before 2.5 mL of acetone, 2.5 mL of toluene and 0.5 mL of water were added. After stirring for 30 min at room temperature, 5 mL of toluene were added. The free acid precipitated as a white powder after a few minutes of stirring. The product was filtered off, washed with toluene and dried in vacuo over KOH pellets. The yield was 0.54 g (32.5%).

Instrumentation

All quantitative fluorescence determinations were performed with a FLUOstar microplate reader from BMG LabTechnologies (Offenburg, Germany) with FLUOstar software version 2.10-0. For the measurements, four different filters were used: 320 nm (bandwidth ± 20 nm) and 470 nm (bandwidth ± 15 nm) filters for excitation and 405 nm (bandwidth ± 25 nm) and 545 nm (bandwidth ± 10 nm) filters for emission. The measurements were performed on Corning (Costar No. 3915, black) 96-wells micro-titration plates, which were purchased at Diagonal (Münster, Germany). For photometric measurements on microplates, a Spectra Max 250 Reader from Molecular Devices (Sunnyvale, CA, U.S.A.) with SOFTmax PRO software version 1.2.0 was used. The transparent flat form 96-wells micromethod plates were purchased from Emergo BV (Landsmeer, The Netherlands).

Fluorescence spectra were recorded using an Aminco Bowman AB2 luminescence spectrometer from Polytec (Waldbronn, Germany) with software version 5.00. The excitation and emission spectra of all fluorophores were recorded for 10^{-4} M solutions in acetonitrile.

Enzymatic assays

Glucose oxidase (GOD) assay [23]: 50 μL of a solution of GOD (10^{-4} u mL^{-1} to 0.1 u mL^{-1}) in acetate buffer (pH 5.5; 0.01 M) were pipetted to 100 μL of a glucose solution ($2 \cdot 10^{-3}$ mol L^{-1}). 1.08 mg MNBDH were dissolved in 10 mL of acetonitrile and 1.4 mL of this solution was added to a solution of 2.64 mg POD (40,000 u L^{-1}) in 10 mL of phosphate buffer (pH 5.8; 0.01 M). 40 μL of this mixture were pipetted after 15 min to the GOD solution. After incubation at room temperature (15 min), the fluorescence was measured at excitation and emission wavelengths of 470 nm and 545 nm, respectively.

Alkaline phosphatase (aP) assay [13]: 50 μL of a solution of 2.36 mg 5-FSAP dissolved in 10 mL of acetonitrile were pipetted to 50 μL of an aP solution ($1 \cdot 10^{-4}$ u L^{-1} to 0.1 u mL^{-1}; Tris buffer; pH 8.5; 0.1 M). 150 μL water were added, and after 15 min, the fluorescence was measured at excitation and emission wavelengths of 320 nm and 405 nm, respectively.

Acid phosphatase (acP) assay [24]: 50 μL of a solution of 2.36 mg 5-FSAP dissolved in 10 mL of acetonitrile were pipetted to 50 μL of an acP solution (0.02 u L^{-1} to 1 u mL^{-1}; citrate buffer; pH 5; 0.02 M). 50 μL of water were added and after 15 min the fluorescence was measured at the excitation and emission wavelengths of 5-FSA.

Peroxidase (POD) assay [25]: 1 mL of a solution of 1.08 mg MNBDH dissolved in 10 mL acetonitrile was added to 25 mL of a 10 mM solution of H_2O_2. 200 μL of this mixture were pipetted to 50.7 μL of a solution of POD

(0.02 u mL^{-1} to 10 u mL^{-1}) in Tris buffer (pH 7.5; 0.1 M). After the sample had been incubated for 15 min at room temperature, fluorescence was measured at excitation and emission wavelengths of MNBDA.

Microperoxidase (MP-11) assay: 1.08 mg MNBDH were dissolved in 10 mL acetonitrile and 1.2 mL of this solution were added to 10 mL of a 30 mM solution of H_2O_2. 65 μL of this mixture were pipetted to 100 μL of a solution of MP-11 ($1 \cdot 10^{-10}$ mol L^{-1} to $1 \cdot 10^{-7}$ mol L^{-1}) in Tris buffer (pH 7.5; 0.1 M). After the sample had been incubated for 15 min at room temperature, the fluorescence was measured at the wavelengths of MNBDA.

Simultaneous enzymatic assays: The assays of the enzymes GOD and aP, GOD and acP as well as aP and MP-11 were performed simultaneously. In all cases, the respective reactions were executed on one microplate by varying the concentrations of the two analytes in different directions. For each concentration of the analytes, multiple determinations were made, in each well of the microtiterplate with a different concentration of the second analyte. The fluorescence intensity of the respective products was read out subsequently. In the case of the parallel determination of GOD and aP and of GOD and acP, it was even possible to excite the fluorescent products with one single wavelength.

GOD and acP determination in honey

For the individual determination of acP and GOD and the simultaneous determination of these two enzymes in a honey sample, 2 g honey were

dissolved in 5 mL citrate buffer (pH 4.8; 0.02 M). All enzyme measurements were performed by means of standard addition for calibration. Therefore, 35 μL honey solution were added to the three reaction solutions.

In order to verify the results, two reference reactions were performed. Determination of GOD with 2,2'-azino-bis-(3-ethylbenzothiazoline-6-sulfonic acid) diammonium salt (ABTS) [23]: 35 μL of the honey solution were pipetted to a solution consisting of 50 μL glucose ($2 \cdot 10^{-3}$ mol L^{-1}) and 25 μL GOD (0 u mL^{-1} to 0.1 u mL^{-1}; citrate buffer). After 15 min, 40 μL of acP (0 u mL^{-1} to 1 u ml^{-1}; citrate buffer), 30 μL POD/MNBDH solution (see above) and 100 μL citrate buffer were added. After a reaction time of 1 h, the product was photometrically determined at a wavelength of 405 nm.

Determination of acP with p-nitrophenyl phosphate (NPP) [24]: 35 μL of the honey solution were pipetted to a solution consisting of 50 μL H_2O and 25 μL GOD (0 u mL^{-1} to 0.1 u mL^{-1}; citrate buffer). Afterwards, 40 μL of acP (0 u mL^{-1} to 1 u ml^{-1}; citrate buffer), 30 μL citrate buffer and 100 μL substrate solution (0.204 g NPP dissolved in 100 mL buffer) were added. After a reaction time of 1 hour, the reaction was stopped by adding 40 μL NaOH solution (0.5 M). The product was photometrically determined at a wavelength of 410 nm.

3.4 Results and Discussion

Goal of this work was the development of a detection scheme for simultaneous bioassays based on fluorescence spectroscopy. This should meet the following criteria:

- The detection of at least two different (groups of) enzymes (e.g., an oxidoreductase as peroxidase and a hydrolase as alkaline phosphatase) should be possible from a single reaction solution without interferences between the two assays.
- The analytical figures of merit (limit of detection, limit of quantification, linear range for calibration) should be similar to those of the individual assays.
- To allow the immediate application in routine laboratories, commercially available instrumentation (microplate fluorescence spectrometers, standard filters) should be used, and no chemometric tools should be required.

Selection of the fluorophores

To obtain assay conditions, which allow low limits of detection and a linear range of the assay over at least two decades of concentration, the selection of the fluorophores was based on some additional criteria:

- Upon enzymatic conversion, non-fluorescent substrates should be converted into strongly fluorescent products.

- To be able to simultaneously detect two or more fluorophores, without using mathematical tools like chemometrics, the emission bands should not overlap significantly.
- The substrates should be stable during storage over a reasonable period of time.
- The enzymatic conversions and, if possible, the detection should be carried out at or close to physiological pH.

Table 3.1: *Fluorescence excitation and emission maxima for selected fluorophores.*

	Excitation maximum [nm]	Emission maximum [nm]
7-Amino-4-(trifluoromethyl)coumarin	361	492
5-FSA	313	418
7-Hydroxycoumarin	345	453
6-Nitro-3,4-benzocoumarin	395	479
7-Methoxycoumarin	346	391
Fluorescein	468	518
Diflunisal	313	420
MNBDA	468/335	522

A series of fluorophores comprising coumarin, fluorescein, salicylate and 4-nitrobenzoxadiazole (NBD) backbones was investigated with respect to their excitation and emission maxima. These data are provided in Table 3.1. A detailed comparison of all excitation and emission spectra led to the conclusion that only few combinations could allow to meet all criteria mentioned above. Only a combination of 5-FSA or diflunisal with fluorescein or MNBDA would, in principle, be possible. Finally, 5-FSA and MNBDA were selected for the following reasons: Under the conditions investigated 5-FSA is a triplicate stronger fluorophore than diflunisal. MNBDA is characterized by a second excitation maximum, which shows some overlap with the excitation maximum of diflunisal or 5-FSA. This is presented in Figure 3.1 and could enable the use of a common excitation wavelength for both compounds. The emission spectra of 5-FSA and MNBDA overlap only slightly, and with the use of appropriate emission filters, chances to obtain no cross selectivity into both directions appeared to be good for this pair of compounds.

Simultaneous detection of 5-FSA and MNBDA

The conditions for the simultaneous detection of the two fluorophores 5-FSA and MNBDA were investigated in the following. Both fluorophores were simultaneously determined, and concentrations were varied. In Table 3.2, the detection wavelengths for the filter-based microplate spectrofluorimeter and the limits of detection for both substances obtained in the individual measurement (both compounds in different wells of the microplate) and in the simultaneous determination (both compounds in one common well of the microplate) are provided. For both approaches and both compounds, the

limits of detection are identical with 10 nmol L^{-1}, thus proving that there are no interferences of one fluorophore with respect to the other from the detection point of view.

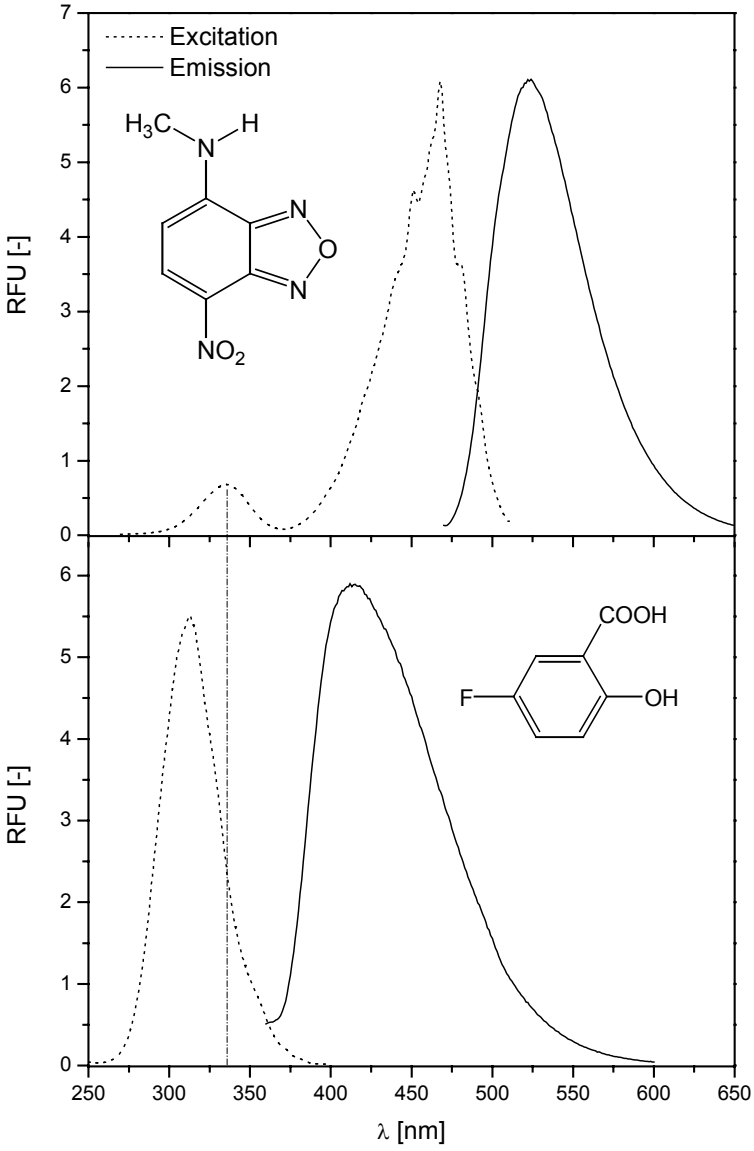

Figure 3.1: *Fluorescence excitation and emission maxima for selected fluorophores; MNBDA (above) and 5-FSA (below).*

Table 3.2: Limits of detection for the individual and the simultaneous determination of the fluorophores MNBDA and 5-FSA.

	λ_{ex} [nm]	λ_{em} [nm]	Individual determination (ind) [10^{-8} mol L^{-1}] LOD	LOQ	Simultaneous determination (sim) [10^{-8} mol L^{-1}] LOD	LOQ	Linear range [mol L^{-1}]	RSD [%] ($1 \cdot 10^{-7}$ mol L^{-1}) ind	sim	RSD [%] ($1 \cdot 10^{-5}$ mol L^{-1}) ind	sim
MNBDA	468	524	1	3	1	3	$3 \cdot 10^{-8}$ - $1 \cdot 10^{-5}$	3.0	2.4	1.0	1.3
5-FSA	313	415	1	3	1	3	$3 \cdot 10^{-8}$ - $1 \cdot 10^{-5}$	5.0	8.7	1.0	2.0

Synthesis of substrates

4-(N-methylhydrazino)-7-nitro-2,1,3-benzooxadiazole (MNBDH) has recently been introduced as reagent for the analysis of aldehydes and ketones [21], for nitrite analysis [26] and as substrate for peroxidase [23]. MNBDH was synthesized according to literature procedures [21] as described above. The respective reaction is presented in Figure 3.2.

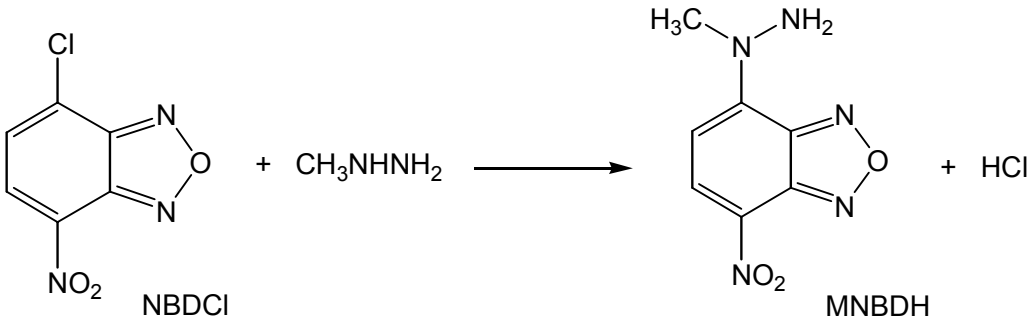

Figure 3.2: *Reaction scheme for the synthesis of MNBDH.*

5-FSA has been described previously as substrate for alkaline phosphatase in enzyme-amplified lanthanide luminescence (EALL) assays, in which it is formed as hydrolysis product of 5-fluorosalicylic phosphate (5-FSAP) and coordinated with Tb(III) ions [13]. 5-FSAP has been synthesized, as shown in Figure 3.3.

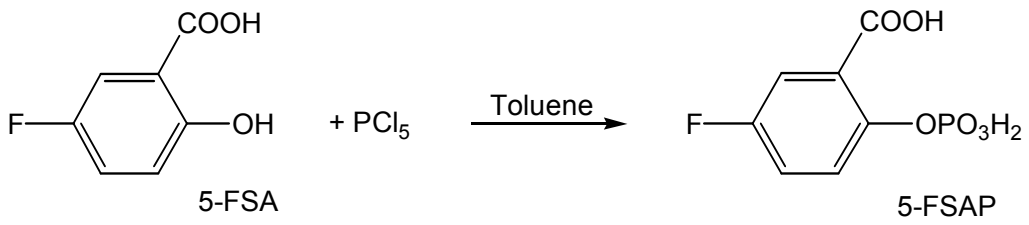

Figure 3.3: *Reaction scheme for the synthesis of 5-FSAP.*

Enzyme detection schemes

The enzymatic reactions, which are carried out with MNBDH and 5-FSAP are presented in Figure 3.4. Glucose oxidase catalyzes the oxidation of glucose by oxygen under formation of gluconolactone and hydrogen peroxide. The latter oxidizes, in the presence of peroxidase as catalyst, the non-fluorescent MNBDH to the fluorescent MNBDA. The non-fluorescent 5-FSAP is hydrolyzed under catalysis of phosphatase to the fluorescent 5-FSA.

Despite the excellent fluorescence properties of MNBDA, its peroxidase-catalyzed formation is comparably slow. For this reason, the substrate is only applicable in those cases, where POD can be used in higher concentrations, e.g., to detect hydrogen peroxide formed in a previous reaction step. Preliminary investigations, however, showed that the microperoxidase MP-11 rapidly catalyzes the conversion of MNBDH to MNBDA by hydrogen peroxide and that MNBDH can therefore be considered to be an excellent new substrate for this microperoxidase.

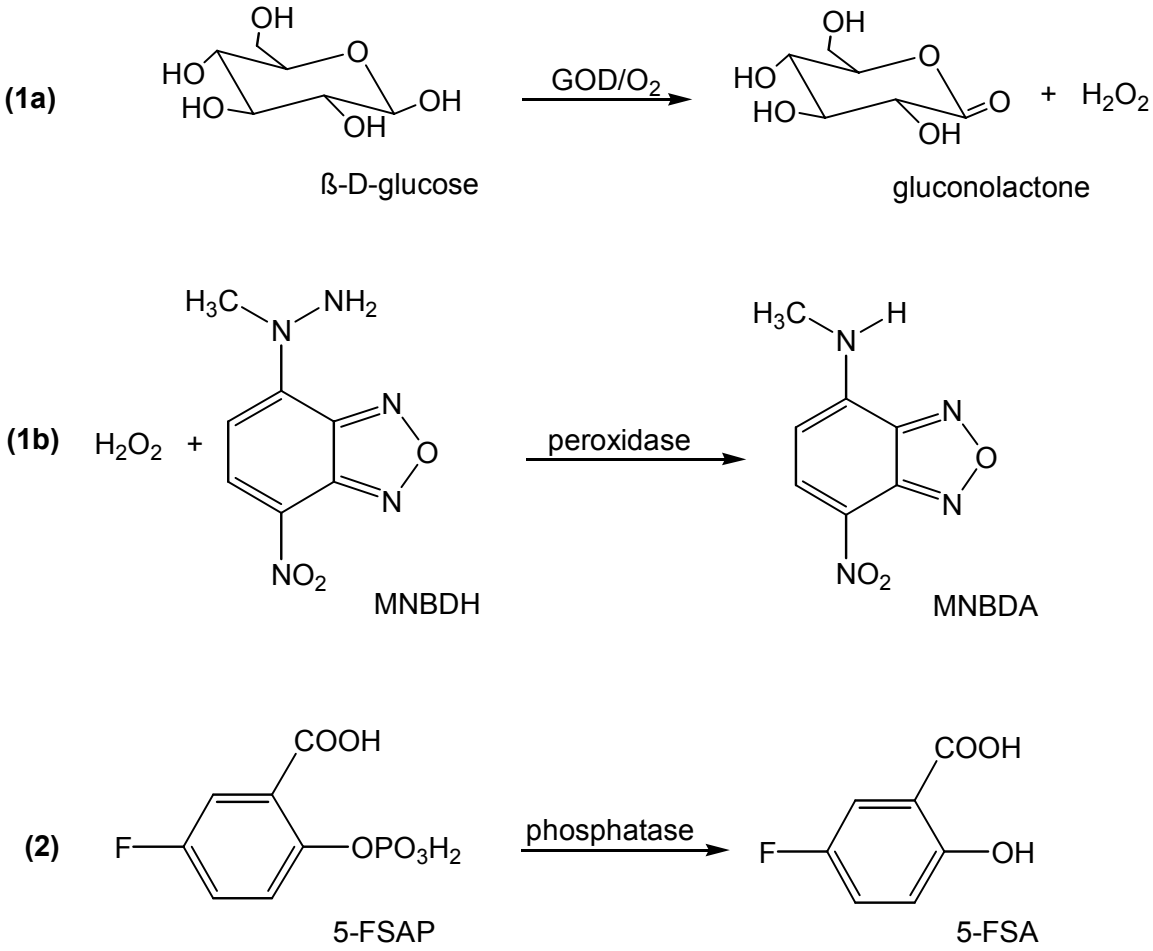

Figure 3.4: *Enzymatic reactions for the determination of GOD, POD and MP-11 using MNBDH and for the determination of phosphatases using 5-FSAP.*

(1a) GOD-catalyzed oxidation of glucose by atmospheric oxygen; (1b) POD- or MP-11-catalyzed reaction of MNBDH to MNBDA with H_2O_2; (2) aP- or acP-catalyzed reaction of 5-FSAP to 5-FSA.

The limits of detection were optimized for POD and MP-11. As is obvious from Table 3.3, the limits of detection of MP-11 are improved by more than a factor of 100 compared with POD. While only 17 nmol L^{-1} are achieved as LOD for

POD, 100 pmol L^{-1} are observed for MP-11. Linear ranges of the calibration functions are observed from $5 \cdot 10^{-8}$ mol L^{-1} to $2 \cdot 10^{-6}$ mol L^{-1} for POD and from $3 \cdot 10^{-10}$ mol L^{-1} to $1 \cdot 10^{-7}$ mol L^{-1} for MP-11. The limits of quantification are $5 \cdot 10^{-8}$ mol L^{-1} and $3 \cdot 10^{-10}$ mol L^{-1}. The relative standard deviations (n = 8) were determined for two different concentrations of POD and MP-11 each. As expected, the RSDs for POD and MP-11 are much lower for the higher concentrations. In general, the RSDs for MP-11 are slightly lower compared with those for POD.

Table 3.3: *Limits of detection and relative standard deviations (n = 8) for multiple analysis of POD and MP-11 solutions at selected concentrations*

Method	LOD [mol L^{-1}]	LOQ [mol L^{-1}]	Linear range [mol L^{-1}]	RSD [%] ($2 \cdot 10^{-7}$ mol L^{-1})	RSD [%] ($2 \cdot 10^{-6}$ mol L^{-1})	RSD [%] ($2 \cdot 10^{-10}$ mol L^{-1})	RSD [%] ($5 \cdot 10^{-8}$ mol L^{-1})
POD	$2 \cdot 10^{-8}$	$5 \cdot 10^{-8}$	$5 \cdot 10^{-8}$- $2 \cdot 10^{-6}$	15.8	5.3	-	-
MP-11	$1 \cdot 10^{-10}$	$3 \cdot 10^{-10}$	$3 \cdot 10^{-10}$- $1 \cdot 10^{-7}$	-	-	11.3	2.2

pH-Optimization for the simultaneous determinations

Different enzymatic reactions may demand different pHs for the optimum performance. Therefore, assay conditions had to be optimized for the simultaneous enzyme-substrate reactions. The GOD assay is usually performed at pH 5.5-6, whereas the aP-catalyzed reaction should be carried out in the alkaline pH range from 9 to 10. In order to find a pH, which is acceptable for both reactions, the individual assays were performed with a pH variation in 0.5 steps between pH 5.5 and pH 9.5, resulting in pH 7.5 as a compromise for both reactions. The parallel determination of aP and MP-11 was tested at pH 8.5 in comparison to pH 7.5, with better results being obtained in the latter case. The simultaneous measurements of acP and GOD were carried out at pH 4.8, the optimum pH value for acP, which was also acceptable for the GOD-catalyzed reaction.

Table 3.4: *Limits of detection for the individual and for the simultaneous determination of selected enzymes based on their reactions with MNBDH and 5-FSAP*.

Method	Individual determination LOD	Individual determination LOQ	Simultaneous determination with	LOD	LOQ
GOD	$5 \cdot 10^{-4}$ [u mL^{-1}]	$2 \cdot 10^{-3}$ [u mL^{-1}]	aP (λ_{ex} = 320 nm)	$1 \cdot 10^{-3}$ [u mL^{-1}]	$3 \cdot 10^{-3}$ [u mL^{-1}]
			aP	$5 \cdot 10^{-4}$ [u mL^{-1}]	$3 \cdot 10^{-3}$ [u mL^{-1}]
			acP	$5 \cdot 10^{-4}$ [u mL^{-1}]	$3 \cdot 10^{-3}$ [u mL^{-1}]
aP	$5 \cdot 10^{-4}$ [u mL^{-1}]	$2 \cdot 10^{-3}$ [u mL^{-1}]	GOD	$5 \cdot 10^{-4}$ [u mL^{-1}]	$3 \cdot 10^{-3}$ [u mL^{-1}]
			MP-11	$5 \cdot 10^{-4}$ [u mL^{-1}]	$3 \cdot 10^{-3}$ [u mL^{-1}]
acP	$5 \cdot 10^{-2}$ [u mL^{-1}]	$2 \cdot 10^{-1}$ [u mL^{-1}]	GOD	$5 \cdot 10^{-2}$ [u mL^{-1}]	$2 \cdot 10^{-1}$ [u mL^{-1}]
MP-11	$1 \cdot 10^{-10}$ [mol L^{-1}]	$3 \cdot 10^{-10}$ [mol L^{-1}]	aP	$2 \cdot 10^{-10}$ [mol L^{-1}]	$6 \cdot 10^{-10}$ [mol L^{-1}]

Simultaneous enzyme determination in solution

The simultaneous two-enzyme determination was investigated for different couples of enzymes, as summarized in Table 3.4. In most cases, the limit of detection is identical for the individual and the parallel determination. There is no interference of one enzymatic reaction with respect to the other.

Only the limit of detection of MP-11 in the simultaneous measurement with aP increases by a factor of 2 in comparison to the single determination. As expected, the limit of detection of GOD in the simultaneous determination with aP by exciting the fluorescent products of both assays with one single excitation wavelength increases also by a factor of 2. MNBDA was in this case excited at its lower excitation maximum at 320 nm (compare with Figure 3.1).

Simultaneous enzyme detection in honey

Honey is known to contain different enzymes in significant concentrations, including acid phosphatase and glucose oxidase. Therefore, honey is well-suited to investigate the applicability of the simultaneous detection scheme for the analysis of real samples. To validate the results, enzyme detection systems based on established chromophores were used in parallel with the individual and the simultaneous determination based on the new method described in this chapter. Calibration was performed based on standard addition for all newly developed and reference methods, as external calibration could not be performed for any of the methods due to matrix

interferences. The results plus the respective RSDs (n = 5) for a honey sample are presented in Table 3.5. For GOD as well as for acP determination, all data obtained correlate well under consideration of the RSDs.

Table 3.5: *Concentrations of GOD and acP determined with the newly developed method and with reference methods in a honey sample.*

Method	Individual determination [u mL^{-1}]	RSD [%] (n = 5)	Simultaneous determination [u mL^{-1}]	RSD [%] (n = 5)
GOD (λ_{ex}= 470 nm)	28.6	6.0	27.1	12.9
GOD (λ_{ex}= 320 nm)	29.3	11.5	29.2	14.7
GOD Ref_{ABTS}	27.6	5.0		
acP	382.5	10.0	411.0	13.3
acP Ref_{NPP}	378.9	8.8		

3.5 Conclusions

The simultaneous dual-enzyme determination of GOD or MP-11 and aP or acP has been demonstrated. In case of aP and GOD, it has also been shown

that it is possible to excite MNBDA and 5-FSA with one single excitation wavelength by yielding only a slightly higher LOD for GOD in comparison to two individual optimum excitation wavelengths. MNBDH has been introduced as an excellent new substrate for MP-11, and its combination with 5-FSAP as phosphatase substrate allows the simultaneous determination with only slightly reduced performance data compared with the individual determination. The applicability of the method was demonstrated for a honey sample containing GOD and acP. The possibility for expansion of this detection scheme to other enzymes, e.g., other oxidases as xanthine oxidase, can be assumed by analyzing these results provided that similar reaction products are generated. Future work could be directed towards the development of a two-analyte immunoassay and on a simultaneous two-enzyme post-column detection system for liquid chromatographic separations.

3.6 References

[1] W. Gerhartz, Enzymes in Industry, VCH: Weinheim, 1990.

[2] H.-J. Rehm, G. Reed, Biotechnology, VCH: Weinheim, 1995.

[3] T. K. Christopolous, E. P. Diamandis, Immunoassay, San Diego, CA: Academic Press, 1996.

[4] E. Engvall, P. Perlmann, Immunochemistry 8 (1971) 871-874.

[5] D. Wahler, J.-L. Reymond, Biotechnology 12 (2001) 535-544.

[6] R. A. Evangelista, H. E. Wong, E. F. Gudgin Templeton, T. Granger, B. Allore, A. Pollak, Anal. Biochem. 203 (1992) 218-226.

[7] Q. Wang, J. Scheigetz, M. Gilbert, J. Snider, C. Ramachandran, Biochim. Biophys. Acta 1431 (1999) 14-23.

[8] C. J. Veiopoulou, E. S. Lianidou, P. C. Ioannou, C. E. Efstathiou, Anal. Chim. Acta 335 (1996) 177-184.

[9] G. G. Guilbault, P. J. Brignac, M. Juneau, Anal. Chem. 40 (1968) 1256-1263.

[10] X.–Y. Zheng, J.–Z. Lu, Q.–Z. Zhu, J.–G. Xu, Q.–G. Li, Analyst 122 (1997) 455-458.

[11] R. Dondon, V. P. Khilya, A. D. Roshal, S. Fery-Forgues, New J. Chem. 23 (1999) 923-927.

[12] I. Hemmilä, Anal. Chem. 57 (1985) 1676-1681.

[13] R. A. Evangelista, A. Pollak, E. F. Gudgin Templeton, Anal. Biochem. 197 (1991) 213-224.

[14] C. J. Murphy, Appl. Spectrosc. 56 (2002) 16A-27A.

[15] E. R. Goldman, E. D. Balighian, H. Mattoussi, M. K. Kuno, J. M. Mauro, P. T. Tran, G. P. Anderson, J. Am. Chem. Soc. 124 (2002) 6378-6382.

[16] E. R. Goldman, G. P. Anderson, P. T. Tran, H. Mattoussi, P. T. Charles, J. M. Mauro, Anal. Chem. 74 (2002) 841-847.

[17] D. M. Willard, Anal. Bioanal. Chem. 376 (2003) 284-286.

[18] T. Soukka, H. Härmä, J. Paukkunen, T. Lövgren, Anal. Chem. 73 (2001) 2254-2260.

[19] T. Soukka, K. Antonen, H. Härmä, A.-M. Pelkkikangas, P. Huhtinen, T. Lövgren, Clin. Chim. Acta 328 (2003) 45-58.

[20] Z. Kaul, T. Yaguchi, S. C. Kaul, T. Hirano, R. Wadhwa, K. Taira, Cell Research 13 (2003) 503-507.

[21] A. Büldt, U. Karst, Anal. Chem. 71 (1999) 1893-1898.

[22] R. A. Evangelista, E. F. G. Templeton, A. Pollak, (Kronem Systems, Inc.) US 5 262 299, 1993.

[23] J. Meyer, A. Büldt, M. Vogel, U. Karst, Angew. Chem. Int. Ed. 39 (2000) 1453-1455.

[24] H. U. Bergmeyer, Methoden der enzymatischen Analyse, VCH: Weinheim, 1974.

[25] J. Meyer, N. Jachmann, A. Büldt, U. Karst, DE 199 32 380.1, 2000.

[26] A. Büldt, U. Karst, Anal. Chem. 71 (1999) 3003-3007.

Chapter 4

Fluorescence and Mass Spectrometric Detection Schemes for Simultaneous Enzymatic Conversions: Method Development and Comparison [*]

[*] C. Hempen, A. Liesener, U. Karst, *Anal. Chim. Acta* **2005,** 543, 137-142.

4.1 Abstract

Fluorescence and mass spectrometric detection schemes are developed and compared for the simultaneous activity determination of two enzymes in solution. As model system, the following reactions are used: The alkaline phosphatase (aP)-catalyzed reaction with 5-fluorosalicyl phosphate (5-FSAP) yields the fluorescent 5-fluorosalicylic acid (5-FSA), whereas microperoxidase 11 (MP-11) reacts with 4-(N-methylhydrazino)-7-nitro-2,1,3-benzooxadiazole (MNBDH) and hydrogen peroxide to the strongly fluorescent 4-(N-methylamino)-7-nitro-2,1,3-benzooxadiazole (MNBDA). As the emission spectra of the fluorescent products as well as the molecular masses of substrates and products do not interfere with each other (shown in Chapter 3), it is possible to determine both reactions in parallel with both detection schemes. The measurements resulted in the same limits of detection, limits of quantification and linear ranges of the single/simultaneous enzyme determination for fluorescence and MS detection. While the relative standard deviations were significantly lower in case of fluorescence detection (1.4%-3.2%) than in mass spectrometry (5.7%-10.1%), the latter proved to be the more versatile approach for multianalyte determination.

4.2 Introduction

Enzymatic assays play an important role in clinical chemistry and related fields [1,2]. Therefore, it is desirable to improve enzymatic assays with respect to

throughput and limits of detection. Thus, the simultaneous identification and/or quantification of several analytes using simple and readily available instrumentation is advantageous (see also Chapter 3). In the case of the most frequently applied conversion of colorless substrates to colored products and subsequent UV/vis detection, there are hardly possibilities for simultaneous multianalyte determination. In contrast, fluorescence-based enzymatic assays with their low limits of detection and large linear ranges for calibration, resulting from the low background, do in principle allow the simultaneous determination of different analytes. Prerequisites for parallel fluorescence measurements are non-overlapping emission bands of the fluorescent products [3,4]. In Chapter 3, a multiplexing detection scheme of two different enzymes, a phosphatase and a peroxidase or glucose oxidase, respectively, based on microtiter plates fluorescence measurements of the fluorophores 5-fluorosalicylic acid (5-FSA) and 4-(N-methylamino)-7-nitro-2,1,3-benzooxadiazole (MNBDA) has already been introduced [5].

An alternative approach for monitoring two independent enzyme-catalyzed conversions is electrospray ionization mass spectrometry (ESI-MS). Since in MS, different compounds are separated solely by their mass-to-charge ratio (m/z), this detection method is independent from the spectroscopic properties of the analytes. Therefore, a multiplexing analysis without further separation is generally possible as long as the substrate and product species present in the assay exhibit different m/z ratios. The principle of using ESI-MS as means of detection in enzymatic bioassays was introduced in 1989 by Henion and co-workers [6]. Since this first publication, the interest in this field has been steadily

growing. The first approaches to a multiplexing analysis were presented by the group of Gelb and colleagues. They developed an assay scheme, which was based on the coupling of affinity chromatography for the extraction of the substrate and product species from the reaction mixture with ESI-MS for the parallel quantification of those compounds. This assay scheme allowed the parallel assessment of enzymatic activities in cell lysates providing a tool for the diagnosis of enzyme deficiency related diseases [7-12]. Basile et al. developed a direct flow-injection ESI-MS assay, which allowed the *in vivo* differentiation of bacteria by their aminopeptidase activity profiles. These profiles were generated by incubation of living bacterial cells with a mixture of different substrates and the quantification of substrates and products after a defined incubation time. Four sorts of bacteria were used as models and each was found to exhibit different enzymatic activities towards the substrates resulting in unique activity profiles [13].

In this chapter, a comparative study on the simultaneous quantitative determination of the two enzymes alkaline phosphatase and microperoxidase 11 is presented. The possibility of MS detection as an alternative method to fluorescence-based enzymatic assays was investigated by means of direct flow-injection measurements on a coupled fluorescence/mass spectrometric detection system. The reactions were carried out at-line, thus generating time-resolved reaction profiles.

4.3 Experimental

Chemicals

All chemicals were purchased from Aldrich (Steinheim, Germany), Merck (Darmstadt, Germany) and Fluka (Neu-Ulm, Germany) in the highest quality available. Acetonitrile and water for the flow-injection measurements were LC/MS grade and purchased from Biosolve (Valkenswaard, The Netherlands). Microperoxidase MP-11 and alkaline phosphatase aP (E.C. 3.1.3.1) were purchased from Sigma (Deisenhofen, Germany). The syntheses of 4-(N-methylhydrazino)-7-nitro-2,1,3-benzooxadiazole (MNBDH) and 5-fluorosalicyl phosphate (5-FSAP) were performed as described in literature [14, 15] (compare also Chapter 3).

Instrumentation

The flow-injection measurements with fluorescence and MS detection were performed with the following system: two LC-10AS pumps, degasser GT-154, SIL-10A autosampler, software Class LC-10 version 1.6, CBM-10A controller unit and RF-10AXL fluorescence detector (all components from Shimadzu, Duisburg, Germany). Fluorescence for 5-FSA was determined at excitation and emission wavelengths of 313 nm and 418 nm, respectively. For MNBDA, the excitation wavelength was set to 470 nm and the emission to 545 nm. The subsequent MS detection was performed by means of an esquire 3000*plus* ion trap mass spectrometer from Bruker Daltonics (Bremen, Germany). All MS results were obtained using electrospray ionization (ESI) in the negative ion mode. Ions were generated and guided towards the mass analyzer with

2049 V at the transfer capillary inlet, –102.6V on the capillary exit and –40.0 V at the skimmer. Mass spectra were recorded in the full scan mode, scanning from m/z = 50 to m/z = 1000. The ion count cumulative target for the ion trap mass analyzer was set to 10000, with a maximum accumulation time of 200 ms. Further ion source parameters were 45 psi nebulizer gas (nitrogen) and 10.0 L/min of drying gas (nitrogen) at a temperature of 365 ^{o}C.

The injection volume was 5 μL. For elution, a mixture (1:1, v/v) of methanol and 15 mmol L^{-1} NH_4Ac buffer (pH 7.3) was used.

Alkaline phosphatase (aP) assay [16]

For the single determination of aP, 300 μL of a 5-FSAP solution (10^{-3} mol L^{-1}; acetonitrile) were pipetted to 300 μL of an aP solution ($5 \cdot 10^{-4}$ u L^{-1} to 0.1 u L^{-1}; NH_4Ac buffer, pH 7.3, 15 mmol L^{-1}). Subsequently, 950 μL NH_4Ac buffer were added. Afterwards, every 2 min (20 times) 50 μL of the reaction solution were pipetted to 950 μL methanol in order to quench the enzymatic assay. Samples of every reaction time were injected in triplicate into the flow-injection set-up as described above.

Microperoxidase (MP-11) assay [5]

For the single determination of MP-11, 0.9 mL of a MNBDH solution ($5 \cdot 10^{-4}$ mol L^{-1}) were added to 7.5 mL of a 30 mmol L^{-1} solution of H_2O_2. 550 μL of this mixture were pipetted to 1000 μL of a solution of MP-11 ($1 \cdot 10^{-9}$ mol L^{-1} to $2 \cdot 10^{-7}$ mol L^{-1}) in NH_4Ac buffer (pH 7.3; 15 mmol L^{-1}). Afterwards, every

2 min (20 times) 50 μL of the reaction solution were pipetted to 950 μL methanol in order to quench the enzymatic assay. Samples of every reaction time were injected in triplicate into the flow-injection set-up as described above.

Simultaneous enzymatic assays [5]

The assays of the enzymes aP and MP-11 were performed simultaneously. For each reaction solution, 150 μL aP ($1 \cdot 10^{-3}$ u L^{-1} to 0.2 u L^{-1}; NH_4Ac buffer, pH 7.3, 15 mmol L^{-1}), 150 μL FSAP ($2 \cdot 10^{-3}$ mol L^{-1}; acetonitrile) and 475 μL buffer were mixed with 500 μL MP-11 ($2 \cdot 10^{-9}$ mol L^{-1} to $4 \cdot 10^{-7}$ mol L^{-1}) and 275 μL of the MNBDH/H_2O_2 mixture (0.9 mL of MNBDA; $1 \cdot 10^{-3}$ mol L^{-1} / 7.5 mL H_2O_2; 60 mmol L^{-1}). The concentrations of all enzyme and substrate solutions were twice as high as for the single determinations of aP and MP-11, so that all final concentrations were the same. Again, every 2 min (20 times) 50 μL of the reaction solution were pipetted to 950 μL of methanol in order to quench the enzymatic assay. Samples of every reaction time were injected in triplicate into the flow-injection set-up described above. The fluorescence of the respective products was read out for the two fluorescent products subsequently, due to technical limitations of the fluorescence detector available for this study. The MS detection of MNBDA and 5-FSA was performed simultaneously.

Kinetic MP-11 determination

The fluorescence measurements of the MP-11 reaction in quartz cuvettes were performed using an Aminco Bowman AB2 luminescence spectrometer from Polytec (Waldbronn, Germany) with software version 5.00. For this reaction, 2584 μL NH_4Ac buffer (pH 7.3; 15 mmol L^{-1}), 200 μL MP-11 ($2 \cdot 10^{-8}$ mol L^{-1}), 200 μL MNBDH ($5 \cdot 10^{-4}$ mol L^{-1}) and 16 μL H_2O_2 were mixed in a cuvette. Approximately every 5 seconds, the fluorescence intensity of MNBDA was measured at an excitation wavelength of 470 nm and an emission wavelength of 545 nm.

4.4 Results and Discussion

Quantification of alkaline phosphatase (aP) was achieved by means of the catalyzed reaction of 5-FSAP to the fluorescing 5-FSA, whereas microperoxidase 11 (MP-11) could be determined by the conversion of the non-fluorescent MNBDH into the strongly fluorescent MNBDA as depicted in Figure 4.1. The reactions were carried out both individually and simultaneously. While both individual reactions were already analyzed earlier using fluorescence spectroscopy, mass spectrometric detection has not been described for the analysis of either of these reactions.

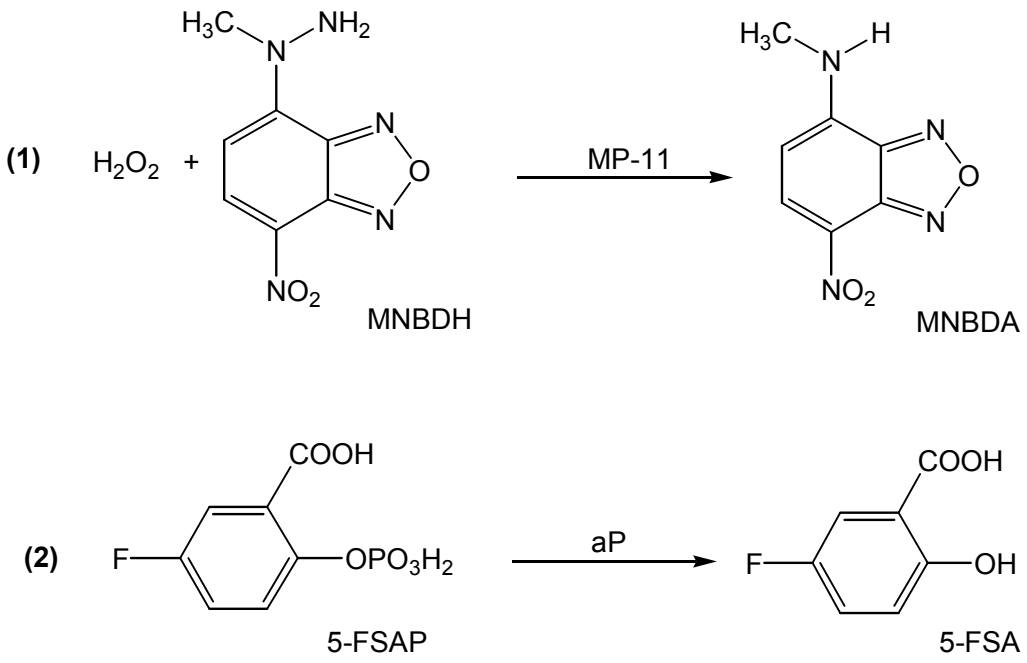

Figure 4.1: *Enzymatic reactions for the determination of MP-11 (1) using MNBDH and for the determination of aP (2) using 5-FSAP.*

The reaction substrates were mixed manually, and after approximately every 2nd minute, a sample aliquot (50 µL) of the reaction solution was pipetted into a vial with an excess of methanol in order to stop the reaction and to obtain information about the progress of the two reactions over a period of 40 minutes (20 samples). This was performed for eight concentrations of each enzyme in the case of individual determinations as well as for simultaneous measurements with the second enzyme. Afterwards, the samples were injected into the FIA system and analyzed by means of the fluorescence detector and subsequently by means of the connected mass spectrometer.

A drawback of fluorescence detection is that it is not possible to switch between different excitation and emission wavelengths in one single run. Consequently,

two injections of the simultaneous reaction solution, with different detection wavelengths, had to be performed, thus not allowing a truly simultaneous detection of both reaction products. In contrast, the ESI-MS-detection enabled the simultaneous determination of aP and MP-11.

Figure 4.2 shows a mass spectrum of the simultaneous determination of the two enzymes, with an aP concentration of 5 u L^{-1} and a MP-11 concentration of $2 \cdot 10^{-8}$ mol L^{-1}.

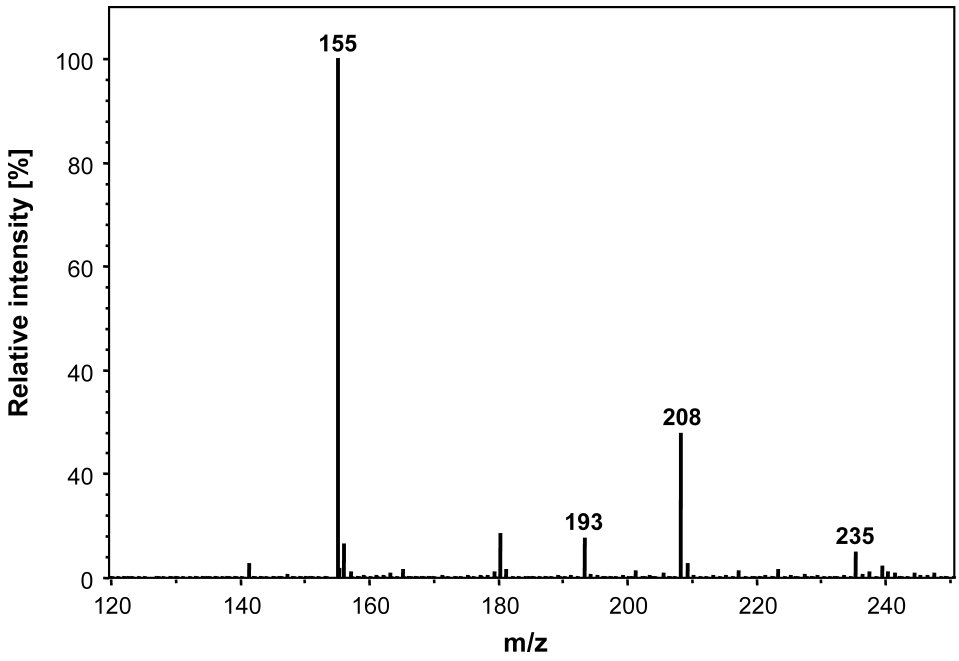

Figure 4.2: *ESI-MS spectrum showing the educts (5-FSAP: $[M-H]^-$ = 235; MNBDH: $[M-H]^-$ = 208) and the products (5-FSA: $[M-H]^-$ = 155; MNBDA: $[M-H]^-$ = 193) of a simultaneous enzyme reaction (c_{aP} = 5 u L^{-1} and $c_{MP-11} = 2 \cdot 10^{-8}$ mol L^{-1}; reaction time: 6 min).*

The signals at m/z = 155 and m/z = 235 correspond to the deprotonated 5-FSA and 5-FSAP, respectively. Furthermore, the signals at m/z = 193 and m/z = 208 are assigned to the deprotonated MNBDA and MNBDH.

A comparison of the figures of merit for the single and parallel determination of aP and MP-11 by means of fluorescence and ESI-MS detection after flow-injection is presented in Table 4.1. The limits of detection, the limits of quantification and the linear ranges are determined for the reaction time of 18 minutes, whereas the RSD is calculated for all measurements of each enzyme at all concentrations and times (n = 960 for the single/parallel fluorescence measurements and for the single MS determination; n = 480 for the simultaneous MS measurements). The values for the LOD, the LOQ and the linear range of the MS detection correspond to the results for the fluorescence detection. Both detection methods yield a LOD of $2 \cdot 10^{-3}$ u L^{-1}, a LOQ of $6 \cdot 10^{-3}$ u L^{-1} and a linear range from $6 \cdot 10^{-3}$ u L^{-1} to $5 \cdot 10^{-2}$ u L^{-1} for the single aP determination.

For the simultaneous measurement with MP-11, the LOD and LOQ of aP are higher by approximately a factor of 2. In case of the single MP-11 determination, the LOD is $5 \cdot 10^{-9}$ mol L^{-1} and the LOQ $1.5 \cdot 10^{-8}$ mol L^{-1}. The linear range is observed from $1.5 \cdot 10^{-8}$ mol L^{-1} to $2 \cdot 10^{-7}$ mol L^{-1}. The figures of merit for the simultaneous measurements of MP-11 are lower by factor of five for the fluorescence as well as for the MS detection. Comparing the relative standard deviations for all measurements, it can be observed that the values are much lower, especially in case of the simultaneous measurements, for fluorescence

detection. The RSDs for the single determination of aP and MP-11 are lower by factor 2 and 4, respectively, whereas the RSDs for the parallel measurements differ in factor 3 and 10 for aP and MP-11.

In Figures 4.3 and 4.4, the comparative reaction profiles for the reaction of aP (c_{aP} = 10 u L^{-1}) with 5-FSAP and for the reaction of MP-11 ($c_{MP\text{-}11}$ = $2 \cdot 10^{-7}$ mol L^{-1}) with hydrogen peroxide and MNBDH are presented. In all cases, the signals for the different reaction times of the single determinations are shown. The upper trace displays each with the fluorescence detection of the products 5-FSA (313 nm/418 nm) and MNBDA (470 nm/545 nm), whereas in the respective second traces the ESI(-)-MS-detection for 5-FSA (m/z = 155) and MNBDA (m/z = 193) can be seen. In Figure 4.3, a typical kinetic behavior of an enzymatic reaction can be observed for the fluorescence as well as for the mass spectrometric detection of 5-FSA. In the beginning of the reaction, the signals have a relatively low intensity, which increases and reaches a maximum value with longer reaction times. Figure 4.4 shows, in contrast, different kinetic properties for MP-11. The plateau, which is reached after a reaction time of approximately 28 min for aP, is in this case already achieved after 4 minutes, which means that the MP-11 reaction proceeds much faster than the aP-reaction.

Table 4.1: *Figures of merit for the single and simultaneous determinations of the enzymes MP-11 and aP after a reaction time of 18 minutes for the fluorescence detection in comparison to the MS detection (n = 3).*

	Fluorescence				ESI-MS			
	LOD	LOQ	Linear range	RSD [%]	LOD	LOQ	Linear range	RSD [%]
aP_{Single}	$2 \cdot 10^{-3}$ [u mL^{-1}]	$6 \cdot 10^{-3}$ [u mL^{-1}]	$6 \cdot 10^{-3}$-$5 \cdot 10^{-2}$ [u mL^{-1}]	3.2	$2 \cdot 10^{-3}$ [u mL^{-1}]	$6 \cdot 10^{-3}$ [u mL^{-1}]	$6 \cdot 10^{-3}$-$5 \cdot 10^{-2}$ [u mL^{-1}]	6.3
$MP\text{-}11_{Single}$	$5 \cdot 10^{-9}$ [mol L^{-1}]	$1.5 \cdot 10^{-8}$ [mol L^{-1}]	$1.5 \cdot 10^{-8}$-$2 \cdot 10^{-7}$ [mol L^{-1}]	1.9	$5 \cdot 10^{-9}$ [mol L^{-1}]	$1.5 \cdot 10^{-8}$ [mol L^{-1}]	$1.5 \cdot 10^{-8}$-$2 \cdot 10^{-7}$ [mol L^{-1}]	8.3
$aP_{Simultaneous}$	$5 \cdot 10^{-3}$ [u mL^{-1}]	$1.5 \cdot 10^{-2}$ [u mL^{-1}]	$1.5 \cdot 10^{-2}$-$5 \cdot 10^{-2}$ [u mL^{-1}]	1.7	$5 \cdot 10^{-3}$ [u mL^{-1}]	$1.5 \cdot 10^{-2}$ [u mL^{-1}]	$1.5 \cdot 10^{-2}$-$5 \cdot 10^{-2}$ [u mL^{-1}]	5.7
$MP\text{-}11_{Simultaneous}$	$1 \cdot 10^{-9}$ [mol L^{-1}]	$3 \cdot 10^{-9}$ [mol L^{-1}]	$3 \cdot 10^{-9}$-$1 \cdot 10^{-7}$ [mol L^{-1}]	1.4	$1 \cdot 10^{-9}$ [mol L^{-1}]	$3 \cdot 10^{-9}$ [mol L^{-1}]	$3 \cdot 10^{-9}$-$2 \cdot 10^{-7}$ [mol L^{-1}]	10.1

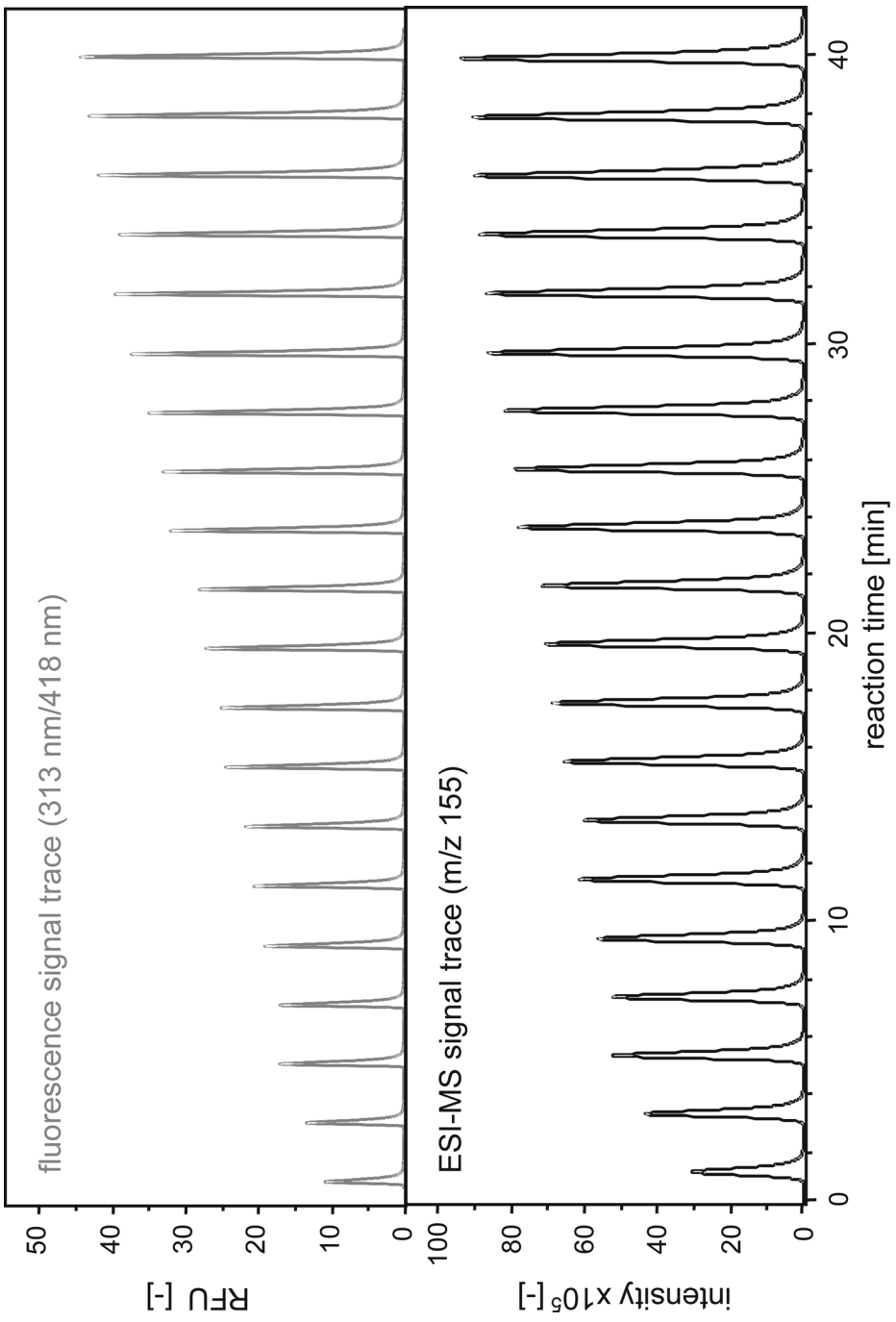

Figure 4.3: *Comparative reaction profile for the reaction of aP (c_{aP} = 10 u/L) with 5-FSAP over 40 minutes (reaction time between each signal approximately 2 minutes). In the upper trace, the fluorescence detection of the product 5-FSA (313 nm/418 nm) is shown, whereas the lower trace shows the ESI(-)-MS-detection for 5-FSA (m/z = 155).*

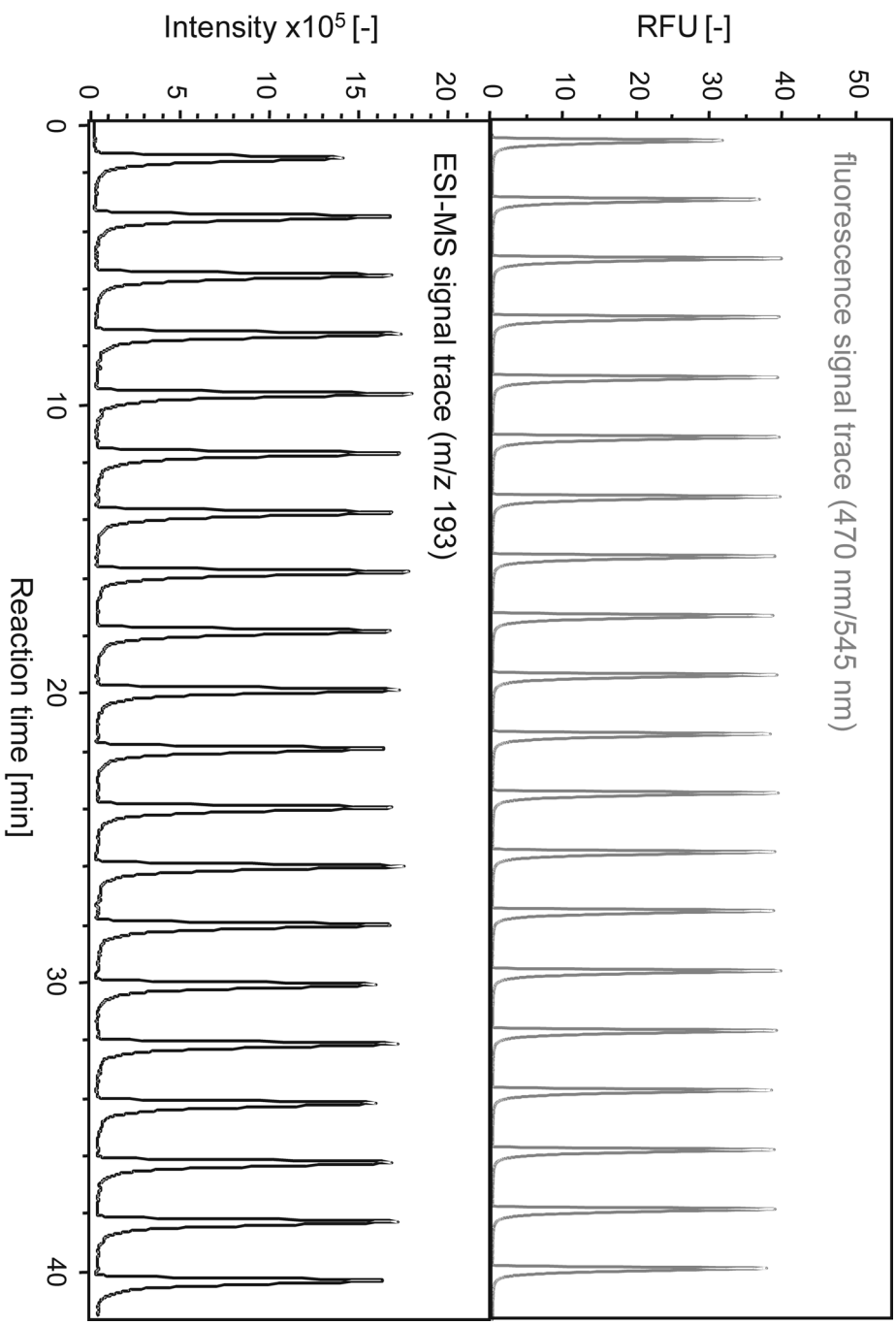

Figure 4.4: *Comparative reaction profile for the reaction of MP-11 (c_{MP-11} = $2 \cdot 10^{-7}$ mol L^{-1}) with MNBDH and H_2O_2 over 40 minutes (reaction time between each signal approximately 2 minutes). In the upper trace, the fluorescence detection of the product MNBDA (470 nm/545 nm) is presented, whereas the lower trace shows the ESI(-)-MS-detection for MNBDA (m/z = 193).*

The major difference in the kinetic behavior of aP and MP-11 is the fact that the height of the plateau value is in case of the MP-11-mediated conversion strongly dependent on the concentration of MP-11, while the aP-catalyzed reaction are all running to the same plateau level. This indicates that MP-11 is after a certain number of conversions inactivated, and thus not working like a true enzymatic catalyst as aP.

Spee et al. have found for different microperoxidases to be relatively efficient catalysts for the reaction with aniline and H_2O_2 [17].

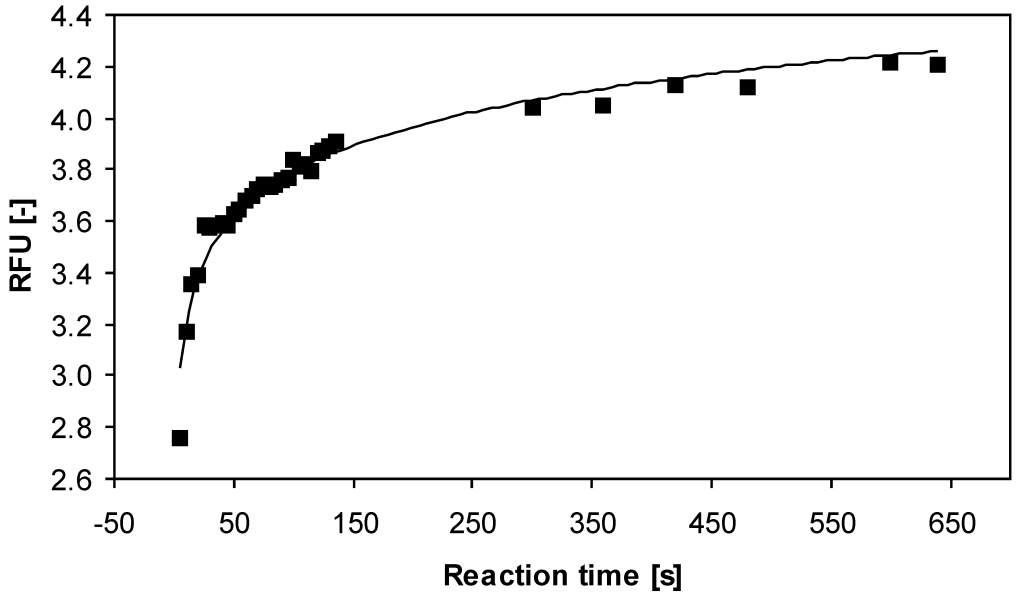

Figure 4.5: *Progress of the MP-11-catalyzed reaction with MNBDH and H_2O_2 in the first 10 minutes ($c_{MP-11} = 2 \cdot 10^{-8}$ mol L^{-1}).*

However, they also observed reaction profiles for different conversions, which were characterized by a steep slope in the beginning and a rapid decrease of

the reaction rate after 2 minutes. Similar investigations for the MP-11 reaction with MNBDH and H_2O_2 are presented in Figure 4.5.

This MP-11 reaction was performed in quartz cuvettes and the fluorescence intensity increase of the product MNBDA has been observed for circa 10 minutes. It can be seen that the fluorescence intensity increases steeply in the first 2 minutes, whereas afterwards it rises very slowly to a plateau, which is in agreement with the result of the flow-injection measurements. The logarithmic fit ($y = 0.2528 \cdot \ln(x) + 2.6269$) confirms this observation: The calculated fluorescence intensity changes significantly in case of small increasing x-values (time). Longer reaction times do not influence the result in a considerably way. In Figure 4.6, a comparison of the reaction profiles of the single and simultaneous aP reaction ($c_{aP} = 2 \cdot 10^{-2}$ u L^{-1}) detected by means of ESI-MS is presented. It is observed that the development of the reaction product with time is very similar for both reaction schemes. These results stress that there is no interference of one enzymatic reaction with respect to the other.

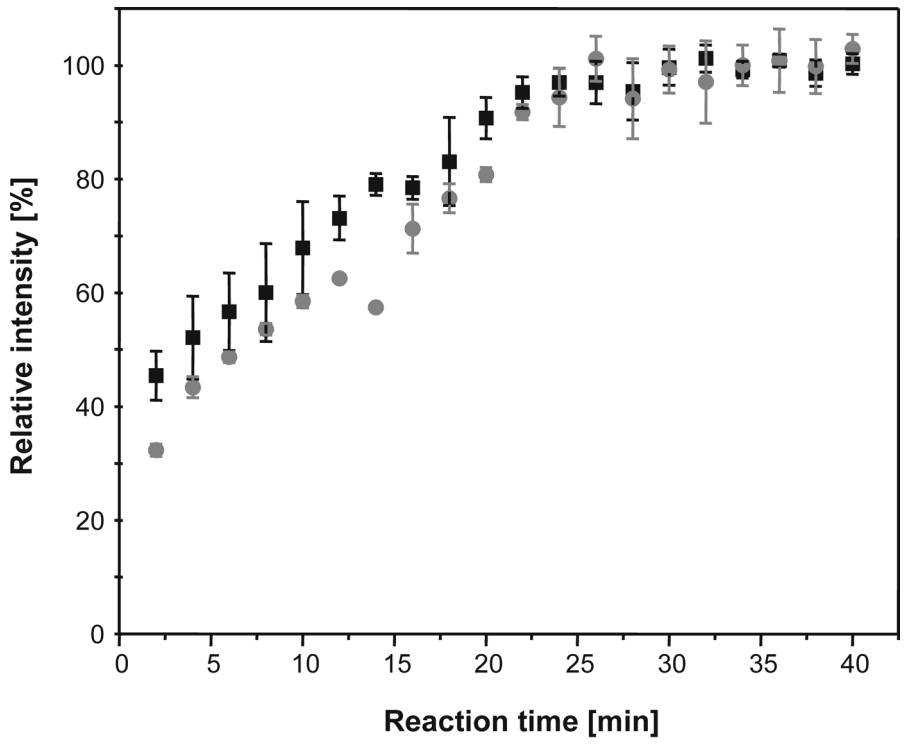

Figure 4.6: *Comparison of the reaction profile of the single aP-reaction (black) with the profile of the simultaneous determination (grey) (c_{aP} = 2·10^{-2} u L^{-1}), both detected by means of ESI-MS.*

4.5 Conclusions

A comparative study for the simultaneous determination of enzymes by means of flow-injection measurements with fluorescence and subsequent ESI-MS detection is presented. The results of these investigations, which also provide mechanistical information on the reaction schemes, show that both detection methods do in principle allow the simultaneous determination of MP-11 and aP. The advantage of fluorescence detection is a better reproducibility, which is expressed by significantly lower RSDs. However, the

reproducibility and accuracy of the ESI-MS detection method might be improved by employing an on-line sample clean-up feature (such as turbulent flow chromatography), in order to remove matrix components, which might have deteriorating effects on the ionization and thus the signal response. Therefore, flow-injection measurements with fluorescence but also with MS detection are qualified as validation method for enzymatic assays on microtitration plates. However, as long as the technical properties of commercially available fluorescence detectors still do not allow the detection at two different pairs of wavelengths simultaneously, it is advantageous to use MS detection, especially with respect to the sample throughput demands in studies of enzymatic reactions on microtitration plates due to possible parallel product detection. Mass spectrometry additionally enables the detection of two reaction products as well as of the respective reaction educts at the same time. Future work could be directed towards investigations on the on-line inhibition of parallel enzymatic assays in flow-injection systems.

4.6 References

[1] H.-J. Rehm, G. Reed, Biotechnology, VCH: Weinheim, 1995.

[2] W. Gerhartz, Enzymes in Industry, VCH: Weinheim, 1990.

[3] I. Hemmilä, Anal. Chem. 57 (1985) 1676-1681.

[4] D. M. Willard, Anal. Bioanal. Chem. 376 (2003) 284-286.

[5] C. Hempen, U. Karst, Anal. Chim. Acta 521 (2004) 117-122.

[6] E. D. Lee, W. Mueck, J. Henion, T. R. Covey, J. Am. Chem. Soc. 111 (1989) 4600-4604.

[7] S. A. Gerber, C. R. Scott, F. Turecek, M. H. Gelb, J. Am. Chem. Soc. 121 (1999) 1102-1103.

[8] X. Zhou, F. Turecek, C. R. Scott, M. H. Gelb, Clin. Chem. 47 (2001) 874-881.

[9] S. A. Gerber, C. R. Scott, F. Turecek, M. H. Gelb, Anal. Chem. 73 (2001) 1651-1657.

[10] S. A. Gerber, F. Turecek, M. H. Gelb, Bioconjugate Chem. 12 (2001) 603-615.

[11] Y. Li, Y. Ogata, H. H. Freeze, C. R. Scott, F. Turecek, M. H. Gelb, Anal. Chem. 75 (2003) 42-48.

[12] Y. Li, C. R. Scott, N. A. Chamoles, A. Ghavani, B. M. Pinto, F. Turecek, M. H. Gelb, Clin. Chem. 50 (2004) 1785-1796.

[13] F. Basile, I. Ferrer, E. T. Furlong, K. J. Voorhees, Anal. Chem. 74 (2002) 4290-4293.

[14] A. Büldt, U. Karst, Anal. Chem. 71 (1999) 1893-1898.

[15] R. A. Evangelista, E. F. G. Templeton, A. Pollak, (Kronem Systems, Inc.) US 5 262 299, 1993.

[16] R. A. Evangelista, A. Pollak, E. F. Gudgin Templeton, Anal. Biochem. 197 (1991) 213-224.

[17] J. H. Spee, M. G. Boersma, C. Veeger, B. Samyn, J. Van Beeumen, G. Warmerdam, G. W. Canters, W. M. A. M. van Dongen, I. M. C. M. Rietjens, Eur. J. Biochem. 241 (1996) 215-220.

Chapter 5

Liquid Chromatographic/Mass Spectrometric Investigation on the Reaction Products in the Peroxidase-Catalyzed Oxidation of o-Phenylenediamine by Hydrogen Peroxide [*]

[*] C. Hempen, S. M. Van Leeuwen, H. Luftmann, U. Karst, *Anal. Bioanal. Chem.* **2005,** 382, 234-238.

5.1 Abstract

Mass spectrometric evidence was obtained to confirm that the main reaction product of the horseradish peroxidase (POD)-catalyzed oxidation of o-phenylenediamine (OPD) by hydrogen peroxide is 2,3-diaminophenazine. Although this reaction is one of the most widespread detection schemes in enzyme-linked immunosorbent assays (ELISAs), the literature data on the identity of the reaction product(s) are strongly contradictory throughout the last decades. Liquid chromatography with UV/vis and mass spectrometric detection as well as exact mass measurements after LC fraction collection have led to the unambiguous identification of 2,3-diaminophenazine as main reaction product. 2,2´-Diaminoazobenzene, which is frequently described in other publications to be the major reaction product was not detected at all.

5.2 Introduction

The POD-catalyzed oxidation of OPD by hydrogen peroxide is the most widely-applied detection scheme in immunoassays of the ELISA type. The enzyme-catalyzed reaction results in the formation of an orange-red reaction product, which is most frequently detected by UV/vis absorbance using microplate readers in the wavelength range between 425 and 450 nm [1, 2, 3]. Often, sulfuric acid is added to stop the enzymatic reaction. This leads to a change in the UV/vis absorbance of the product, which is then best detected

at 492 nm [4]. The reaction has also been used frequently in combination with electroanalytical methods [5, 6, 7].

Whereas OPD has already been known and has successfully been applied for more than a century, the discussion about the structure of the generated oxidation product is still on-going in literature: In many cases, 2,3-diaminophenazine is supposed to be the product of the OPD oxidation, but frequently 2,2´-diaminoazobenzene is mentioned as main oxidation product instead. The oxidation with the two possible reaction products is presented in Figure 5.1.

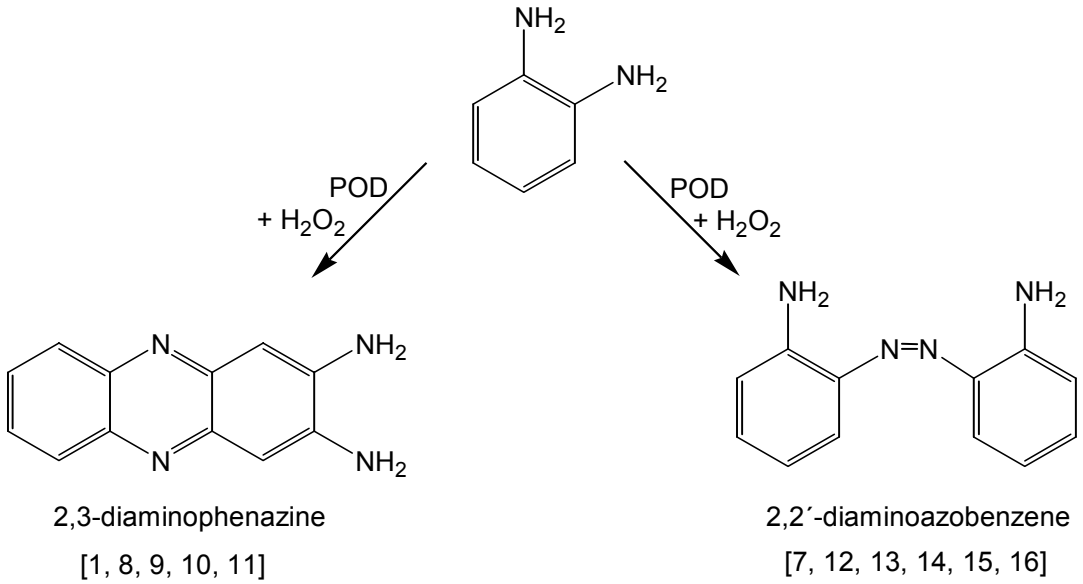

Figure 5.1: *Formation of the reaction products described in literature in the POD-catalyzed oxidation of OPD by hydrogen peroxide.*

In 1871, 2,3-diaminophenazine was described for the first time by Griess as product of the reaction of OPD with iron (III) chloride [8]. In 1918, Knoevenagel referred to investigations regarding the reaction of OPD with

iodine, which resulted in 2,3-diaminophenazine as oxidation product [9]. Tarcha et al. characterized in 1987 the reaction product of OPD with H_2O_2 in the presence of POD by melting point, ^{13}C- and ^{1}H-NMR spectra and the mass spectrum by electron impact measurements [10]. Although the result of the melting point determinations did not correspond to the results of Knoevenagel, they claimed 2,3-diaminophenazine as reaction product due to their other measurements. In 2000, Zhang et al. [1] and, even more recently, Niu et al. [11] confirmed the earlier findings of 2,3-diaminophenazine to be the product of the enzyme-catalyzed OPD reaction. In the latter case, the product was characterized by UV/vis, IR and NMR measurements. It should, however, be noted that the earlier measurements described above were based on different oxidation schemes, while some of the more recent investigations did not use reaction conditions which are identical to those typically used in ELISAs.

However, in the same time period, 2,2´-diaminoazobenzene was frequently claimed to be main product of the OPD oxidation. In 1971, Omote et al. identified it as the product of the reaction of OPD with atmospheric oxygen in the presence of sodium hydride by melting point measurements [12], although the reaction mechanism could not be unambiguously clarified. Berchmans et al. described the same product in 1995 by investigating the electrochemical oxidation of OPD [7]. In the years 1982 – 2000, Gallati et al. [13], Song et al. [14], Huangxian et al. [15] and Azek et al. [16] performed conventional ELISAs by using the typical substrates POD and H_2O_2 and claimed, thereupon, 2,2´-diaminoazobenzene to be the product of the OPD reaction.

In order to clarify the conflicting results described in literature, the OPD reaction was investigated under reaction conditions similar to the ELISA, and the products were identified by means of LC/UV/APCI-MS and ESI-MS after LC fraction collection.

5.3 Experimental

Chemicals

All chemicals were purchased from Aldrich (Steinheim, Germany) and Merck (Darmstadt, Germany). For LC/MS measurements, acetonitrile and water were LC/MS grade (Biosolve, Valkenswaard, The Netherlands). Horseradish peroxidase POD (E.C. 1.11.1.7; 113 purpurogallin units/mg solid) and o-phenylenediamine OPD (purity 99%) were purchased from Sigma (Deisenhofen, Germany).

LC/MS conditions

For LC/MS investigations, an Agilent Technologies (Waldbronn, Germany) HP1100 liquid chromatograph for binary gradient elution (pump model G1312A), including an autosampler (G1313A) and a DAD (G1315B), coupled to an esquire 3000*plus* ion trap mass spectrometer from Bruker Daltonics (Bremen, Germany) was used. For the LC separation, a binary gradient system consisting of buffer A (NH_4Ac/HAc, both 0.05 mol L^{-1}, pH 4) and acetonitrile (B) with a flow rate of 0.5 mL min^{-1} was used. The gradient profile was as follows:

time [min]	0	2	10	15	16	24
c_B [%]	35	35	90	90	35	stop

The injection volume was 20 µL. A Prontosil C18-ace-EPS column (Bischoff Chromatography, Leonberg, Germany) was used; particle size 3.0 µm, pore size 120 Å; column dimensions 150 mm x 3.0 mm.

All LC/MS results were obtained using atmospheric pressure chemical ionization (APCI) in the positive ion mode. Ions were generated with 2500 nA corona current and guided towards the mass analyzer with –3525 V at the transfer capillary inlet, 145 V on the capillary exit and 16.4 V at the skimmer. Mass spectra were recorded in the full scan mode, scanning from m/z = 50 to m/z = 500. The ion count cumulative target for the ion trap mass analyzer was 5000, with a maximum accumulation time of 200 ms. Further ion source parameters were 50 psi nebulizer gas and 5.0 L/min of drying gas with a temperature of 205 ^{o}C. MS/MS experiments were carried out in the autofragmentation mode with 1.10 V fragmentation amplitude, selecting one precursor from the included ions of interest.

Exact mass measurements

Exact mass measurements of the collected LC fractions were performed in the positive ion mode using a microTOF instrument (Bruker Daltonics) equipped with an ESI probe.

HPLC fraction collection

The liquid chromatographic separations were performed with the following system (all components from Shimadzu, Duisburg, Germany): two LC-10AS pumps, degasser GT-154, SPD-M10Avp diode array detector, SIL-10A autosampler, software Class LC-10 version 1.6. and CBM-10A controller unit. For the HPLC separation, conditions as described above were used.

OPD reaction

In order to identify the products, the reaction mixture was directly injected into the LC-MS system. The reaction was performed as follows: To 2.5 mL of a $3.7 \cdot 10^{-3}$ mol L^{-1} OPD solution (in acetic acid/ammonium acetate buffer, 0.05 mol L^{-1}, pH 5), 100 µL H_2O_2 solution (0.35 mass % in H_2O) were added. 250 µL of this solution were mixed with 125 µL POD solution (20 u L^{-1}, buffer) and made up to 3.75 mL with the same buffer. After a reaction time of at least 10 min, aliquots of the reaction solution were injected.

5.4 Results and Discussion

The goal of this work was to clarify the conflicting reports regarding the products of the POD-catalyzed reaction of OPD with H_2O_2. Before respective MS investigations were started, the reaction conditions were optimized on microtitration plates. Initial experiments on microtitration plates and by LC/MS confirmed that, as Bovaird et al. [3] have already published in 1982, citrate buffer at pH 5 is best suited for the reaction. However, these measurements

also resulted in the finding that ammonium acetate/acetic acid buffer at pH 5, which is superior for MS measurements to citrate buffer, is appropriate for the OPD reaction as well and that the same products are formed in both cases. Therefore, this buffer was selected for all MS studies. Initial flow-injection ESI-MS measurements using these reaction conditions proved that separation of the reaction mixture is required for proper identification of the products. Therefore, some comparative and optimizing studies were performed: different gradients for the separation of the reaction solution on a reversed-phase Prontosil C18-ace-EPS column were tested using acetonitrile and ammonium acetate/acetic acid buffer at pH 5 (as in the reaction mixture) and at pH 4. Finally, the above-described gradient was identified to be very well suited for LC separation of the reaction products (data not shown). The results of the ESI-MS measurements were compared with respective APCI-MS measurements. Both interfaces performed equally well for this purpose, and the APCI interface was selected

Prior to MS detection, the compounds of the reaction solution were first detected by means of UV/vis absorbance. Figure 5.2 shows the UV/vis chromatograms of the reaction solution recorded at different wavelengths. Three peaks were observed: The main peak at approximately 10 min in the survey chromatogram A can also be seen in chromatograms B and C, which were recorded at 290 nm and 450 nm, respectively. The same applies for the smaller peak at about 8 min. The peak at 4 min is also detected at 290 nm, but not at a wavelength of 450 nm, which confirms, in addition to the retention time, the identity of the substance as residual colorless substrate OPD.

In agreement with the UV signals discussed above, Figure 5.3 shows the mass spectrometric detection of peaks at approximately 5, 8 and 10 minutes. The main peak, showing up in the latter case, is observed with m/z = 211. This m/z ratio can be assigned to the protonated 2,3-diaminophenazine, which would mean that this substance and not the azo dye (M = 212 g/mol) is the main reaction product. The peaks observed at the same retention time in the mass traces with m/z = 212 and m/z = 213 correspond to the respective ^{13}C isotopic patterns due to the observed peak intensities (note the respective scaling).

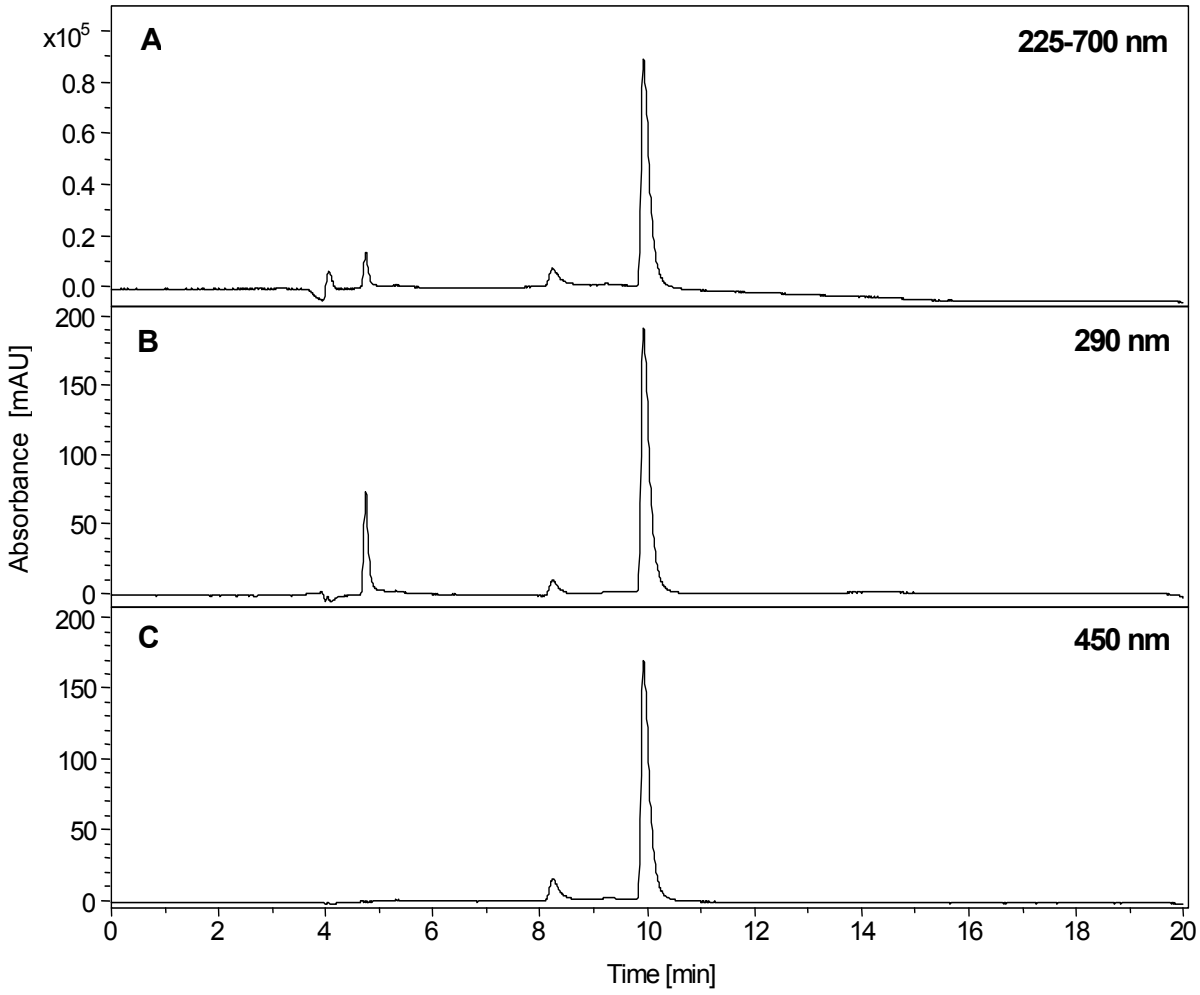

Figure 5.2: *UV/vis chromatograms of the OPD reaction solution after LC separation recorded in the range of 225-700 nm (A), at 290 nm (B) and at 450 nm (C).*

In order to confirm the elemental composition of the main reaction product, exact mass measurements using electrospray-time of flight (ESI-TOF) mass spectrometry were performed. Therefore, peak fractions of the chromatographic separation were collected. These measurements confirmed the first interpretation regarding the peak with m/z = 211. The molecular formula generated from exact mass measurements fits to that of 2,3-diaminophenazine (measured: 211.0992; theoretical: 211.0978 for

$C_{12}H_{11}N_4$). This compound is thus verified as main product of the OPD reaction.

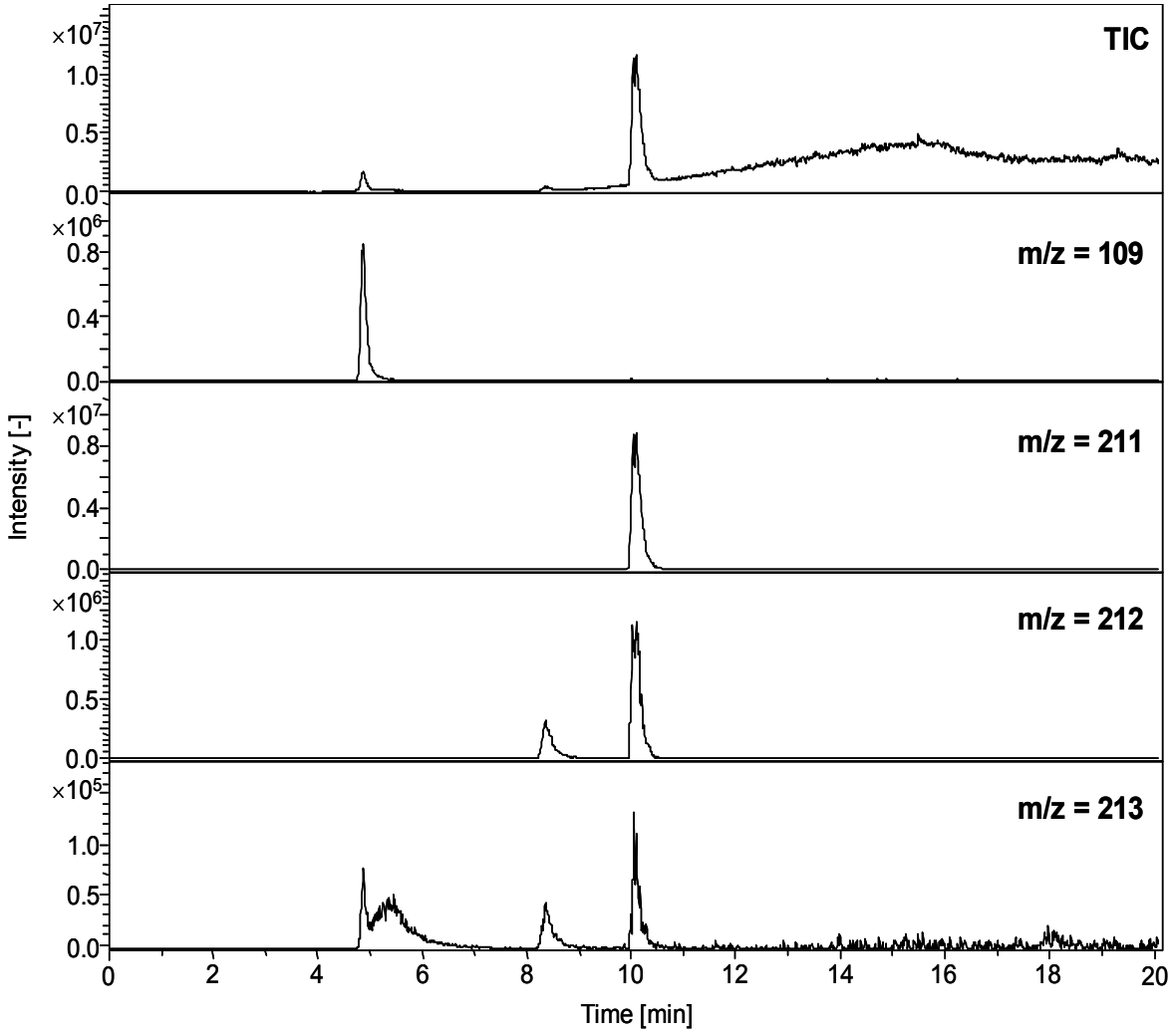

Figure 5.3: *APCI(+)-MS chromatogram of the OPD reaction solution after LC separation; recorded in the scan mode (m/z = 50 – 500) and the respective extracted mass traces of m/z = 109, 211, 212 and 213.*

The main side product, eluting after 8 minutes, is observed at m/z = 212 under LC/MS conditions with low mass accuracy. This mass could possibly indicate the presence of the radical cation of the 2,2´-diaminoazobenzene. However,

accurate mass measurements after fraction collection indicate that this is not the case (measured: 212.0816; theoretical: 212.1062 for $C_{12}H_{12}N_4$). The data rather indicate the presence of a protonated product with a similar structure than 2,3-diaminophenazine, but with one NH_2 group exchanged by an OH group. The calculated mass for this species with a sum formula of $C_{12}H_{10}N_3O$ is 212.0818, which deviates by only 1 ppm from the measured exact mass. However, the present data do not allow to propose an exact structure of this compound.

The first peak in the chromatogram is observed at m/z = 109, thus exactly matching the protonated OPD. At the same time, a signal at m/z = 213 is observed, probably due to oxidation of OPD in the APCI interface, as confirmed by MS/MS investigations of the m/z = 213 as well as by LC/MS determinations of OPD without any added substrates. Furthermore, the mass trace of m/z = 213 shows a peak, directly after the previously described peak, at a retention time of approximately 5.5 minutes. This peak was not observed in the UV chromatograms. The mass would fit to protonated 2,2'-diaminoazobenzene. However, the peak shape (Figure 5.3) as well as the decreasing signal intensity upon longer reaction time (Figure 5.4) strongly indicate a reactive species.

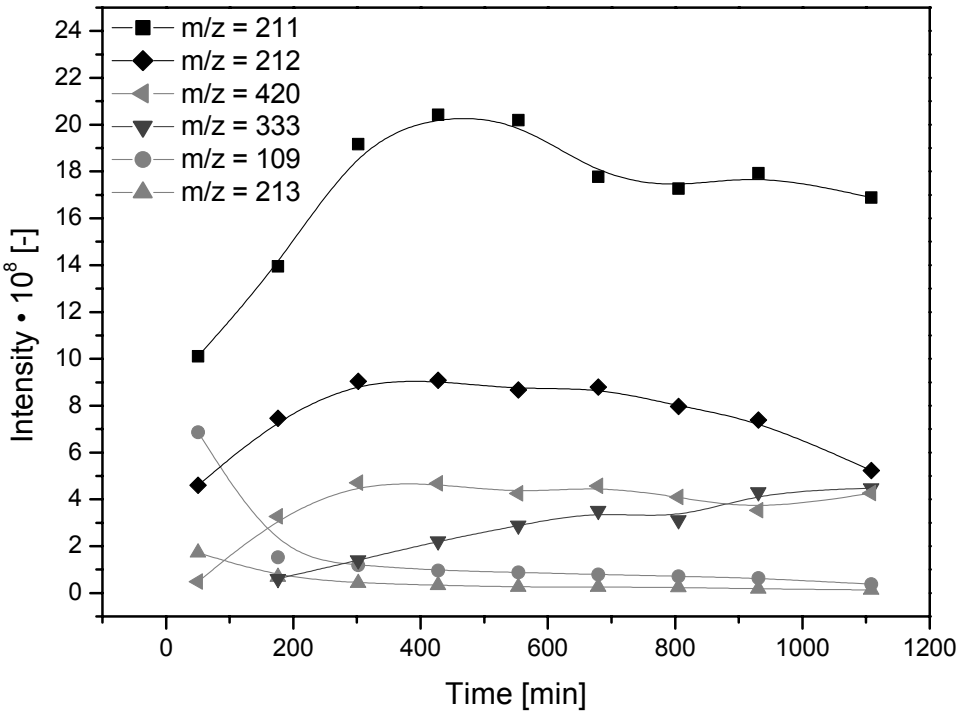

Figure 5.4: *Overview of product development of different m/z ratios: 211, 212, 420 (amplification factor 50), 333 (amplification factor 50), 109 (amplification factor 10) and 213 (amplification factor 10).*

In the reaction forming the diaminophenazine, an intermediate with two NH bridges in the central ring could be imagined. Tandem MS data of this peak, providing a fragment with m/z = 107, are in agreement with this assumption, as m/z = 107 fits to the half mass of the intermediate in the protonated form, resulting from cleavage of both N bridges.

A recent paper of Li et al. [17] investigates the intermediates and products of the methemoglobin-catalyzed oxidation of OPD in two aqueous-organic phases. Although the reaction conditions and the catalyst differ from the work carried out here, their findings may be seen as additional evidence for this

reaction pathway. Herewith, the main path of the POD-catalyzed reaction of OPD with H_2O_2 can be summarized as in Figure 5.5.

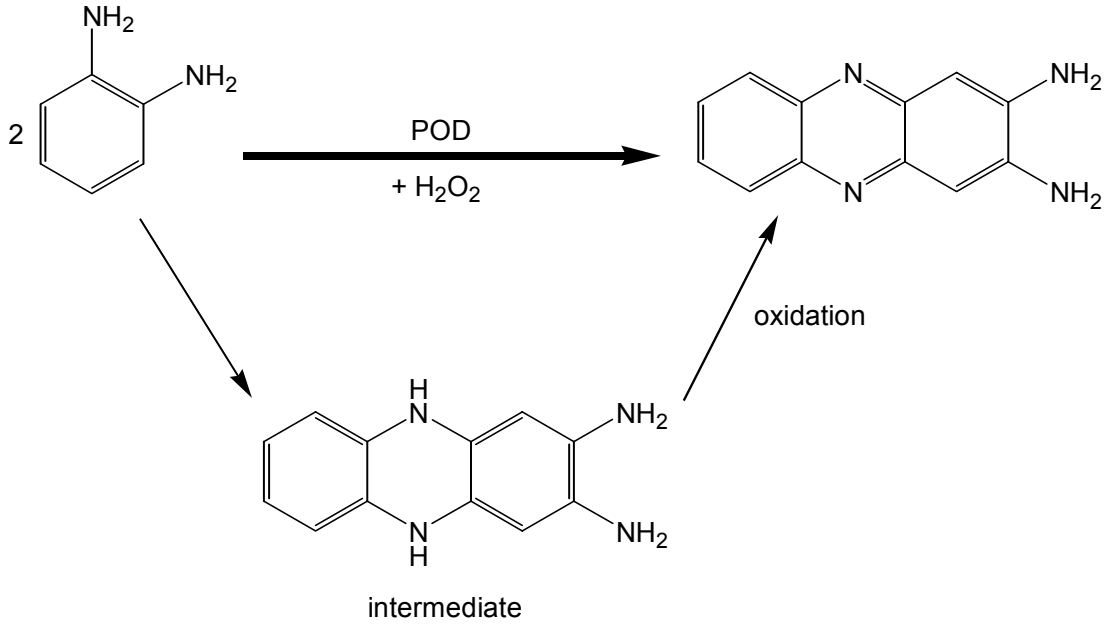

Figure 5.5: *Formation of the main reaction product in the POD-catalyzed oxidation of OPD by hydrogen peroxide.*

In literature, different reaction times are used for the oxidation of OPD in ELISA schemes. Therefore, it is in principle possible that different products are observed depending on the reaction time applied. This effect has therefore been thoroughly studied. Figure 5.4 gives an overview of the product development against the reaction time. Additionally to the mass traces shown in Figure 5.3, the very small signals of m/z = 333 and m/z = 420 are plotted as well. In the chromatogram, the peak with m/z = 333 is observed after approximately 6 min, whereas the product with m/z = 420 is detected after ca. 9 min. As can be seen in Figure 5.4, these signals have a relatively

low intensity, especially in comparison to the main product (with m/z = 211). For high POD concentrations (50 u L^{-1}) and relatively long reaction times (5 - 10 h, thus much longer than used in ELISAs), a second peak for both m/z = 333 and m/z = 420 is observed with even lower intensity. However, due to the fact that the intensity of all peaks with m/z = 333 or m/z = 420 is dependent on the POD concentration and that these masses are only observed after relatively long reaction times (30 min and longer), these products are not relevant for discussions about the reaction product observed in ELISAs.

5.5 Conclusions

By means of LC/APCI-MS investigations, 2,3-diaminophenazine could be unambiguously identified as the main product of the POD-catalyzed oxidation of OPD by hydrogen peroxide. This result was confirmed by exact mass measurements using ESI-TOF-MS. The formation of significant concentrations of the second literature-discussed product, 2,2´-diaminoazobenzene, could be excluded. Two more low abundance products have been identified as an intermediate in the formation of the main product and as an oxygen-containing species. The data provide sufficient evidence on the main reaction product to terminate the contradictory discussion in literature.

5.6 References

[1] K. Zhang, R. Cai, D. Chen, L. Mao, Anal. Chim. Acta 413 (2000) 109-113.

[2] Product information o-phenylenediamine dihydrochloride, Sigma Aldrich.

[3] J. H. Bovaird, T. T. Ngo, H. M. Lenhoff, Clin. Chem. 28 (1982) 2423-2426.

[4] G. Wolters, L. Kuijpers, J. Kacaki, A. Schuurs, J. Clin. Path. 29 (1976) 873-879.

[5] P. J. Elving, A. F. Krivis, Anal. Chem. 30 (1958) 1648-1652.

[6] S. Wawzonek, T. W. McIntyre, J. Electrochem. Soc. 114 (1967) 1025-1029.

[7] S. Berchmans, R. J. Vijayavalli, Electrochem. Soc. India 44 (1995) 162-166.

[8] P. Griess, J. Prakt. Chem. 3 (1871) 143-144.

[9] E. Knoevenagel, J. Prakt. Chem. 89 (1914) 25-75.

[10] P. J. Tarcha, V. P. Chu, D. Whittern, Anal. Biochem. 165 (1987) 230 233.

[11] S. Y. Niu, S. S. Zhang, L. B. Ma, K. Jiao, Bull. Korean Chem. Soc. 25 (2004) 829-832.

[12] Y. Omote, Y. Nakada, R. Kobayashi, N. Sugiyama, Chem. Ind. 35 (1971) 996.

[13] H. Gallati, H. Brodbeck, J. Clin. Chem. Clin. Biochem. 20 (1982) 221-225.

[14] J. F. Song, X. F. Kang, W. Guo, Fresenius J. Anal. Chem. 357 (1997) 127-129.

[15] J. Huangxian, G. Yan, F. Chen, H. Chen, Electroanalysis 11 (1999) 124-128.

[16] F. Azek, C. Grossiord, M. Joannes, B. Limoges, P. Brossier, Anal. Biochem. 284 (2000) 107-113.

[17] D. J. Li, X. W. Li, Y. X. Xie, X. Q. Cai, G. L. Zou, Biochem. (Moscow) 70 (2005) 92-99.

Chapter 6

Analysis of Microperoxidases Using Liquid Chromatography, Post-Column Substrate Conversion and Fluorescence Detection [*]

[*] R. Haselberg, C. Hempen, S. M. Van Leeuwen, M. Vogel, U. Karst, *J. Chromatogr. B*, submitted for publication

6.1 Abstract

A liquid chromatographic method with on-line activity determination for microperoxidases has been developed. After enzymatic digestion of a cytochrome, which is supposed to occur under formation of microperoxidases, the product mixture is separated by reversed-phase liquid chromatography. The products first pass a diode array detector, and are then subject to a reaction with 4-(N-methylhydrazino)-7-nitro-2,1,3-benzooxadiazole (MNBDH) and hydrogen peroxide. In a reaction coil, microperoxidases catalyze the reaction under formation of the fluorescent 4-(N-methylamino)-7-nitro-2,1,3-benzooxadiazole (MNBDA). Quantification of the microperoxidases is performed using a fluorescence detector at an excitation wavelength of 470 nm and an emission wavelength of 545 nm, respectively. For this LC-based system, limits of detection are $3 \cdot 10^{-8}$ mol L^{-1}, limits of quantification are $9 \cdot 10^{-8}$ mol L^{-1}, and a linear range from $9 \cdot 10^{-8}$ mol L^{-1} to $3 \cdot 10^{-6}$ mol L^{-1} is obtained for the microperoxidases MP-9 and MP-11. A highly active microperoxidase MP-6 was found in the reaction of cytochrome c from bovine heart with protease from *streptomyces griseus*.

6.1 Introduction

Horseradish peroxidase (POD) is one of the most widely used enzymes in analytical chemistry [1,2]. POD catalyzes the oxidation of an organic substrate by hydrogen peroxide. The POD-catalyzed reaction can be detected in

different ways. Frequently, organic substrates are oxidized under formation of colored or fluorescent products, thus enabling the use of optical detection techniques. The large number of POD applications includes the use as a marker enzyme in immunoassays [3,4] and as a catalyst in various biosensors [5,6] (shown in Chapter 2). Another relevant field is environmental analysis of hydrogen peroxide and primary hydroperoxides [7,8]. The most important drawbacks of POD for analytical applications are its limited compatibility with organic solvents and its high molecular mass.

Microperoxidases have been known since decades as products of the digestion of cytochrome c with proteolytic enzymes [9-11]. Microperoxidases contain the heme group of the cytochrome c plus a peptide chain with at least five amino acids. Their name results from their catalytic properties, which are similar to those of POD. They are named according to the number of amino acids, which are still attached to the heme group. For example, MP-8 is a microperoxidase with an octapeptide chain. The molecular masses of the most commonly used microperoxidases, MP-8, MP-9 and MP-11, are in the range between 1500 and 2000 Da. Due to their lower molecular masses, they can be coupled to other biomolecules (e.g., for immunochemical applications) in a more defined way than the large enzyme POD with its multiple functional groups. Furthermore, compatibility with organic solvents is improved compared with POD [12].

However, surprisingly few analytical applications of microperoxidase have been described up to now. These comprise various biosensors [13-15],

chemiluminescence detection schemes with [16-20] and without [21,22] initial liquid chromatographic or capillary electrophoretic separation. The chemiluminescence assay takes advantage of the catalytic effect of microperoxidases on the oxidation of luminol or related compounds under generation of an intense emission signal. For the determination of fatty acid hydroperoxides, Schmitz et al. [23] used laser-induced fluorescence detection after oxidation of p-hydroxyphenylacetic acid to a fluorescent dimer in the presence of microperoxidase 11 as a catalyst. Recently, our group described 4-(N-methylhydrazino)-7-nitro-2,1,3-benzooxadiazole (MNBDH) as a new substrate for MP-11 [24]. Its oxidation to the fluorescent 4-(N-methylamino)-7-nitro-2,1,3-benzooxadiazole (MNBDA) by hydrogen peroxide in the presence of MP-11 was used as one part of a dual substrate enzyme assay.

These examples show that attractive analytical applications of microperoxidases are already available. On the other hand, their further use is hampered by their high price, their limited availability and the lack of a method to rapidly test the activity of newly synthesized microperoxidases. Therefore, a chromatographic system should be developed, being able to provide on-line information of the character and the activity of a microperoxidase or a mixture of different microperoxidases, which are formed in a proteolytic digest. The development of such a system is described within this chapter.

6.2 Experimental

Chemicals

All chemicals were purchased from Aldrich (Steinheim, Germany), Merck (Darmstadt, Germany) and Fluka (Neu-Ulm, Germany) in the highest purity available. Acetonitrile and water for HPLC were from Biosolve (Valkenswaard, The Netherlands), gradient grade. For LC/MS measurements, acetonitrile and water were LC-MS grade (Biosolve, Valkenswaard, The Netherlands). Microperoxidases MP-11 and MP-9 (both from equine heart cytochrome c), trypsin and protease type XIV from *streptomyces griseus* (Pronase E) as well as cytochrome c from bovine heart were purchased from Sigma (Deisenhofen, Germany). The synthesis of MNBDH was performed as described in literature [25].

Instrumentation

The optimization of the experimental parameters was performed using a microplate reader from BMG LabTechnologies (Offenburg, Germany) with FLUOstar software version 2.10-0 and FLUOstar Galaxy software version 4.30-0. For the measurements, the following filters were used: 470 nm (bandwidth $\pm$ 15 nm) for excitation and 545 nm (bandwidth $\pm$ 10 nm) for emission. Corning (Costar No. 3915, black) 96-wells micro-titration plates used for these measurements were purchased from Diagonal (Münster, Germany).

Liquid chromatographic separation and detection were performed with the following system (all components from Shimadzu, Duisburg, Germany): two LC-10AS pumps, degasser GT-154, SPD-M10Avp diode array detector, RF-10AXL fluorescence detector, SIL-10A autosampler, software Class LC-10 version 1.6, and CBM-10A controller unit. The injection volume was 10 µL. A Prontosil 120-5-phenyl column (Bischoff Chromatography, Leonberg, Germany) was used; particle size 5 µm, pore size 120 Å; column dimensions 250 mm x 3 mm.

For HPLC separation, the following binary gradient consisting of buffer A (NH_4Ac/HAc, both 10 mmol L^{-1}, pH 7) and 5% A in acetonitrile (B) with a flow rate of 0.3 mL min^{-1} was used:

time (min)	0.03	12.5	25	26	28
c_B (%)	10	30	30	10	10

The post-column derivatization set-up is shown in Figure 6.1. After separation and UV/vis-detection, the analytes were mixed with the substrate solution consisting of MNBDH ($5 \cdot 10^{-4}$ mol L^{-1} in acetonitrile) and H_2O_2 (0.167 mol L^{-1} in water), which were delivered by a Sp230iw syringe pump (World Precision Instruments, Berlin, Germany) equipped with two gas tight 1 mL SGE syringes (Supelco, Bellefonte, PA, U.S.A.). The reagents were added with a flow rate of 0.5 µL min^{-1}. The subsequent reaction loop was a 25-m knitted Teflon tubing coil with an inner diameter of 0.3 mm. The reaction products were detected with the fluorescence detector at an excitation wavelength of 470 nm and an emission wavelength of 545 nm, respectively.

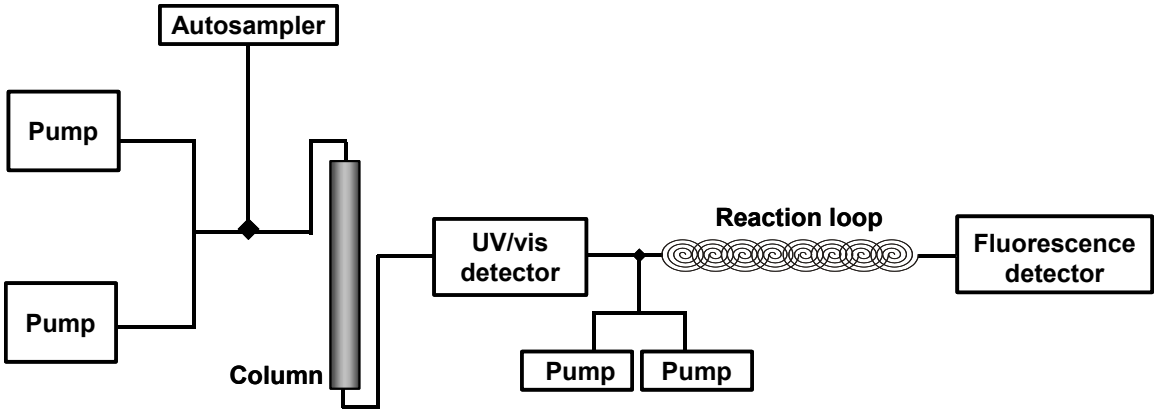

Figure 6.1: *Set-up for the separation and post-column derivatization of microperoxidases.*

For LC-MS investigations, an Agilent Technologies (Waldbronn, Germany) HP1100 liquid chromatograph for binary gradient elution (pump model G1312A), including an autosampler (G1313A) and a DAD (G1315B), coupled to an esquire 3000*plus* ion trap mass spectrometer from Bruker Daltonics (Bremen, Germany) was used. The LC separation of the analytes was carried out under the same conditions as described above.

All MS measurements were performed by means of electrospray ionization in the positive ion mode. Mass spectra were recorded in the full scan mode, scanning from m/z = 500 to m/z = 3,000. The ion count cumulative target for the ion trap mass analyzer was 100,000, with a maximum accumulation time of 200 ms. The electrospray voltage was 3750 V. Other ion source parameters were 145 V on the transfer capillary exit, 40 V at the skimmer, 40 psi nebulizer gas and 10.0 L/min of drying gas with a temperature of 365 ^{o}C. In case of MS/MS experiments, auto-fragmentation was performed with

one precursor selection (excluding the mass range m/z = 500 to m/z = 685) and a fragmentation amplitude of 1.20 V.

The detected masses of the different microperoxidases were confirmed by means of comparison with the information on the expasy peptide database [26].

pH Optimization

In order to find the best suitable pH for the post-column reaction, the conversion of MNBDH by means of MP-11 and H_2O_2 was performed on microtitration plates in 0.5 pH steps in the pH range from 2 to 7.5. For every pH, 100 µL of a blank and of five MP-11 concentrations ($1 \cdot 10^{-7}$ mol L^{-1} to $1 \cdot 10^{-9}$ mol L^{-1}) were pipetted in fourfold onto a microtitration plate. Subsequently, 50 µL of a H_2O_2 ($1.67 \cdot 10^{-3}$ mol L^{-1})/MNBDH ($5 \cdot 10^{-4}$ mol L^{-1}) mixture (ratio 8.3:1) were added to each well. After incubation at room temperature, fluorescence was measured at excitation and emission wavelengths of 470 nm and 545 nm, respectively.

Opimization of acetonitrile content

The influence of the acetonitrile content on the MP-11 reaction was investigated by performing the conversion of MNBDH by means of MP-11 and H_2O_2 on microtitration plates. In this case, the reaction was executed at pH 7, and the acetonitrile amount was varied. For each acetonitrile concentration

(2, 10, 20, 30, 40 and 50%), the reaction was carried out as described above, and the microtitration plate was read out in the same way.

Digestion

For the digestion, each of the four above-mentioned cytochromes was dissolved to a $2 \cdot 10^{-4}$ mol L^{-1} solution in a NH_4HCO_3 buffer (15 mmol L^{-1}, pH 8). For the trypsin solution, 0.145 mg were dissolved in 1 mL of the same buffer and diluted by a factor of 100 just prior to use ($4 \cdot 10^{-8}$ mol L^{-1}). Equal amounts of protein solution and enzyme solution were added to each other, and this mixture was placed in a stove for an overnight digestion at 37 ^{o}C. The digestion with the unspecific protease was performed in the same way, but with the difference that 2 mg of the enzyme were dissolved in 10 mL of bis-tris-propane buffer (10 mmol L^{-1}, pH 7). The digests were analyzed both by means of the HPLC post-column method described above and by LC-MS, respectively.

6.4 Results and Discussion

Initial work regarding the substrate MNBDH resulted in the finding that, despite the attractive spectroscopic properties of the substance, its applicability for the detection of enzymatic conversions is limited [24]. The reason is its slow conversion by horseradish peroxidase (POD), which allows the use of MNBDH as a substrate only in those cases when POD is present in excess concentrations. Therefore, the determination of hydrogen peroxide,

glucose or glucose oxidase leads to favorable analytical figures of merit [27], while the attempt to detect POD itself does not. More recently, it was found that MNBDH may rapidly be converted by microperoxidases [24]. The respective reaction is presented in Figure 6.2.

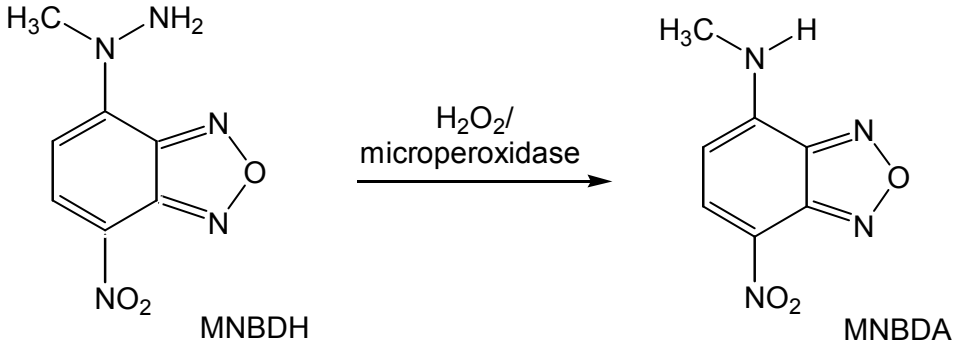

Figure 6.2: *Conversion of the non-fluorescent MNBDH to the strongly fluorescent MNBDA under microperoxidase catalysis.*

In combination with liquid chromatographic separation and post-column conversion, this reaction should thus allow the detection of different microperoxidases within a single chromatographic run. Aim of this work was the development of a respective system and its application to the detection of microperoxidases in cytochrome c digests.

Optimization of the reaction of microperoxidase with MNBDH/H_2O_2

The MNBDH/H_2O_2 system was optimized with respect to all those parameters being significant for the development of an enzyme-catalyzed post-column reaction. Regarding the optimization, MP-11 was selected as a model microperoxidase, and all reactions were carried out using microtitration plates

and a microplate fluorescence reader. The optimization of the pH is presented in Figure 6.3. It is obvious that the highest signals are obtained between pH 6 and 7. Thus, the buffer system NH_4Ac/HAc (both 10 mmol L^{-1}, pH 7) was chosen as the mobile phase in LC. The reaction time has only a minor influence: Already at a reaction time of 30 seconds, a strong signal is observed, and the increase of signal intensity with time (up to 6 minutes) is small.

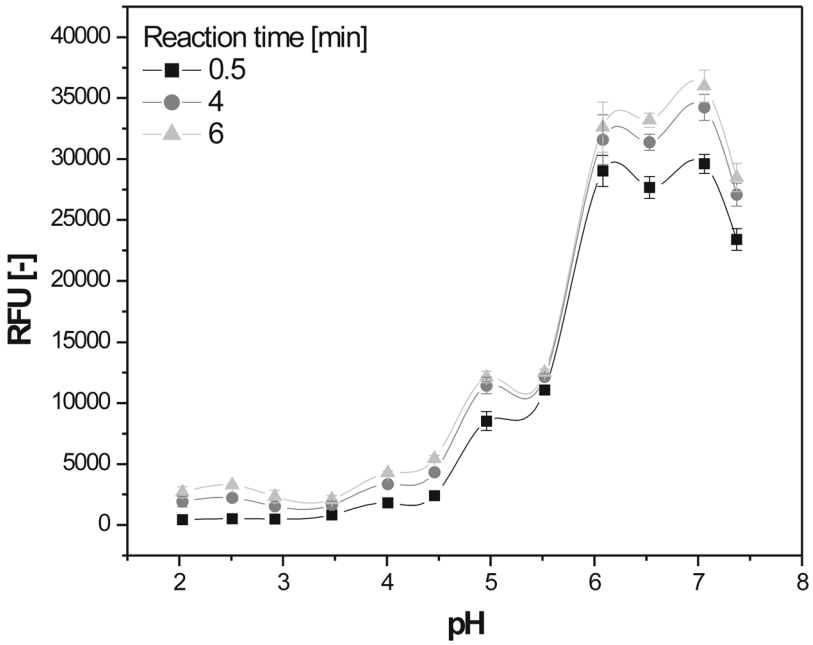

Figure 6.3: *Dependency of the MP-11-catalyzed oxidation of MNBDH by hydrogen peroxide on the pH at different reaction times (c_{MP-11} = 10 nmol L^{-1}).*

For the LC separations, reversed-phase systems are most favorable with respect to ease of use. However, most enzymatic reactions experience strong adverse effects in the presence of increasing organic solvent concentration. Therefore, representative for the entire group of microperoxidases, the MP-11 reaction was investigated in the presence of acetonitrile, as shown in Figure

6.4. Obviously, the signal intensity decreases with increasing acetonitrile concentration. However, the signal intensity at 10% acetonitrile is higher than the intensity in the absence of acetonitrile. A possible reason for this phenomenon is the known dependency of the fluorescence intensity of benzooxadiazole derivatives on the solvent composition. Typically, mixed aqueous-organic solutions or even purely organic solvents are more advantageous than water [28]. It is therefore assumed that the optimum at 10% acetonitrile is the best compromise between enzymatic conversion and spectroscopic properties. In practice, the acetonitrile content should not be higher than 30% to still obtain a reasonable signal.

These findings were subsequently used to develop a suitable LC method for the separation of microperoxidases MP-11 and MP-9. The phenyl-modified RP column in combination with the NH_4Ac/HAc buffer (A) and the 5% buffer in acetonitrile (B) mixture turned out to be appropriate for the separation. Applying the gradient mentioned above, which did not reach more than 30% of organic solvent, a baseline separation of the two microperoxidases within 22 minutes could be achieved. All applied conditions were in good accordance with a favorable post-column reaction.

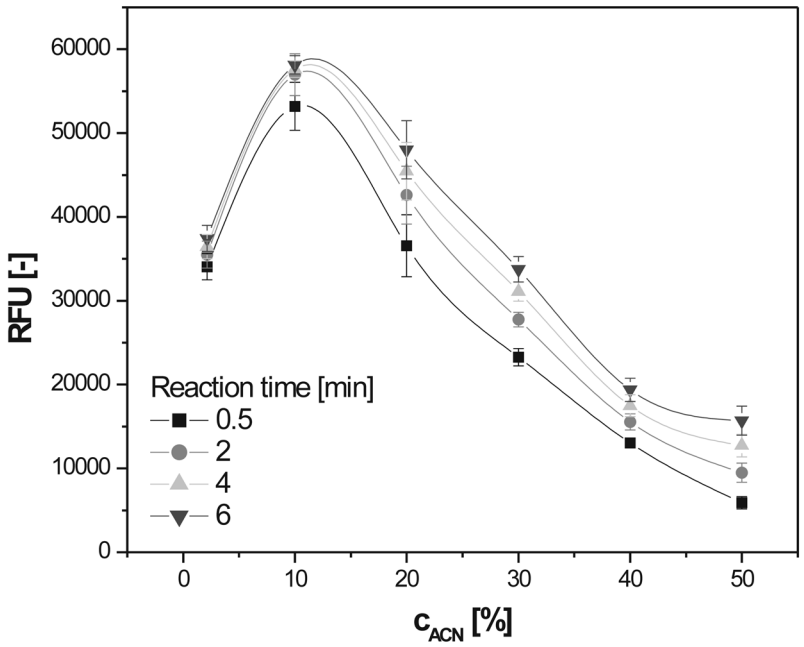

Figure 6.4: *Dependency of the MP-11-catalyzed oxidation of MNBDH by hydrogen peroxide on the concentration of acetonitrile (ACN) at different reaction times (c_{MP-11} = 10 nmol L^{-1}).*

HPLC separation and post-column derivatization of microperoxidase standards

The set-up of the separation and post-column detection system is presented in Figure 6.1. A binary gradient was used with a high-pressure gradient system. An UV/vis detector was used to monitor the column effluent prior to addition of the reagents. For stability reasons, the solutions of MNBDH and hydrogen peroxide were stored in separate syringes and delivered with one pump. The two solutions were mixed in a mixing tee prior to the addition to the LC eluent. A reaction loop of poly(tetrafluoroethylene) with a length of 25 m (inner diameter: 0.3 mm) was used to achieve a high turnover of the

microperoxidase-catalyzed reaction. Finally, a fluorescence detector was used to monitor the concentration of the formed MNBDA. This set-up, using a flow rate of 0.3 mL min^{-1}, caused a delay of 1 minute between the UV/vis and fluorescence detector traces, which is sufficient for the performance of the MP reaction. This was shown in Chapter 4 when investigating the kinetic properties of the MP reaction. Standards of MP-11 and MP-9 (each of 3 µmol L^{-1}) were analyzed using the post-column system. As presented in Figure 6.5, a good chromatographic resolution between the two microperoxidases was obtained.

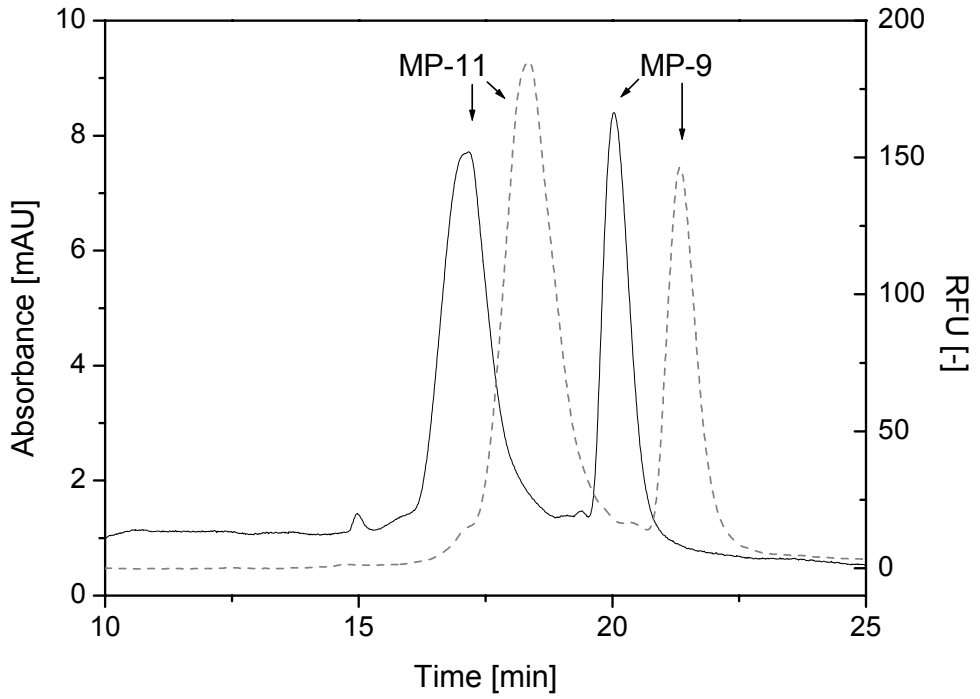

Figure 6.5: *Separation of MP-11 and MP-9 standards (3 µmol L^{-1} each) with UV/vis (solid line) and fluorescence (dashed line) detection*.

In respect of the LC-based detection system, limits of detection were $3 \cdot 10^{-8}$ mol L^{-1}, limits of quantification were $9 \cdot 10^{-8}$ mol L^{-1}, and the linear range was from $9 \cdot 10^{-8}$ mol L^{-1} to $3 \cdot 10^{-6}$ mol L^{-1} for both microperoxidases. The RSD for multiple determination at the concentration of $3 \cdot 10^{-7}$ mol L^{-1} was 3.6% for MP-9 and 7.3% for MP-11 (n = 3). The figure shows that fluorescence detection is superior to UV/vis detection owing to more stable baselines and higher signal intensities. This is due to the inherently better limits of detection of fluorescence versus UV/vis detection as well as due to the selectivity of the post-column detection system, combining both the advantages of the selective LC separation and the selective enzymatic reaction, respectively. The limits of detection are inferior for the LC-based system compared with the microtitration plate system because of shorter reaction times, the presence of organic solvents, lower amounts of the analyte in the detection system and the dilution of the analytes during separation. However, the limits of detection are still better than required for the identification and quantification of microperoxidases from cytochrome c digests, as demonstrated in the following.

Tryptic digestion of cytochrome c from bovine heart and analysis of products

Digests of cytochrome c were carried out using various proteolytic enzymes. The detailed procedures are described in the Experimental Section. For the digest of cytochrome c from bovine heart with trypsin, only MP-9 was detected (Figure 6.6). This was also predicted due to the very specific cleavage

properties of trypsin. The identity of MP-9 was confirmed by electrospray ionization mass spectrometry.

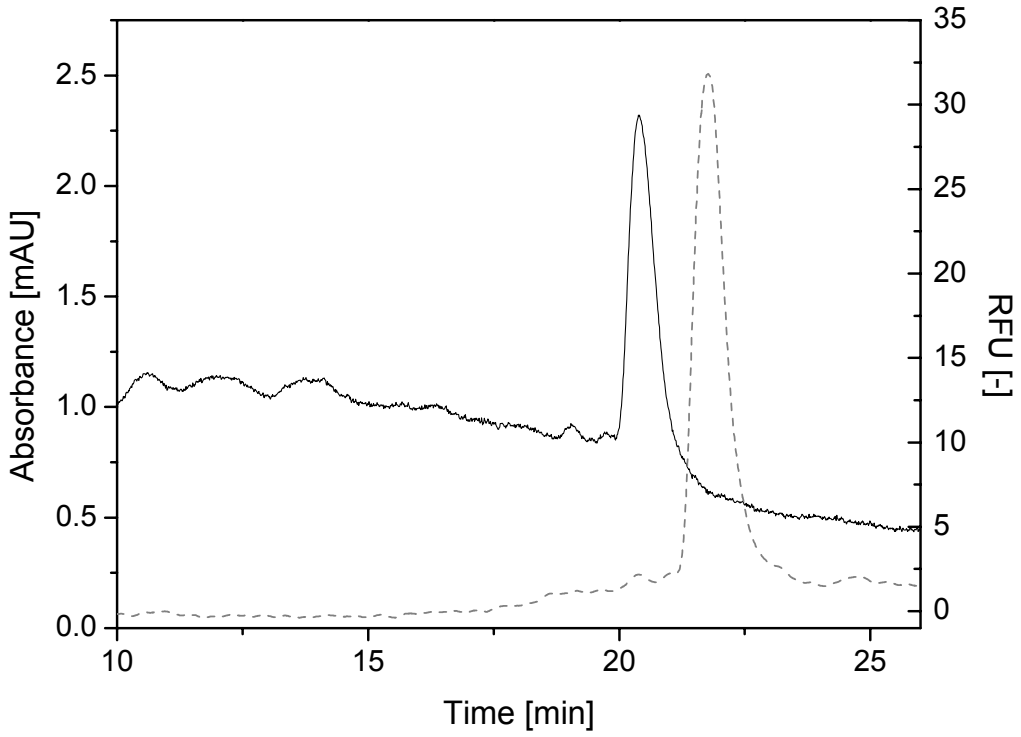

Figure 6.6: *Chromatogram of a digest of cytochrome c from bovine heart (1 µmol L^{-1}) with trypsin. Only MP-9 is detected by means of UV/vis (solid) and fluorescence (dashed) spectroscopy.*

In Figure 6.7, the ESI mass spectra of the respective digest (1) and of commercially available MP-9 (2) are compared. In both spectra, the peak of m/z = 1635.1 is the $[M+H]^+$ of MP-9, which has only a very low abundance (see insert). The $[M+2H]^{2+}$ peak is the base peak in these mass spectra and has an m/z of 817.6, whereas the $[M+H+Na]^{2+}$ peak of m/z = 828.6 has a lower intensity again. Although the comparison of both spectra shows a higher

signal-to-noise ratio for (1), which is due to a higher MP-9 concentration, it is also visible that the noise itself is very similar for both samples.

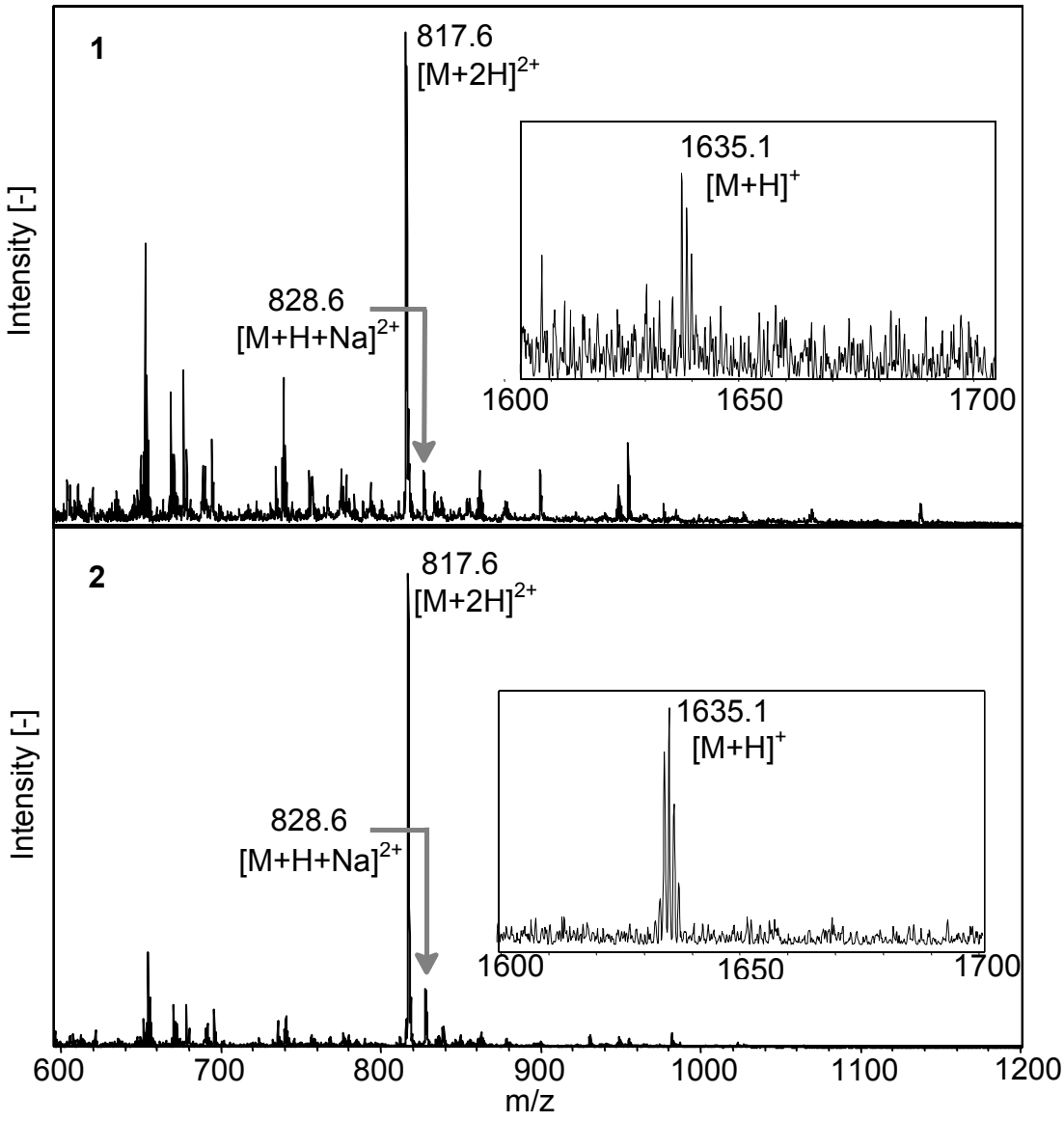

Figure 6.7: *1) ESI-MS spectrum of a digest of cytochrome c from bovine heart (1 µmol L^{-1}) with trypsin. 2) ESI-MS spectrum of commercially available MP-9 (1 µmol L^{-1}). The peak at m/z = 1635.1 is caused by MP-9 (both spectra), thus confirming the data of the LC method (compare with Figure 6.6).*

Digestion of cytochrome c from bovine heart with a protease from *streptomyces griseus* and analysis of products

The digest of cytochrome c from bovine heart with a protease from *streptomyces griseus* was investigated as well. In Figure 6.8, the chromatogram of the digest with UV/vis (solid) and fluorescence (dashed) detection is presented.

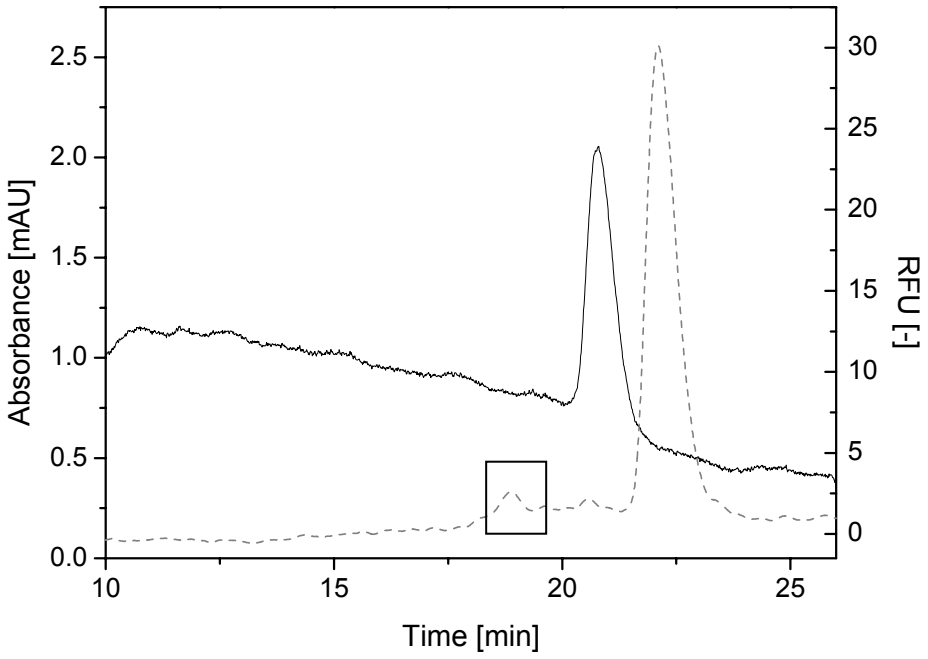

Figure 6.8: *Chromatogram of a digest of cytochrome c from bovine heart (1 µmol* L^{-1}*) with protease. Only one large peak is detected with UV/vis (solid) and fluorescence (dashed) detection at a retention time similar to, but still different from MP-9. Another small peak is detected (marked with a frame) only in the fluorescence trace.*

An intense signal is obtained with both detectors. This has a similar, but not the same retention time as MP-9. It is therefore assumed that the unknown

peak represents another type of microperoxidase. A smaller peak (framed in Figure 6.8) was observed only in the fluorescence trace at the retention time of MP-11, thus indicating that the conversion rate to the unknown microperoxidase is slightly lower than 100%.

Identification of the unknown peak was performed by means of electrospray MS again, as presented in Figure 6.9. With similar abundance, the $[M+H]^+$ (m/z = 1277.8) and the $[M+2H]^{2+}$ (m/z = 639.6) confirm that the unknown substance is a microperoxidase MP-6. In Figure 6.10, the structure of MP-6 is presented in comparison to the microperoxidases MP-9 and MP-11, which were used in this study.

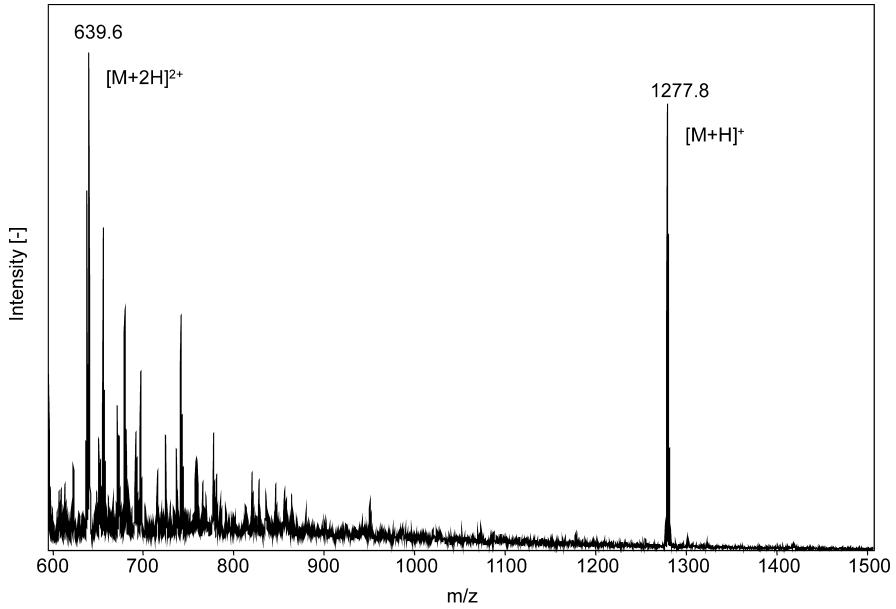

Figure 6.9: *ESI-MS spectrum of a digest of cytochrome c from bovine heart (1 µmol* L^{-1}*) with protease. The peak at m/z = 1277.8 is related to MP-6.*

Although MP-6 is known from the biochemical literature [2], there is no analytical use up to now. Owing to its high activity and its even lower molecular mass in comparison with MP-9 and MP-11, MP-6 could be an excellent candidate for analytical applications.

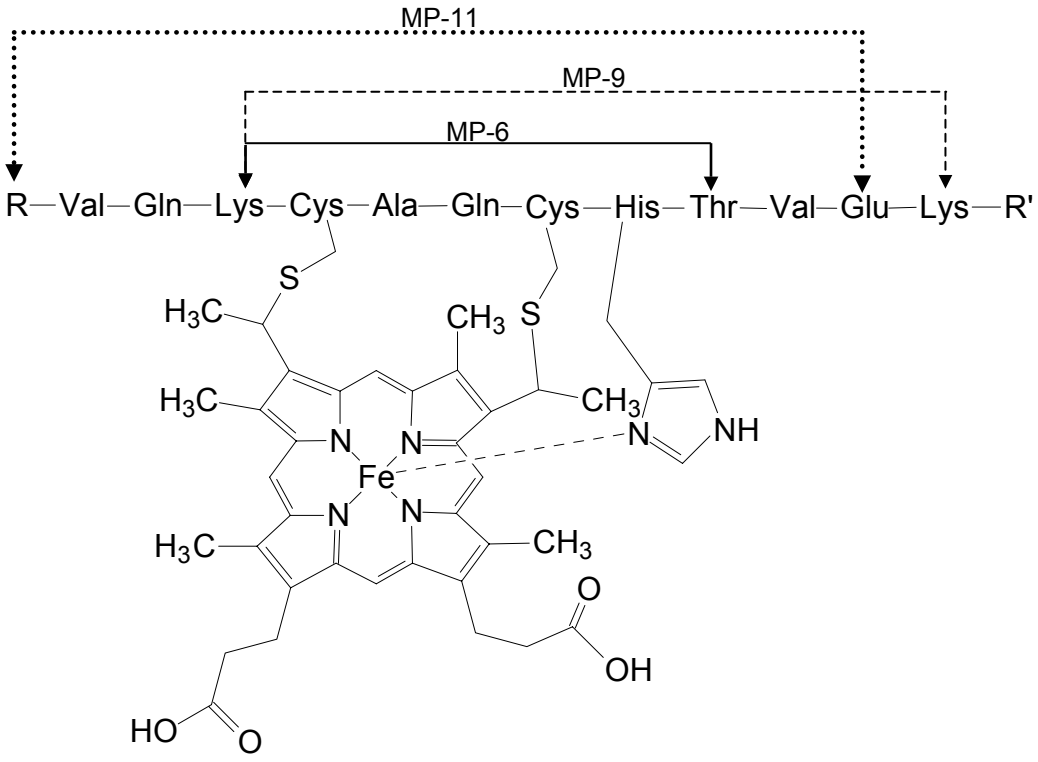

Figure 6.10: *Part of the primary structure of cytochrome c from bovine heart. Dotted lines indicate the cleavage sites to obtain MP-11, dashed lines those for MP-9 and the solid lines those for MP-6.*

In future work, larger amounts of MP-6 shall be isolated, and it shall be investigated if MP-6 exhibits the high activity not only in case of the MNBDH/MNBDA substrate system, but also with other substrates, e.g.,

o-phenylenediamine. Due to its lower molecular mass, it could become an attractive analytical tool in solution as well as immobilized on solid supports.

6.5 Conclusions

A new HPLC/post-column reaction/fluorescence detection system has been developed and applied to the determination of microperoxidases in proteolytic digests of cytochrome c from bovine heart. This set-up is well suited for the activity measurement of microperoxidases. Whereas the digestion of cytochrome c with trypsin yielded the expected MP-9, which was detected by means of fluorescence and confirmed by ESI-MS measurements, the digestion with the unspecific protease from *streptomyces griseus* resulted in a microperoxidase, which was characterized as MP-6, a literature-known but not yet analytically used microperoxidase. Due to high catalytic activity, investigations regarding possible analytical application of MP-6 are planned for future work.

6.6 References

[1] B. C. Saunders, A. G. Holmes-Siedle, B. P. Stark, Peroxidase (1964) Butterworths, London.

[2] J. Everse, K. E. Everse, M. B. Grisham, Peroxidases in Chemistry and Biology Vol. 2 (1991) CRC Press, Boca Raton.

[3] D. S. Hage, Anal. Chem. 65 (1993) 420R-424R.

[4] J. M. van Emon, V. Lopez-Avila, Anal. Chem. 64 (1992) 79A-88A.

[5] E. P. Medyantseva, E. V. Khaldeeva, G. K. J. Budnikov, J. Anal. Chem. 56 (2001) 886-900.

[6] M. P. Marco, D. Barcelo, Meas. Sci. Technol. 7 (1996) 1547-1562.

[7] S. Gäb, W. V. Turner, S. Wolff, Atmos. Environment 29 (1995) 2401-2407.

[8] G. K. Moortgat, D. Grossmann, A. Boddenberg, G. Dallmann, A. P. Ligon, W. V. Turner, S. Gäb, F. Slemr, W. Wieprecht, K. Acker, M. Kibler, S. Schlomski, K. Bächmann, J. Atmosph. Chem. 42 (2002) 443-463.

[9] C. L. Tsou, Biochem. J. 49 (1951) 362-367.

[10] P. A. Adams, M. P. Byfield, R. D. Goold, A. E. Thumser, J. Inorg. Biochem. 37 (1989) 55-59.

[11] W. J. Chuang, Y. D. Chang, W. Y. Jeng, J. Inorg. Biochem. 75 (1999) 93-97.

[12] H. Wariishi, M. Kabuto, J. Mikuni, M. Oyadomari, H. Tanaka, Biotechnol. Prog. 18 (2002) 36-42.

[13] E. Katz, V. Heleg-Shabtai, A. Bardea, I. Willner, H. K. Rau, W. Haehnel, Biosens. Bioelectron. 13 (1998) 741-756.

[14] S. Yakubi, F. Mizutani, Y. Hirata, Electrochemistry 68 (2000) 853-855.

[15] W. M. Huang, J. B. Jia, Z. L. Zhang, X. J. Han, J. L. Tang, J. G. Wang, S. J. Dong, E. K. Wang, Biosens. Bioelectron. 18 (2003) 1225-1230.

[16] A. Dapkevicius, T. A. van Beek, H. A. G. Niederländer, A. de Groot, Anal. Chem. 71 (1999) 736-740.

[17] H. A. G. Niederländer, C. Gooijer, N. H. Velthorst, Anal. Chim. Acta 285 (1994) 143-159.

[18] J. Ishida, H. Arakawa, M. Takada, M. Yamaguchi, Analyst 120 (1995) 1083-1086.

[19] S. D. Mangru, D. J. Harrison, Electrophoresis 19 (1998) 2301-2307.

[20] J. Y. Zhao, J. Labbe, N. J. Dovichi, J. Microcolumn Separations 5 (1993) 331-339.

[21] L. J. van Look, C. H. van Peteghem, Anal. Chim. Acta 248 (1991) 207-211.

[22] H. C. Yeh, W. Y. Lin, Anal. Bioanal. Chem. 372 (2002) 525-531.

[23] O. Schmitz, D. Melchior, W. Schuhmann, S. Gäb, J. Chromatogr. A 814 (1998) 261-265.

[24] C. Hempen, U. Karst, Anal. Chim. Acta 521 (2004) 117-122.

[25] A. Büldt, U. Karst, Anal. Chem. 71 (1999) 1893-1898.

[26] http://www.expasy.org/tools/peptide-mass.html

[27] J. Meyer, A. Büldt, M. Vogel, U. Karst, Angew. Chem. Int. Ed. 39 (2000) 1453-1455.

[28] S. Uchiyama, T. Santa, K. Imai, Anal. Chem. 73 (2001) 2165-2170.

Chapter 7

Immunoassay and Liquid Chromatography/Mass Spectrometry Methods for the Determination of Telmisartan in Human Blood Plasma*

* C. Hempen, L. Gläsle-Schwarz, U. Kunz, U. Karst, *Anal. Chem.*, submitted for publication

7.1 Abstract

Telmisartan is an angiotensin II receptor antagonist and a known drug against high blood pressure. In this chapter, two new and rapid analytical techniques, a liquid chromatography/atmospheric pressure chemical ionization-tandem mass spectrometry (LC/APCI-MS/MS) method and an enzyme-linked immunosorbent assay (ELISA) for the determination of telmisartan in human blood plasma are introduced, compared and applied. These independent analytical methods turned out to yield comparable results for the analysis of the pharmacokinetic profile of the analyte in human blood plasma. For LC/MS/MS the limit of detection was 0.3 ng mL^{-1}, the limit of quantification was 0.9 ng mL^{-1} and the linear range extended from 0.9 - 1000 ng mL^{-1}. For the ELISA, the limit of detection was 0.1 ng mL^{-1}, limit of quantification was 0.3 ng mL^{-1} and the range extended from 0.3 - 300 ng mL^{-1}. 48 samples from 4 volunteers were analyzed to obtain pharmacokinetic profiles of telmisartan in plasma samples.

7.2 Introduction

High blood pressure (hypertension) is a widespread disease and an important risk factor for vascular disease, renal and cardiac insufficiency [1]. The drug telmisartan, 4-[(2-n-propyl-4-methyl-6-(1-methylbenzimidazol-2-yl)-benz-imidazole-1-yl)methyl]-biphenyl-2-carboxylic acid (Figure 7.1), is an angiotensin II receptor antagonist, which is highly selective for angiotensin II

(AT_1) receptors. Angiotensin II is generated from angiotensin I and affects the blood pressure [2, 3] owing to different mechanisms: Increasing the activity of the sympathetic nervous system, by causing a boosted sodium revertive resorption in the kidneys and by promotion of the secretion of aldosterone in the adrenal glands. Telmisartan is a benzimidazole derivative, which selectively inhibits the receptor of angiotensin II. Therefore, the effect of angiotensin II is blocked resulting in a steady vascular dilatation and abated blood pressure [4].

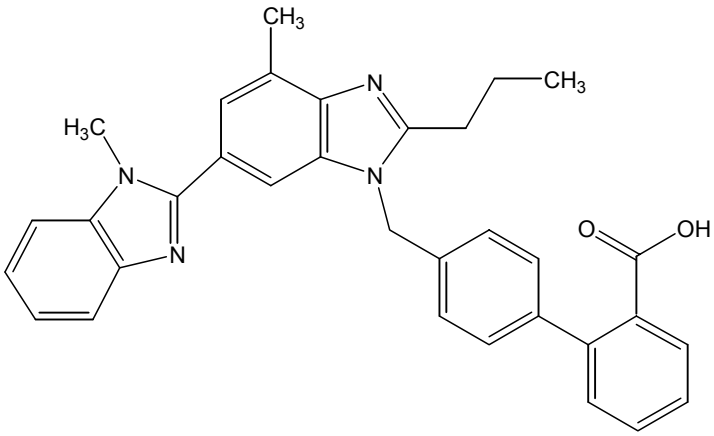

Figure 7.1: *Chemical structure of telmisartan.*

The need for drugs abating high blood pressure is evident and is still increasing due to the increasing number of humans in the western society who fulfil the risk factors for hypertension (e.g., stress, wrong food, overweight, alcohol). Regarding this, the pharmacokinetic investigation of telmisartan in human blood plasma or in urine is important.

However, already many publications discuss the pharmacokinetic behavior and the properties of telmisartan [5, 6]. Due to its high lipophilicity and a high volume distribution, telmisartan shows a good tissue penetration. It is highly bound to plasma proteins (99.5%) [6]. A long half-life results in a recommendation of usually 40 mg once per day. Telmisartan is subject to a very limited phase-I-metabolism so that the potential of interaction of this pharmaceutical is also low with respect to other drugs (e.g., paracetamol). Ebner et al., among others, investigated the chemical stability of telmisartan in the human body [7]. It undergoes only minimal biotransformation in the liver to form its major inactive metabolite, telmisartan 1-O-acrylglucuronide. Besides the studies on the decompositon of telmisartan in the human body, on the dose as well as on the combination of telmisartan with other drugs [6], not many investigations on this drug applying analytical methods as chromatography, mass spectrometry, photometric/fluorescence spectroscopic detection schemes or immunoassays have been published yet.

In 2002, Gonzalez et al. [8] screened several angiotensin II receptor antagonists, amongst them telmisartan, by means of capillary zone electrophoresis (CZE) with UV/vis detection. They were able to separate seven angiotensin II receptor antagonists within 8 minutes. Comparative HPLC measurements took 25 minutes to obtain the same resolution. In the same year, similar CZE/UV/vis investigations were performed by Hillaert et al. [9]. They described the separation of candesartan, eprosartan, irbesartan, losartan potassium, telmisartan and valsartan. The limit of quantification was in the range of 0.05 mg mL^{-1} to 0.07 mg mL^{-1} for the determined drugs. In

2003, they transferred the separation of these angiotensin II receptor antagonists to micellar electrokinetic chromatography [10]. The sensitivity was comparable with the initial CZE investigations

Maotin et al. developed a polarographic method for the determination of telmisartan [11, 12], which was applied to its determination in pharmaceutical preparations and in biological samples such as human serum. They achieved a detection limit of 0.05 mg mL^{-1}.

In 2003, Torrealday et al. published investigations on the fluorescence detection of the native telmisartan [13] after LC separation of urine samples, which were cleaned up previously by means of solid-phase extraction (SPE). However, although both selectivity and sensitivity of fluorescence detection (approximately 1 ng mL^{-1}) are superior to those of UV/vis absorbance, it is doubtful if the analytical figures of merit, which can be achieved with this method, are sufficient for highly complex samples.

Although telmisartan has already been available on the market since the late 1990s, these few publications available regarding the analysis of this drug are mainly published later than 2000. However, HPLC-based methods with either UV/vis [14] or fluorescence [15, 16] detection are also published for some other angiotensin II receptor antagonists as ,e.g., losartan potassium, candesartan or irbesartan. A LC/electrospray-tandem MS method applying an off-line sample extraction procedure for the characterization of metabolites of

the angiotensin II receptor antagonist candesartan cilexetil in rat blood plasma was presented by Kondo et al. in 1996 [17].

To meet the requirements of low limits of detection in combination with high selectivity and short analysis times, two other methods have frequently been applied for the analysis of pharmaceuticals in body fluids: While liquid chromatography with tandem mass spectrometry (LC/MS/MS) currently is the method of choice for the analysis of highly polar pharmaceuticals and offers the capability of simultaneous multianalyte determination, enzyme-linked immunosorbent assays (ELISAs) are characterized by extremely low limits of detection and high selectivity for the analyte and, depending on the antibodies used, a limited number of very closely related compounds. Additional advantages are the possibility of high sample throughput and low operating costs. However, the successful development of an LC/MS/MS method using the "soft" atmospheric pressure ionization (API) methods as electrospray ionization (ESI) or atmospheric pressure chemical ionization (APCI) was not certain due to the low polarity of the analyte [18]. Furthermore, it was considered to be favorable to utilize two independent high-sensitivity methods for cross-validation. Thus, it was decided to develop both a LC/MS/MS method with automated on-line sample clean-up using turbulent flow chromatography and an ELISA method based on the glucose oxidase-catalyzed reaction of MNBDH to the fluorescent MNBDA [19, 20] for the determination of telmisartan in human plasma samples. It is the first time that MNBDH is used as substrate in an immunoassay. This reaction system, yielding MNBDA as product, was chosen due to usually higher sensitivity and

selectivity of fluorescent detection schemes in comparison to UV/vis detection.

7.3 Experimental

Chemicals

Telmisartan (4-[(2-n-propyl-4-methyl-6-(1-methylbenzimidazol-2-yl)-benzimidazole-1-yl)methyl]-biphenyl-2-carboxylic acid, the hapten telmisartan-(2-amino acetic acid) (Tel-AAA) (see also Figure 7.2), which is coupled to the enzyme glucose oxidase, the biotin-labeled rabbit anti-telmisartan IgG as well as all plasma samples (12 single plasma samples, 1 pooled plasma sample) and the internal telmisartan standard (deuteration degree of the propyl group over seven hydrogen atoms: 78%) were kindly provided by Boehringer Ingelheim GmbH & Co. KG (Biberach, Germany). Acetonitrile and water for LC/MS measurements were from Biosolve (Valkenswaard, The Netherlands), LC/MS grade. Bovine serum albumin (BSA) was purchased from Serva (Heidelberg, Germany). The enzymes glucose oxidase (GOD, E.C 1.1.3.4) and horseradish peroxidase (POD, E.C. 1.11.1.7) as well as avidin were purchased from Sigma (Deisenhofen, Germany). The synthesis of 4-(N-methylhydrazino)-7-nitro-2,1,3-benzoxadia-zole (MNBDH) was performed as described in literature [21]. All other chemicals were purchased from Aldrich (Steinheim, Germany), Merck (Darmstadt, Germany) and Fluka (Neu-Ulm, Germany) in the highest quality available.

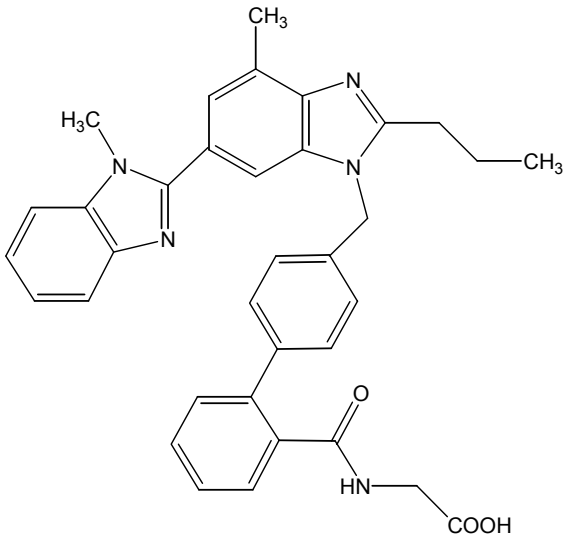

Figure 7.2: *Chemical structure of the hapten used for tracer synthesis (Te-AAA).*

Buffers:

buffer 1: 0.05 mol L^{-1} Na_2HPO_4/KH_2PO_4, 0.15 mol L^{-1} NaCl, pH = 7.4

buffer 2: 0.05 mol L^{-1} Na_2HPO_4/KH_2PO_4, 0.15 mol/L NaCl, 5 g L^{-1} BSA, pH = 7.4

buffer 3: 0.05 mol L^{-1} Na_2HPO_4/KH_2PO_4, 0.15 mol L^{-1} NaCl, 5 g/L BSA, 0.5 g L^{-1} NaN_3, pH = 7.4

Unknown Samples

Human plasma samples of four test persons (male) of a pharmacokinetic clinical study with telmisartan were investigated by means of LC/MS and ELISA measurements. The blood plasma in all four cases was sampled 0.5 h before as well as 0.5 h, 1 h, 1.5 h, 2 h, 4 h, 6 h, 8 h, 12 h, 24 h, 48 h and 72 h after oral intake of 80 mg telmisartan and stored subsequently in aliquots at approximately -20°C.

Enzyme tracer synthesis

The telmisartan-GOD conjugate was synthesized according to the following procedure: A solution of 65 mg GOD in 0.75 mL of $NaHCO_3$ solution (0.13 mol L^{-1}) is mixed under stirring with 0.75 mL DMF (resulting pH ~ 9.6). The pH is adjusted to 7.1, and the solution is cooled in an ice bath (T = 0°C). A solution of 31.3 mg of the hapten Tel-AAA in 1 mL DMF (anhydrous) is cooled under stirring to –25°C. N-Methylmorpholine (11 μL) and isobutyl-chloroformate (6.5 μL) are added, and the mixture is incubated for 10 min at -25°C. Afterwards, 15.3 μL of this solution are pipetted slowly under stirring at 0°C to the GOD solution. The pH is kept at 7.0. The mixture is incubated under stirring at 0°C for 2.5 h.

The synthesized GOD conjugate is purified by means of size-exclusion chromatography: The conjugate is added onto a PD10 Sephadex G25 column (buffer: 0.05 mol L^{-1} Tris, 0.15 mol L^{-1} NaCl, pH = 7.5) and $NH_2OH{\cdot}HCl$ (42.9 mg for each milliliter of conjugate) is added to the conjugate fraction. The mixture is stirred for 30 minutes at room temperature. Afterwards, the GOD tracer is again cleaned on a Sephadex G25 column (buffer: 0.1 mol L^{-1} phosphate, pH = 7.0). For storage at -20°C, 1.125 mL glycerin, 10.6 mg BSA and 1 mg thymol (per mL conjugate) are added to the GOD tracer fraction.

Methods

For LC-MS investigations, an Agilent Technologies (Waldbronn, Germany) HP1100 liquid chromatograph for binary gradient elution (pump model

G1312A), including an autosampler (G1313A) and a diodearray detector (G1315B), coupled to an esquire 3000*plus* ion trap mass spectrometer from Bruker Daltonics (Bremen, Germany) was used. The set-up of the LC/MS system is shown in Figure 7.3. For HPLC separation (pump 2 and pump 3), the following binary gradient consisting of buffer A ($HCOONH_4$/HCOOH, 20 mmol L^{-1}, pH 3) and acetonitrile (B) with a flow rate of 0.4 mL min^{-1} was used:

time [min]	0	1.5	6.5	9.5	9.6	13
c_B [%]	30	30	90	90	30	30

For sample clean-up, turbulent flow chromatography (TFC) using isocratic conditions were used (water, pump 1). The flow rate in this case was 1.2 mL min^{-1} and the injection volume was 100 µL. A Cyclone turboflow (TF) column (Cohesive Technologies Europe, Crownhill, United Kingdom) with the following parameters was used for telmisartan enrichment: Particle size 60 µm, pore size 100 Å, column dimensions 50 mm x 0.5 mm. A Prontosil C18-ace-EPS column (Bischoff Chromatography, Leonberg, Germany) was used for HPLC separation; particle size 3.0 µm, pore size 120 Å; column dimensions 150 mm x 3.0 mm. From 0 min to 1 min, the valve was in the enrichment position. From 1.1 min to 9.5 min, the valve switched to the separation position and at 9.6 min back into the first position again.

All MS measurements were performed by means of atmospheric pressure chemical ionization (APCI) in the negative ion mode. Mass spectra were

recorded in the full scan mode with a mass range from m/z = 100 to m/z = 1000.

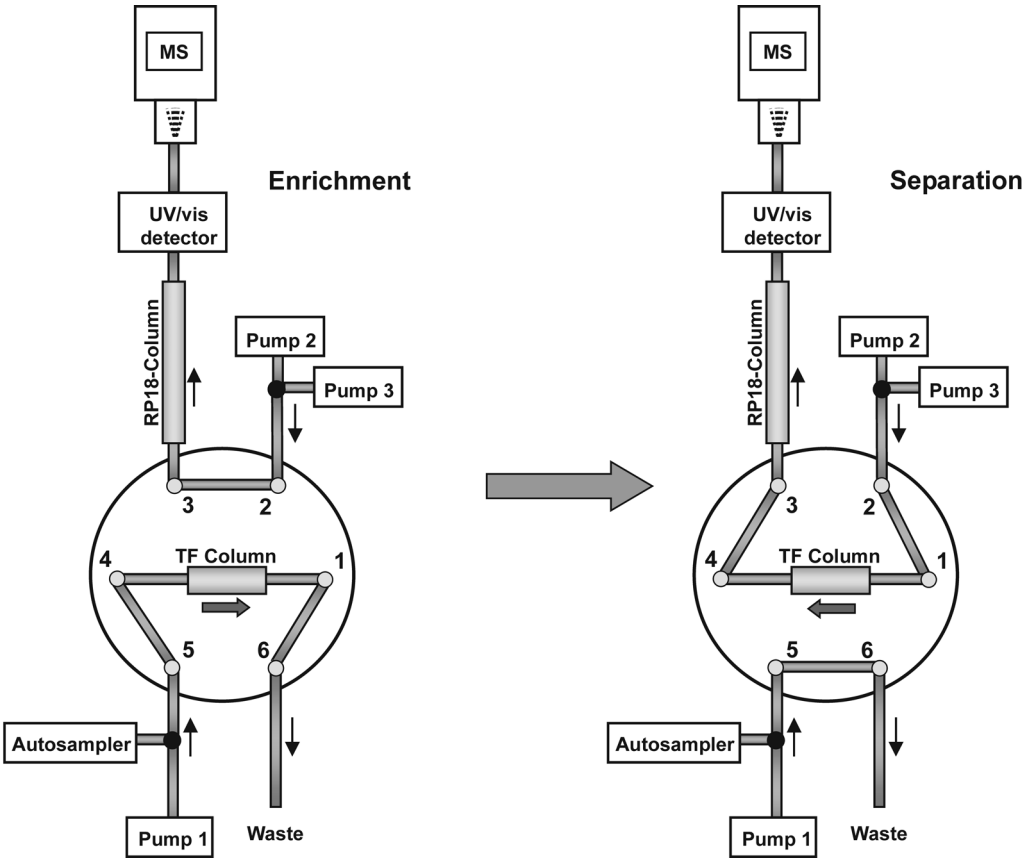

Figure 7.3: *Schematic set-up of the LC/MS system. The switching valve changes between the enrichment and the separation position. In the enrichment position, the TFC column is loaded with the plasma sample, whereas in the separation position, the TFC column is eluted (backflush) and the retained components are separated on the RP18 column and detected by means of UV/vis spectroscopy and APCI-MS.*

Tandem mass spectra of telmisartan were recorded in the multiple reaction monitoring (MRM) mode with a fragmentation amplitude of 1.0 V using the

transition from m/z = 513.2 to m/z = 469.2 for quantification and the transitions from m/z = 513.2 to m/z = 302.2 and m/z = 287.2 additionally for identification. internal standard was determined monitoring the transition from m/z = 519.2 to m/z = 475.2. The ion count cumulative target for the ion trap mass analyzer was 100,000, with a maximum accumulation time of 200 ms. Ions were generated with 10,000 nA corona current and guided towards the mass analyzer with 2582 V at the transfer capillary inlet, -205.7 V on the capillary exit and -49.8 V at the skimmer. Further ion source parameters were 50 psi nebulizer gas and 5.0 L min^{-1} of drying gas with a temperature of 350°C.

The ELISA was performed using a FLUOstar microplate reader from BMG LabTechnologies (Offenburg, Germany) with FLUOstar Galaxy software version 4.30-0. For the measurements, the following filters were used: 470 nm (bandwidth ± 15 nm) for excitation and 545 nm (bandwidth ± 10 nm) for emission. Nunc (Maxisorp, black) 96 well microtitration plates used for these measurements were purchased from VWR International B.V. (Roden, The Netherlands) and Corning (Costar No. 3915, black) microtitration plates were purchased from Diagonal (Münster, Germany).

Optimization of LC/MS parameters

In order to find the best conditions for the LC/MS measurements, several parameters were optimized: Telmisartan was on the one hand determined in initial measurements in the full scan mode and on the other hand in the tandem MS mode, to identify the most sensitive mode. The calibration curve of pooled plasma samples (diluted to 10%) containing standards was compared with the calibration of standards without plasma and with the

results of an internal calibration. Additionally, the breakthrough volume of the TFC column was determined by varying the injection volume between 10 µL, 30 µL, 50 µL, 75 µL and 100 µL and comparing the peak areas of the respective mass traces or transitions.

LC/MS procedure

The telmisartan concentration of the twelve unknown human plasma samples of every test person was determined by means of LC/APCI-MS measurements combined with an on-line TFC sample clean-up step. In case of the external calibration, the standard solutions and the sample solutions were injected in triplicate into the system. Additionally, quality controls of 500 ng mL^{-1} and 20 ng mL^{-1} (in pooled plasma) were analyzed two times in triplicate between the determination of the real human plasma samples. In all cases, the solutions were diluted (buffer 2) to a final plasma concentration of 10%. Therefore, pooled plasma was added to the calibration standards, which were determined in the range of 0.01 ng mL^{-1} to 1000 ng mL^{-1}.

For internal calibration, the response factor was initially determined: Two calibration curves of telmisartan/internal standard mixtures were recorded: On the one hand by mixing solutions of the analyte and the deuterated standard of the same concentration in the range from 0.3 ng mL^{-1} to 1000 ng mL^{-1} and on the other hand by mixing solutions of this concentration range in opposite directions (starting for telmisartan at 0.3 ng mL^{-1} and for the standard at 1000 g mL^{-1}). The response factor was calculated applying the following formula:

$R = (c_{inS} \cdot A_{Telm})/(c_{Telm} \cdot A_{inS})$ with internal standard (inS), area telmisartan (A_{Telm}), and area internal standard (A_{inS}).

This procedure was selected to exclude interferences from very high concentrations of one compound on very low concentrations of the other. Afterwards, the analysis of the plasma samples was carried out by adding the internal standard to each sample in a final concentration of 10.04 ng mL^{-1}. All samples, which were analyzed using an internal standard were also diluted (buffer 2) to a final plasma concentration of 10%. For the two calibration measurements, pooled plasma was added to the solutions again. All measurements based on the use of the internal standard (calibration, real sample determination) were performed in triplicate as well. Furthermore, the telmisartan concentration of quality controls (500 ng mL^{-1}, 20 ng mL^{-1}) containing 10% pooled plasma was again determined two times in triplicate between the human plasma samples. For all measurements, the detection was performed applying UV/vis absorbance spectroscopy and APCI-MS in the MRM mode.

Optimization of ELISA parameter

In order to find the best parameters for the performance of the immunoassay, the ELISA was carried out as described below for different substrate concentrations. The avidin concentration was varied between 0.05 µg mL^{-1}, 0.5 µg mL^{-1} and 5 µg mL^{-1}, the biotin-labeled anti-telmisartan IgG concentration between 0.15 ng mL^{-1}, 1.5 ng mL^{-1}, 45 ng mL^{-1}, 150 ng mL^{-1} and 1500 ng mL^{-1} and the GOD-conjugate dilution between 1:100, 1:300, 1:1000,

1:3000, 1:10,000 and 1:90,000. The immunoassays were performed for calibration standards in the range from 0.01 ng mL^{-1} to 3000 ng mL^{-1}. Additionally, two different types of microtitration plates were tested: The black Maxisorp plate from Nunc and the black Costar 96 microtitration plate from Corning. The different calibration curves were compared.

ELISA procedure

The microtitration plates were coated with avidin (100 µl/well, 0.5 µg mL^{-1}, in buffer 1) and incubated overnight at ambient temperature. Afterwards, the microtiter plates were washed three times (each time 300 µL/well, washing solution: 0.5 g L^{-1} Tween 20), blocked with 250 µL buffer 3, sealed with adhesive foil and stored for at least two weeks at approximately 4°C. Then, the microtitration plates were washed three times again (each time 300 µL/well, washing solution), coated with biotin-labeled anti-telmisartan IgG (100 µL/well, 150 ng mL^{-1} in buffer 3), sealed with adhesive foil and incubated overnight at ambient temperature.

The microplates were washed four times (each time 300 µL/well, washing solution). Then, 25 µL buffer 2 was pipetted into each well and immediately afterwards, 50 µL of the calibration solutions, quality controls (500 ng mL^{-1}, 20 ng mL^{-1}) or unknown samples (all in buffer 2) were added in triplicate onto the microtitration plate. Due to a 1:10 dilution of the unknown samples and quality controls, pooled plasma was added to all calibration standards to obtain a final plasma concentration of 10%. Then, 50 µL of the synthesized telmisartan-GOD conjugate were added to each well. The plate was incubated

for 4 h on a shaker and afterwards washed four times (each time 300 µL/well, washing solution).

In the last step, 75 µL glucose ($2 \cdot 10^{-3}$ mol L^{-1}, in acetate buffer, pH 5.5; 0.01 mol L^{-1}) is added to each well of the microtitration plate. After an incubation time of 15 minutes, 30 µL of a mixture of 1.4 mL MNBDH ($5 \cdot 10^{-4}$ mol L^{-1} in acetonitrile) added to 10 mL POD (2.65 mg dissolved in 10 mL phosphate buffer, pH 5.8; 0.01 mol L^{-1}), are pipetted to each well. The fluorescence intensity of the fluorescent reaction product MNBDA is determined as described above.

Plasma test

The influence of different human plasma samples on the GOD-catalyzed reaction, which was used for detection of the immunoassay, was tested by executing the GOD-catalyzed reaction on microtitration plates without plasma in comparison to the GOD-catalyzed reaction with 13 different plasma samples (see above). Therefore, 25 µL plasma (diluted 1:10 in buffer 2) were pipetted in sixfold into the wells of ten rows of a microtitration plate. In the wells of one row, 25 µL blank solution are added (buffer 2). Afterwards, 50 µL glucose ($2 \cdot 10^{-3}$ mol L^{-1}, in H_2O) are added to each well of the microtitration plate and 25 µL GOD solution (buffer 1) are added in two different concentrations (10 u L^{-1} and 30 u L^{-1}), in a way that every plasma sample and the blank is determined in triplicate for each concentration. After an incubation time of 15 minutes, 20 µL of a mixture of 1.4 mL MNBDH ($5 \cdot 10^{-4}$ mol L^{-1} in acetonitrile) added to 10 mL POD (2.65 mg dissolved in buffer 1), are pipetted

to each well. The fluorescence intensity of the strongly fluorescent 4-(N-methylamino)-7-nitro-2,1,3-benzooxadiazole (MNBDA) is determined as described above. The scheme of the GOD-catalyzed reaction is shown in Figure 7.4.

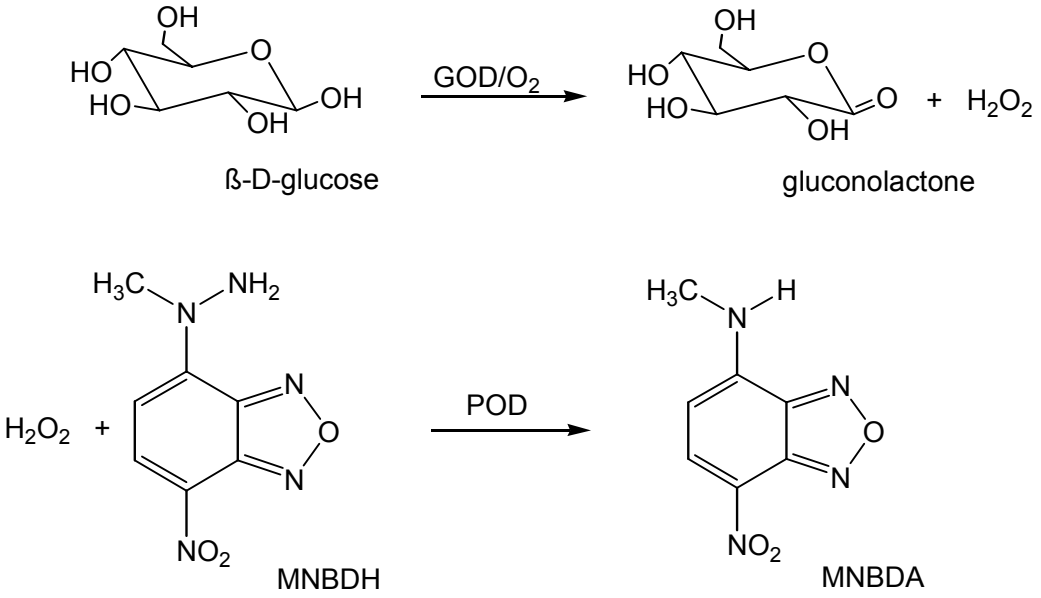

Figure 7.4: *GOD-catalyzed two-step reaction of MNBDH to the fluorescent MNBDA as detection scheme for the immunoassay. I: Reaction of glucose with GOD and atmospheric oxygen to gluconolactone and H_2O_2. II: Reaction of H_2O_2 with MNBDH under POD-catalysis to MNBDA.*

7.4 Results and Discussion

LC/MS method

The LC/APCI-MS/MS technique is the mainly applied method for the determination of drugs and metabolites in complex matrices. The large linear range, reduced suppression problems, ruggedness and reliability are characteristic for this method. The on-line clean-up procedure by means of turbulent flow chromatography enables the automation of the measurements and therefore to rapidly determine the concentration of pharmaceutical compounds in complex matrices, as blood/plasma or urine. As other techniques for the sample preparation like protein precipitation or off-line extraction procedures are usually time-consuming processes, the TF technique is a promising alternative.

The APCI-MS (inserted spectrum) and APCI-MS/MS spectra of a telmisartan calibration standard (10 ng mL^{-1}; solved in buffer 2 including 10% pooled blood plasma) are shown in Figure 7.5. The peak at m/z = 513.2 is caused in both cases by the deprotonated telmisartan, whereas the ion at m/z = 469.2, which can also be observed in both measurements, is due to the loss of carbon dioxide from the carboxylic acid function. The fragment at m/z = 302.2 is caused by cleavage of the C-N bridge between the biphenyl part and the rest of the telmisartan molecule and the fragment at m/z = 287.2 by additional loss of a methyl group.

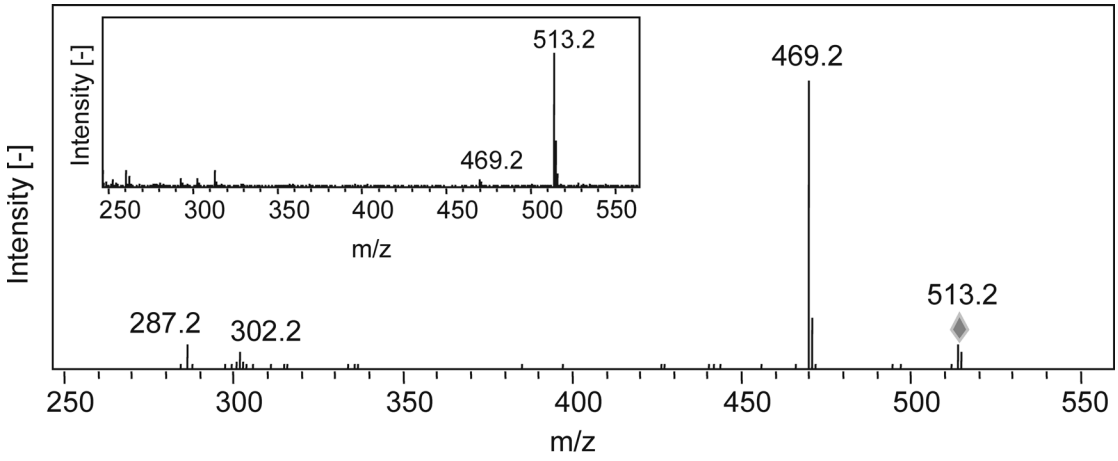

Figure 7.5: *APCI-MS (inserted spectrum) and APCI-MS/MS spectra of a telmisartan calibration standard (10 ng mL^{-1}; dissolved in buffer 2 including 10% pooled blood plasma). The peak at m/z = 513.2 is caused in both cases by telmisartan. The daughter ion at m/z = 469.2 in the tandem mass spectrum is caused by loss of CO_2 from the carboxylic acid group.*

The fragmentation scheme is shown in Figure 7.6. The signal-to-noise ratio for the main MRM signal at m/z = 469.2 is approximately 200:1 at this concentration. Tandem MS techniques have been selected for these investigations due to improved limits of detection in comparison to full scan APCI-MS. In case of the deuterated internal standard, the transition of the main signal at m/z = 519.2 to m/z = 475.2 was observed as expected due to the analogy to the native compound.

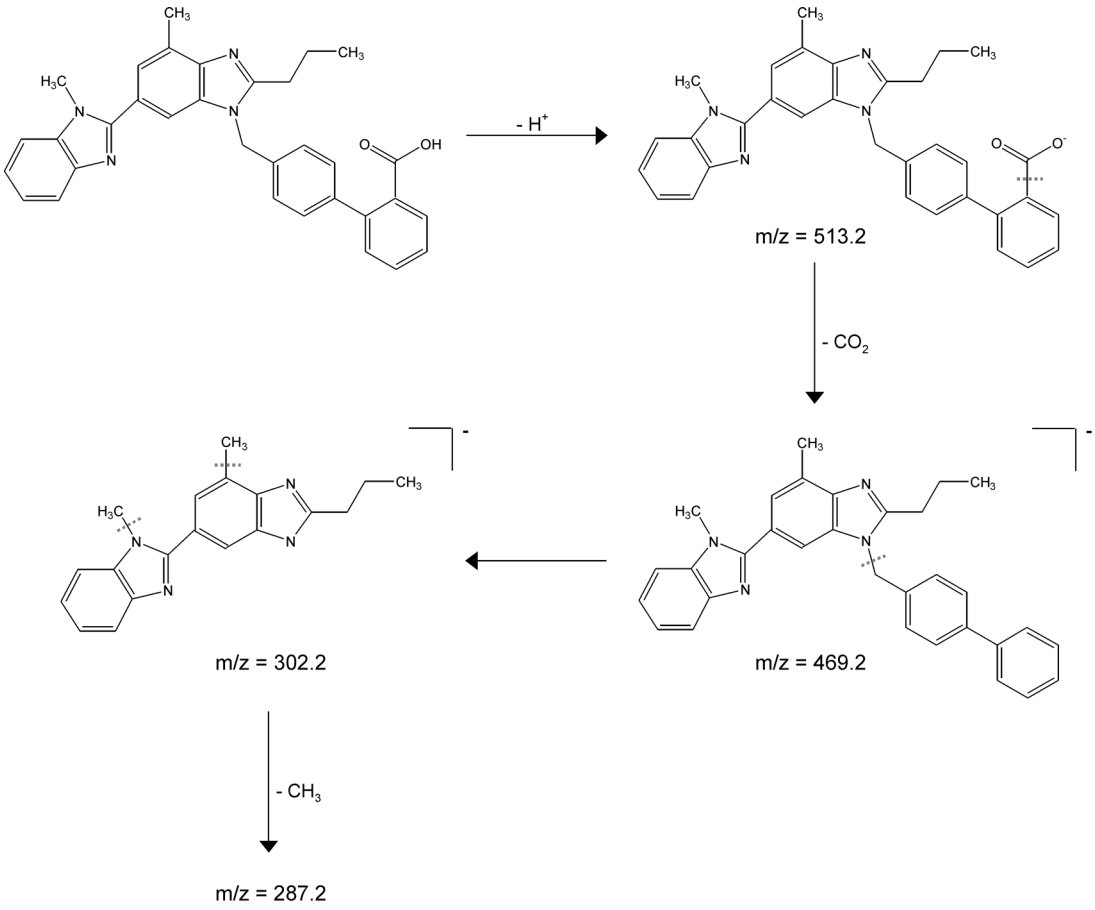

Figure 7.6: *Reaction scheme of the telmisartan fragmentation.*

Figure 7.7 shows the dependency of the signal intensity for the LC/APCI-MS (MRM) measurement on different injection volumes of the peak at m/z = 469.2 (n = 3). Different injection volumes between 10 µL and 100 µL have been selected for these investigations in order to determine the breakthrough volume of the TFC column. The results for higher injection volumes could not be compared due to the maximum volume of 100 µL of the injection loop. The coefficient of linear regression (r^2) is 0.9983 and the mean RSD is 9.2%. As a wide range of telmisartan concentrations could be expected, a large linear

range for the pharmacokinetic investigations was needed. Therefore, an injection volume of 100 µL was selected.

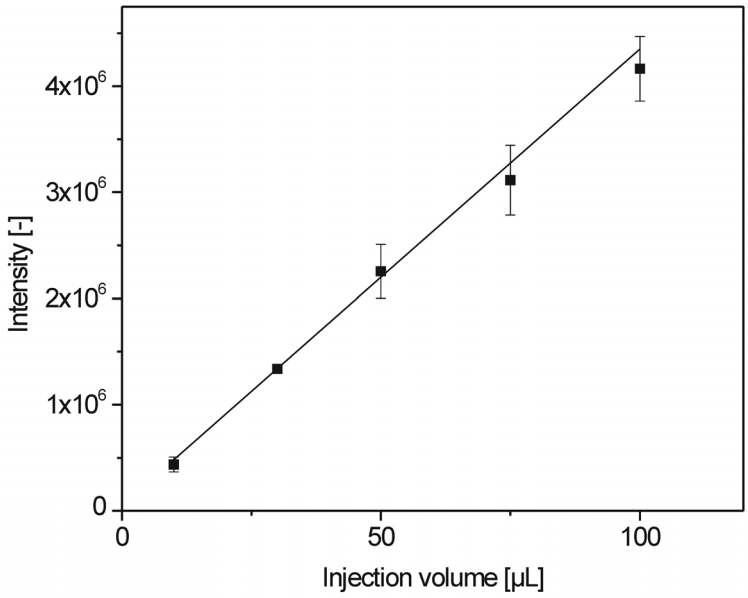

Figure 7.7: *LC/APCI-MS (MRM) investigation regarding the dependency of different injection volumes on the signal intensity of the peak at m/z = 469.2 (n = 3).*

Figure 7.8 shows the APCI(-)-MS and UV/vis chromatograms of a telmisartan calibration solution (1000 ng mL^{-1}; dissolved in buffer 2 including 10% pooled plasma) after TF clean-up. The upper chromatogram shows the TIC, whereas in the middle, the 513.2 → 469.2 transition in the MRM mode is observed. In the TIC chromatogram, the times of changing the switching valve position from enrichment into the separation (1 minute) and back (9.5 minutes) are marked (dashed lines). Both chromatograms show only one peak at approximately 8.5 minutes, which can be assigned to telmisartan. Due to the

low polarity of telmisartan, polar metabolites as the gluconuride are expected to elute earlier from a reversed-phase column than the compound itself. The third window shows the UV/vis chromatogram at the maximum absorption wavelength of 298 nm. Besides the pressure peak resulting from the injection (3.5 minutes), two very small and one larger peak can be seen.

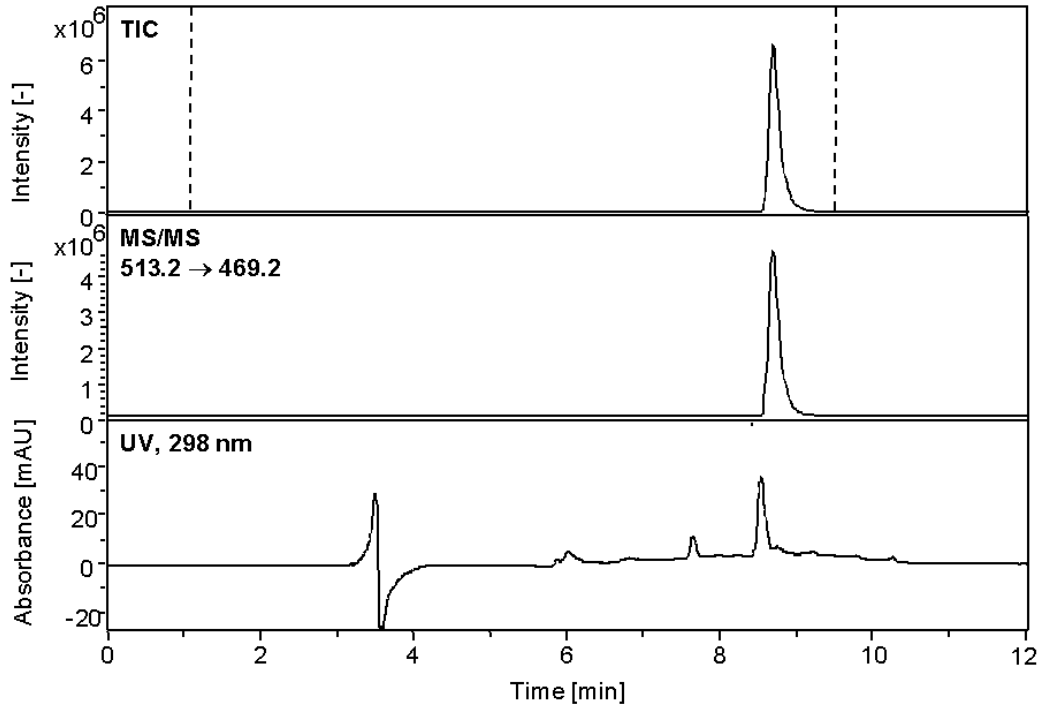

Figure 7.8: *APCI(-)-MS and UV/vis chromatogram of a telmisartan calibration solution (1000 ng mL^{-1}; dissolved in buffer 2 including 10% pooled plasma) after TF clean-up and LC separation recorded in the scan mode (m/z = 50-500), in the MRM mode (m/z = 469.2) and at the respective absorption wavelength of 298 nm.*

The retention time of the large peak corresponds to the telmisartan peaks of the other chromatograms. The two other peaks at approximately 6 and 7.5 minutes, respectively, can be observed in all other performed measurements,

which includes also the determination of unknown samples and the measurement of the telmisartan calibration standard solutions without added plasma. This means that these peaks are probably caused by some additives of telmisartan and not by the plasma itself or by metabolism of telmisartan in the plasma. The comparison of the mass and UV traces shows the difference in sensitivity of the methods. Although the applied telmisartan concentration is very high, the UV peaks show only moderate peak intensities with a much lower signal-to-noise ratio than the MS traces. For the concentrations at the beginning of the linear range, no UV detection was possible. This confirms the argumentation for LC/MS measurements.

Linearity

For the external calibration, eleven telmisartan standard solutions in the concentration range between 0.01 ng mL^{-1} and 1000 ng mL^{-1} were injected in triplicate into the on-line HTLC/LC/MS system. In order to have the same conditions as for the determination of the unknown human plasma samples, all telmisartan standards were diluted in such a way that the final pooled plasma concentration was 10% in buffer 2. The calibration function is provided in Figure 7.9. The limit of detection (LOD), determined according to the concentration to a signal 3 SD above the mean for the blank, is 0.3 ng/mL, the limit of quantification (LOQ), determined according to the concentration to a signal 10 SD above the mean for the blank, is 0.9 ng/mL and the linear range is between 0.9 ng/mL – 1000 ng/mL. The coefficient of linear regression (r^2) is 0.992 and the mean RSD = 7.7% (RSD between 1.0% and 9.6%).

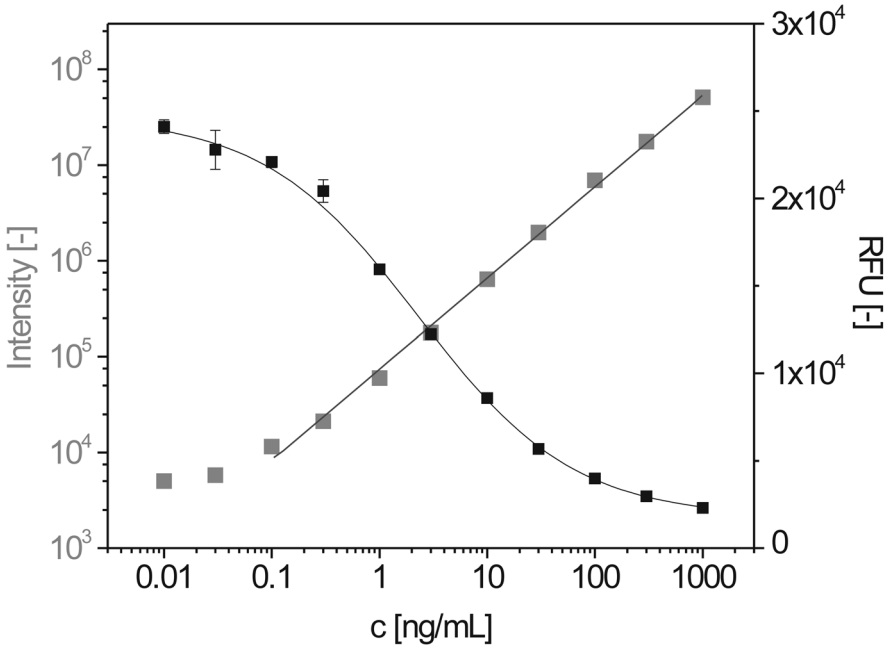

Figure 7.9: *Comparison of the two different types of calibration curves: APCI-MS-calibration (grey) and ELISA-calibration (black).*

For the determination of the response factor for the internal calibration, two calibration curves of telmisartan/internal standard mixtures were measured: On the one hand, by mixing solutions of the native compound and the deuterated standard of the same concentrations (parallel calibration) in the range from 0.3 ng mL^{-1} to 1000 ng mL^{-1} and on the other hand by mixing different concentrations (cross calibration) of these solutions of this range (starting for telmisartan at 0.3 ng mL^{-1} and for the standard at 1000 ng mL^{-1}). Pooled plasma was again added to a final concentration of 10%. The response factor was calculated as 1.77 (SD = 0.20, RSD = 11.31%) as described above by applying the formula $R = (c_{inS} \cdot A_{Telm})/(c_{Telm} \cdot A_{inS})$.

In Table 7.1 (a-d), the results for the LC/MS determination with internal and external calibration of the pharmacokinetic behavior of telmisartan in human blood plasma for four different test persons are presented. Blood plasma samples were taken at twelve different times: Between 30 minutes before delivery of telmisartan and up to 72 hours after administration of the drug. The telmisartan concentration was determined in triplicate after diluting all human plasma samples by a factor of 10 with buffer 2 (and addition of the deuterated standard, in case of the internal calibration) and injecting 100 µL of these solutions for every measurement. In case of the external calibration measurements, the highest telmisartan concentration for test persons 1 and 4, was determined 1 h after application of the drug, for test person 3 already after 30 min and for test person 2 1.5 h after taking telmisartan. The highest (23.8%) and the lowest (0.4%) RSDs for the telmisartan determination were obtained in the measurements regarding volunteer 4.

Table 7.1: *Telmisartan concentration development in human plasma samples for four test persons (a-d). The plasma samples are taken at twelve different times and were diluted with buffer 2 (10%).*

a) **Test person 1**

Time [h]	APCI-MS external (ext.) calibration			APCI-MS internal (int.) calibration			Immunoassay			c(ELISA) compared to c(LC/MS) ext. calibration [%]	c(ELISA) compared to c(LC/MS) int. calibration [%]
	Average [ng/mL]	SD (n = 3)	RSD [%]	Average [ng/mL]	SD (n = 3)	RSD [%]	Average [ng/mL]	SD (n = 3)	RSD [%]		
-0.5	< LOQ	/	/	< LOQ	/	/	< LOQ	/	/	/	/
0.5	186.7	7.2	3.9	199.9	11.9	6.0	115.8	9.2	7.9	62.0	57.9
1.0	334.6	7.2	2.2	372.5	17.3	4.6	244.4	21.1	8.6	73.0	65.6
1.5	279.7	2.0	0.7	318.0	17.5	5.5	227.9	37.5	16.4	81.5	71.7
2.0	245.0	5.7	2.3	284.1	22.8	8.0	208.8	25.3	12.1	85.2	73.5
4.0	102.5	2.4	2.3	108.0	2.5	2.3	85.8	2.3	2.7	83.8	79.4
6.0	63.0	3.9	6.2	66.8	0.6	0.9	52.4	3.7	7.0	83.2	78.4
8.0	64.4	2.1	3.3	65.2	0.8	1.2	64.7	8.6	13.4	100.5	99.3
12.0	42.7	0.5	1.2	45.8	1.8	3.9	40.0	3.8	9.5	93.8	87.4
24.0	21.5	0.8	3.6	26.3	0.9	3.6	22.9	3.1	13.4	106.5	87.1
48.0	< LOQ	/	/	< LOQ	/	/	9.4	0.6	6.3	/	/
72.0	< LOQ	/	/	< LOQ	/	/	< LOQ	/	/	/	/

b) Test person 2

Time [h]	APCI-MS external (ext.) calibration			APCI-MS internal (int.) calibration			Immunoassay			c(ELISA) compared to c(LC/MS) ext. calibration [%]	c(ELISA) compared to c(LC/MS) int. calibration [%]
	Average [ng/mL]	SD (n = 3)	RSD [%]	Average [ng/mL]	SD (n = 3)	RSD [%]	Average [ng/mL]	SD (n = 3)	RSD [%]		
-0.5	< LOQ	/	/	< LOQ	/	/	< LOQ	/	/	/	/
0.5	69.3	0.8	1.2	115.1	1.0	0.9	90.0	1.8	2.0	131.6	78.2
1.0	192.3	4.5	2.3	261.0	9.0	3.5	198.8	12.7	6.4	103.4	76.2
1.5	454.9	4.2	0.9	591.1	14.6	2.5	545.0	26.9	4.9	119.8	92.2
2.0	368.4	3.4	0.9	506.8	20.0	3.9	466.5	33.8	7.3	126.6	92.1
4.0	132.9	4.1	3.1	166.2	12.9	7.8	132.1	13.4	10.2	99.4	79.5
6.0	91.7	5.9	6.5	117.3	2.7	2.3	90.4	5.3	5.8	98.6	77.1
8.0	65.1	2.2	3.4	70.7	1.8	2.5	52.3	5.9	11.2	80.3	74.0
12.0	52.4	0.5	0.9	60.4	1.3	2.1	61.0	10.3	16.9	116.3	100.9
24.0	36.1	1.1	3.1	42.6	1.2	2.8	39.1	4.4	11.2	108.3	91.8
48.0	18.3	0.5	2.7	16.1	0.1	0.9	22.5	0.5	2.0	123.1	139.6
72.0	< LOQ	/	/	< LOQ	/	/	5.8	0.4	6.5	/	/

c) Test person 3

Time [h]	APCI-MS external (ext.) calibration			APCI-MS internal (int.) calibration			Immunoassay			c(ELISA) compared to c(LC/MS) ext. calibration [%]	c(ELISA) compared to c(LC/MS) int. calibration [%]
	Average [ng/mL]	SD (n = 3)	RSD [%]	Average [ng/mL]	SD (n = 3)	RSD [%]	Average [ng/mL]	SD (n = 3)	RSD [%]		
-0.5	< LOQ	/	/	< LOQ	/	/	< LOQ	/	/	/	/
0.5	483.4	19.4	4.0	564.4	59.3	10.5	439.7	22.1	5.0	91.0	77.9
1.0	353.9	17.9	5.0	414.1	53.6	12.9	352.0	42.4	12.0	99.5	85.0
1.5	217.1	4.4	2.0	235.8	4.4	1.9	265.2	16.2	6.1	122.2	112.5
2.0	108.7	2.2	2.0	146.0	17.7	12.1	139.2	2.3	1.7	128.1	95.3
4.0	28.5	0.4	1.3	43.2	3.7	8.5	36.3	4.8	13.2	127.4	84.1
6.0	19.8	1.9	9.4	33.7	0.3	0.8	27.1	1.3	4.7	137.0	80.5
8.0	18.3	1.5	8.3	27.0	1.1	4.2	26.0	3.2	12.1	142.1	96.3
12.0	14.8	1.7	11.2	28.8	2.4	8.2	25.1	0.9	3.6	169.4	87.1
24.0	11.4	1.0	8.5	13.1	0.7	5.5	13.5	2.5	18.6	118.1	103.1
48.0	< LOQ	/	/	11.0	1.9	17.5	6.7	2.0	30.1	/	60.9
72.0	< LOQ	/	/	< LOQ	/	/	< LOQ	/	/	/	/

d) Test person 4

Time [h]	APCI-MS external (ext.) calibration			APCI-MS internal (int.) calibration			Immunoassay			c(ELISA) compared to c(LC/MS) ext. calibration [%]	c(ELISA) compared to c(LC/MS) int. calibration [%]
	Average [ng/mL]	SD (n = 3)	RSD [%]	Average [ng/mL]	SD (n = 3)	RSD [%]	Average [ng/mL]	SD (n = 3)	RSD [%]		
-0.5	< LOQ	/	/	< LOQ	/	/	< LOQ	/	/	/	/
0.5	70.5	6.7	9.5	71.7	2.3	3.3	60.8	6.2	10.2	86.2	84.7
1.0	375.6	9.0	2.4	612.0	14.5	2.4	425.4	96.2	22.6	113.3	69.5
1.5	317.6	1.3	0.4	486.6	1.9	0.4	369.5	31.2	8.4	116.3	75.9
2.0	212.9	50.7	23.8	332.5	26.1	7.9	264.8	2.3	0.9	124.4	79.6
4.0	64.1	0.1	0.2	70.8	0.4	0.5	61.4	9.2	15.0	95.7	86.7
6.0	48.6	0.9	1.8	72.3	7.8	10.7	52.4	5.3	10.1	107.8	72.5
8.0	23.7	0.7	2.8	38.0	2.5	6.5	26.7	2.7	10.1	112.5	70.3
12.0	17.0	0.6	3.5	21.6	2.1	9.7	19.6	1.6	8.3	115.5	90.9
24.0	< LOQ	/	/	10.4	1.0	9.2	8.3	1.5	17.7	/	80.1
48.0	< LOQ	/	/	< LOQ	/	/	5.0	0.4	7.4	/	/
72.0	< LOQ	/	/	< LOQ	/	/	< LOQ	/	/	/	/

In case of the telmisartan determination in human blood plasma samples by means of internal calibration, the concentrations could be calculated by applying the response factor. The results are also listed in Table 7.1. The highest drug concentrations in the plasma samples of each test person were determined in agreement with the results of the external calibration measurements. The highest (17.5%) RSD was obtained for test person 3, the lowest for test person 4 (0.4%).

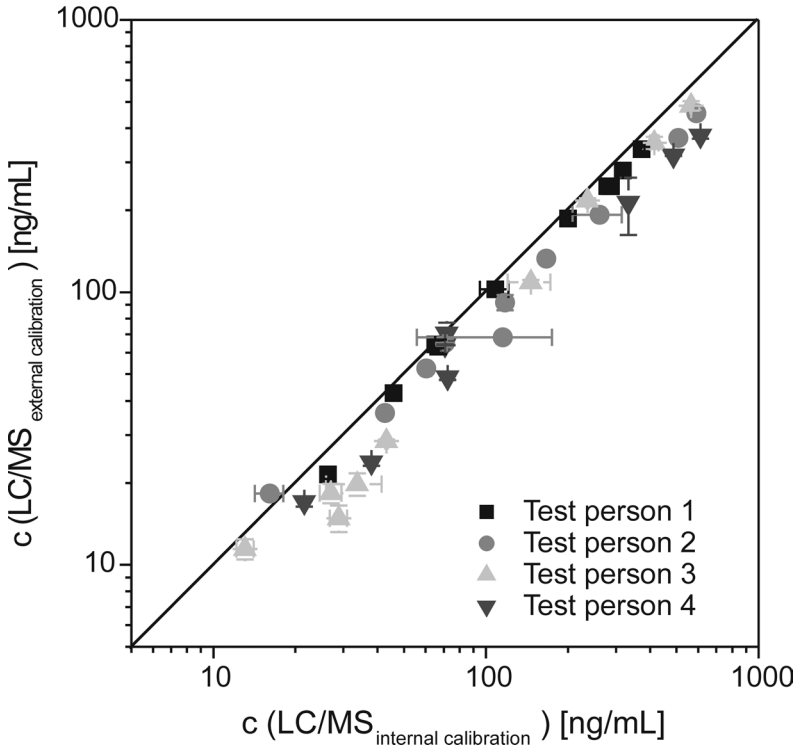

Figure 7.10: *Correlation plot between the determined telmisartan concentrations by means of the LC/MS method with external calibration and with internal calibration.*

By comparing the results of these measurements, two observations are most prominent: First, both series of measurements deliver the same general

tendency for the temporal development of the drug concentration in the plasma samples. This is obvious from Figure 7.10.

However, the second observation, which can be made by comparing the LC/MS results in Table 7.1 and by Figure 7.10 is that the measured telmisartan concentrations are usually higher in case of using the deuterated standard. This result agrees with the very high degree of protein binding of telmisartan. The consequence is that not all telmisartan is retained by means of the TFC column but that it is partly transferred to the waste. Therefore, no quantitative recovery is observed for external calibration. The use of a stable isotope-labeled internal standard, which shows the same degree of protein binding, is the best means to avoid such problems.

ELISA

Immunoassay procedures have already been applied for decades in the fields of bioanalysis and clinical chemistry for the determination of drugs, metabolites or viruses owing to the rapidness (automation/high throughput), the simple sample preparation and low costs (see also Chapter 2). Thus, it is possible to determine antigens, haptens or antibodies in a qualitative and a quantitative way, also in complex matrices. In these enzyme-linked immunosorbent assays (ELISA), the sensitive determination of telmisartan is possible due to the reaction of the marker enzyme with appropriate substrates to a product, which can be determined by means of fluorescence detection, thus usually showing higher sensitivity and selectivity compared with UV/vis

absorbance detection. The large measuring range and the low limits of detection and quantification are the most prominent features of this ELISA.

The results regarding the investigations on the stability of GOD and MNBDH in human plasma are shown in Figure 7.11. The development of the fluorescence intensity over a reaction time of 420 minutes is shown for two different GOD concentrations (10 u L^{-1} part A; 30 u L^{-1} part B). In both cases, the GOD assay performed without added plasma is analyzed and compared with thirteen different plasma-added assays. These measurements are all carried out in triplicate. For the reaction with a GOD concentration of 10 u L^{-1}, the mean RSD over all determined fluorescence intensities (n = 630) was 5.6%. In case of a GOD concentration of 30 u L^{-1}, the mean RSD was 4.8% (n = 630). As can be seen in Figure 7.11, the development of the reaction with time is for all reaction solutions, either without or with added plasma, very similar. This indicates that there is no disturbance or inhibition of the enzyme GOD or of the substrates MNBDH, glucose or POD by added plasma. Therefore, the enzyme-tracer synthesis was performed, and the ELISA based on fluorescence detection was applied for the investigation of telmisartan.

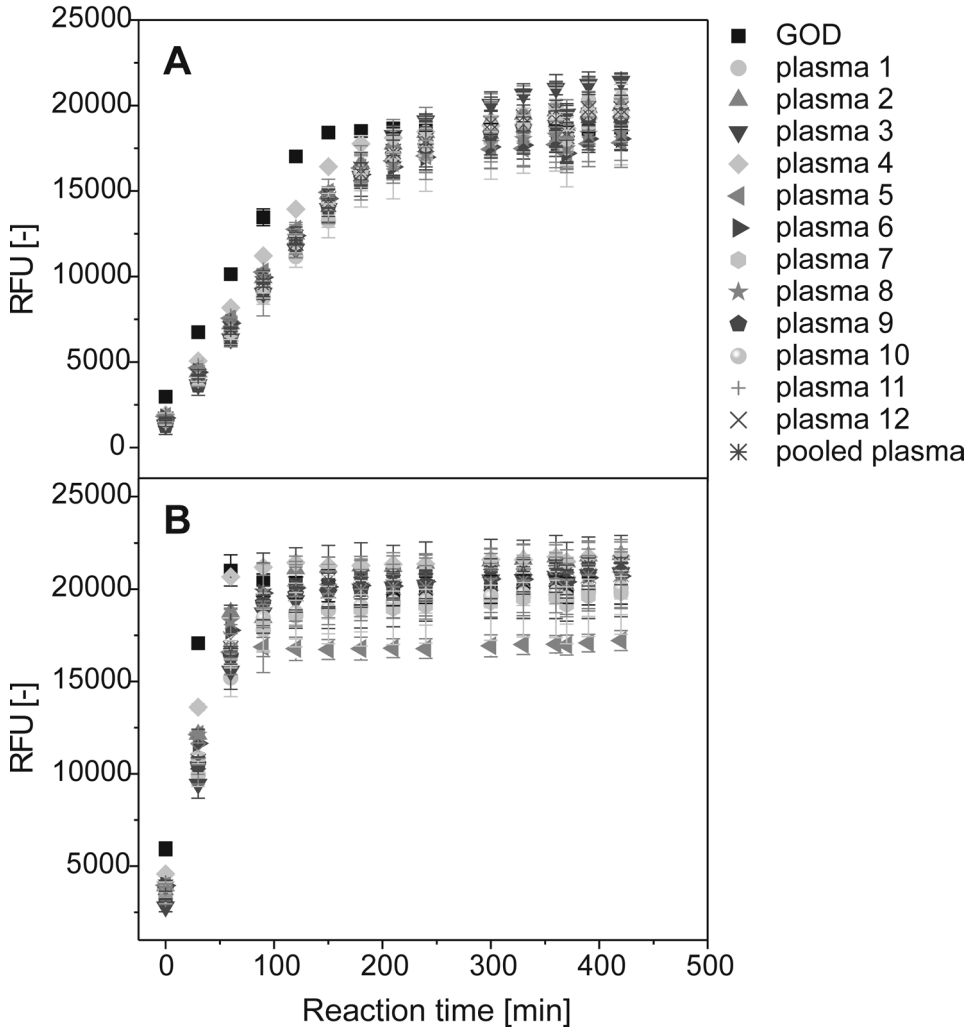

Figure 7.11: *Investigations regarding the stability of GOD and MNBDH in 13 different plasma samples (A: GOD 10 u L^{-1}; B: GOD 30 u L^{-1}).*

The synthesis of the GOD tracer for the immunoassay was performed by means of a mixed-anhydride synthesis as described above. The product was identified by means of activity test measurements of the synthesized enzyme tracer in the MNBDH reaction in comparison to the reaction of commercially available GOD (educt of synthesis). For determining the number of telmisartan molecules, which were bound to the enzyme during the reaction, a MALDI characterization of the product in comparison of the educt GOD was

tried, but failed due to the chemical variability of the carbohydrate part within the GOD structure (different types and numbers of sugar molecules are attached).

For the optimization of the ELISA conditions, several parameters were varied on two different types of microtitration plates (see above). The immunoassay was performed with avidin concentrations between 0.05 µg mL^{-1} and 5 µg mL^{-1} and biotin-labeled anti-telmisartan IgG concentrations between 0.15 ng mL^{-1} and 1500 ng mL^{-1}. The GOD-conjugate was diluted in the range of 1:100 to 1:90,000 and the calibration standards were used in the concentration range between 0.01 ng mL^{-1} and 3000 ng mL^{-1}. Initially, these investigations lead to the result that the black Maxisorp microtitration plates from Nunc are favorable for the immunoassay. Best suited for the ELISA is an avidin concentration of 0.5 µg mL^{-1}, a biotin-labeled anti-telmisartan IgG concentration of 150 ng mL^{-1} and a GOD-tracer dilution of 1:300.

For calibration, eleven telmisartan standard solutions (0 ng mL^{-1}-1000 ng mL^{-1}) were analyzed on the same microtitration plate as the plasma samples. Due to the influence of human blood plasma on the immunoassay, all calibrations were spiked with pooled plasma in such a way that the ratio between buffer 2 and plasma was the same as for the unknown sample solutions (all samples were diluted 1:10 with buffer 2 before the measurements). A typical calibration curve is provided in Figure 7.9. The calculation of the mean B/B_0 values for all calibration measurements (four calibrations each with n = 3) resulted in 0.95 B/B_0 for 0.03 ng mL^{-1}, 0.5 B/B_0

for 3 ng mL^{-1} and 0.05 B/B_0 for 1000 ng mL^{-1}. The LOD of the ELISA, the concentration corresponding to a signal 3 SD above the mean of the blank, was determined as 0.1 ng/mL, the LOQ (10 SD above the mean of the blank) as 0.3 ng mL^{-1} and the range for the measurements was between 0.3 ng mL^{-1} and 300 ng mL^{-1}. The mean RSD was 2.8% including the lowest RSD of 0.8% and the highest RSD of 10.8% of all calibration measurements (n = 84).

Table 7.1 shows, next to the LC/MS results, also the telmisartan concentrations determined using the ELISA during the pharmacokinetic study mentioned above. The telmisartan concentration was determined in triplicate after diluting all human plasma samples by a factor of 10 with buffer 2. The highest values for the telmisartan concentration are determined in agreement with both LC/MS measurements. The lowest RSD was obtained in case of test person 4 (0.9%), whereas the highest RSD was determined for volunteer 3 (30.1%).

Method comparison

The telmisartan concentration data obtained by the two independent methods for human plasma samples out of the pharmacokinetic study were compared. Calibration functions for both methods are provided in Figure 7.9. While the LC/MS/MS method provides a linear calibration curve, the immunoassay calibration typically results in a sigmoidal function.

The development of the determined telmisartan concentration is shown for each test person in Figure 7.12. Here, the results of the immunoassay are

directly compared to the results of the LC/MS/MS method applying internal calibration. It can be seen that the telmisartan profile differs considerably from volunteer to volunteer, but that both analytical methods provide similar concentration profiles, with the largest deviations being observed close to the limit of quantification.

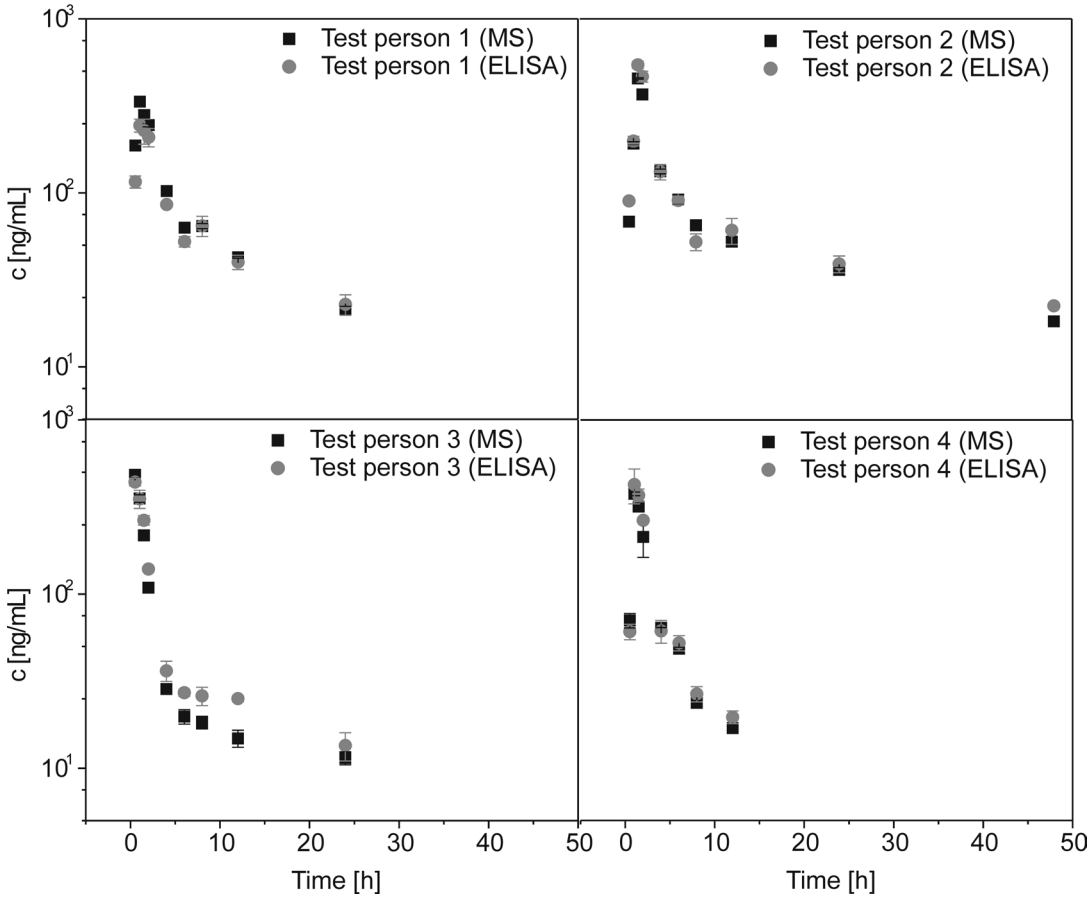

Figure 7.12: *Comparison of the ELISA and LC/MS results regarding the time-dependent development of the telmisartan concentrations in blood plasma of four different probands.*

In Table 7.1, the deviations between ELISA and LC/MS with internal or external calibration are provided for any of the individual samples in the last

two columns. Therefore, the concentrations determined by the ELISA are calculated as RSDs of the LC/MS/MS results achieved by internal or external calibration. By comparing these results, it can be observed that the deviation between ELISA and internal calibration is usually higher than for ELISA and external calibration.

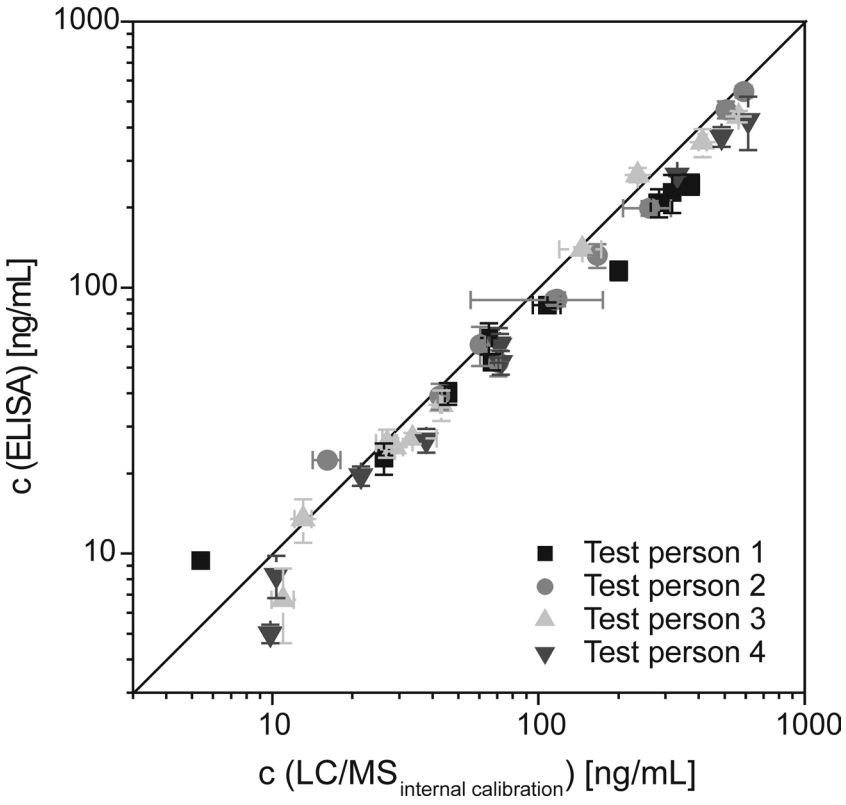

Figure 7.13: *Correlation plot between the telmisartan concentrations as determined by means of immunoassay and LC/MS method.*

Figure 7.13 describes the correlation between the results of the immunoassay and the LC/MS/MS technique with applied internal standard for all four test persons in a scatter plot. The diagonal of the diagram represents the line of 100% agreement of both methods. As all points are concentrated around this

line and no strong outliers can be observed, the two methods show in average and within the scope of the measurements a good correlation. The equation for the linear regression through all points (n = 40) is y = 0.95514x + 0.00742 with the linear regression coefficient (r^2) 0.98665.

The conclusion, which can be drawn from in Figure 7.13 and drawn from Table 7.1, is that the determined telmisartan concentrations are in general slightly lower for the immunoassay than for the LC/MS/MS measurements (averaged: 84.1%). A reason for this might be the external calibration of the immunoassay. For this calibration, pooled human plasma is employed, which probably has different properties than the human plasma of the real samples. Therefore, effects, which appear in case of the real samples and which influence the performance as well as the result of the ELISA might be suppressed by mixing different plasmas. This explanation is confirmed by the results of Table 7.2. Here, the determined telmisartan concentrations of two quality control samples are presented for each method. In this case all samples and all external calibration solutions were dissolved in pooled plasma. First, it can be observed that the results for ELISA and LC/MS measurements with internal calibration differ only slightly from the concentrations of the quality controls.

Table 7.2: *Telmisartan concentrations for quality control samples (500 ng mL^{-1} and 20 ng mL^{-1}) solved in pooled plasma and diluted with buffer 2 (10%).*

c	APCI-MS external (ext.) calibration				APCI-MS internal (int.) calibration				Immunoassay			
[ng mL^{-1}]	Average [ng mL^{-1}]	SD (n = 6)	RSD [%]	Recovery [%]	Average [ng mL^{-1}]	SD (n = 6)	RSD [%]	Recovery [%]	Average [ng mL^{-1}]	SD (n = 12)	RSD [%]	Recovery [%]
500.0	408.3	24.4	6.0	81.7	524.6	7.4	1.4	104.9	492.8	43.3	8.8	98.5
20.0	13.3	0.6	4.5	66.6	17.8	0.9	5.0	89.0	18.2	0.1	0.4	91.1

The deviation in case of the external LC/MS method is higher due to protein adsorption effects. Second, it can also be seen that the differences between the determined concentrations for ELISA and LC/MS with internal standard are negligible.

7.5 Conclusions

Two new independent analytical techniques, a LC/APCI-MS/MS method and an immunoassay for the determination of telmisartan in human blood plasma have been developed. The suitability of the GOD/MNBDH system for the use in immunoassays is presented for the first time. The results of our investigations show that the comparative pharmacokinetic study on telmisartan in human blood plasma by means of the two new introduced methods, which are based on completely different principles was successful. The immunoassay and the on-line TFC/LC/UV/APCI-MS/MS method allow the cross-validation of the obtained results. Both techniques enable a fast, sensitive and selective determination of telmisartan. For future work, further investigations regarding the determination of drugs in blood plasma samples using these measurement principles are foreseen.

7.6 References

[1] G. E. McVeigh, J. Flack, R. Grimm, Drugs 49 (1995) 161-175.

[2] B. Pitt, M. A. Konstam, Am. J. Cardiol. 82 (1998) 47S-49S.

[3] T. Unger, Am. J. Cardiol. 84 (1999) 9S-15S.

[4] R. Willenheimer, B. Dahlöf, E. Rydberg, L. Erhardt, Eur. Heart J. 20 (1999) 997-1008.

[5] W. Wienen, M. Entzeroth, J. C. A. van Meel, J. Stangier, U. Busch, T. Ebner, J. Schmid, H. Lehmann, K. Matzek, J. Kempthorne-Rawson, V. Glaigau, N. H. Hauel, Cardiovas. Drug Reviews 18 (2000) 127-156.

[6] M. Sharpe, B. Jarvis, K. L. Goa, Drugs 61 (2001) 1501-1529.

[7] T. Ebner, G. Heinzel, A. Prox, K. Beschke, H. Wachsmuth, Drug Metabol. Dispos. 27 (1999) 1143-1149.

[8] L. Gonzalez, U. Akesolo, R. M. Jimenez, R. M. Alonso, Electrophoresis 23 (2002) 223-299.

[9] S. Hillaert, W. van den Bossche, J. Chromatogr. A 979 (2002) 323-333.

[10] S. Hillaert, T. R. M. de Beer, J. O. dE Beer, W. van den Bossche, J. Chromatogr. A 984 (2003) 135-146.

[11] T. X. Maotian, J. F. Song, N. Li, Anal. Bioanal. Chem. 377 (2003) 1184-1189.

[12] T. X. Maotian, J. Song, Y. Liang, J. Pharmaceut. Biomed. Anal. 34 (2004) 681-687.

[13] N. Torrealday, L. Gonzalez, R. M. Alonso, R. M. Jimenez, E. O. Lastra, J. Pharmaceut. Biomed. Anal 32 (2003) 847-857.

[14] S. A. Ozkan, J. Liquid Chromatogr. & Rel. Technolog. 24 (2001) 2337-2346.

[15] L. Pastore, A. Tessitore, S. Martinotti, E. Toniato, E. Alesse, M. C. Bravi, C. Ferri, G. Desidri, A. Gulino, A. Santucci, Circulation 100 (1999) 1646-1652.

[16] N. Daneshtalab, R. Z. Lewanczuk, F. Jamali, J. Chromatogr. B 766 (2002) 345-349.

[17] T. Kondo, K. Yoshida, Y. Yoshimura, M. Motohashi, S. Tanayama, J. Mass. Spec. 31 (1996) 873-878.

[18] H. Hayen, U. Karst, J. Chromatogr. A 1000 (2003) 549-565.

[19] J. Meyer, A. Büldt, M. Vogel, U. Karst, Angew. Chemie. Int. Ed. 39 (2000) 1453-1455.

[20] C. Hempen, U. Karst, Anal. Chim. Acta 521 (2004) 117-122.

[21] A. Büldt, U. Karst, Anal. Chem. 71 (1999) 1893-1898

Chapter 8

Concluding Remarks and Future Perspectives

New analytical methods for the determination of analytes in enzymatic and immunoassays have been developed within this thesis. Chapter 2 provides an overview on different labeling strategies for bioassays, including the use of radioactive isotopes, fluorophores and enzymes. These labels are compared with respect to their current applications, and their future perspectives are critically discussed.

Chapter 3 describes the development of a detection scheme for the simultaneous evaluation of two bioassays based on fluorescence spectroscopy. The simultaneous dual-enzyme determination of GOD or MP-11 and aP or acP has been demonstrated with similar results compared to the individual determination of each enzyme. In the case of aP and GOD, an excitation of MNBDA and 5-FSA with one single excitation wavelength was possible due to overlapping excitation bands of the fluorescent products, yielding only a slightly higher LOD for GOD in comparison with the two individual optimum excitation wavelengths. MNBDH has been introduced as an excellent new substrate for MP-11, and its possible combination with 5-FSAP as phosphatase substrate in simultaneous determination could also be demonstrated. Real sample application of this detection scheme was shown by the simultaneous determination of the enzymes GOD and acP in honey. Future work could be directed towards the development of a two-analyte immunoassay and on a simultaneous two-enzyme post-column detection system for liquid chromatographic separations.

Chapter 4 describes a study regarding the comparative reaction scheme for the simultaneous determination of enzymes by means of flow-injection measurements with fluorescence and subsequent ESI-MS detection. The results of these investigations, which also provide kinetic data of both reaction schemes, show that ESI-MS detection is an attractive alternative detection method for the determination of MP-11 and aP. This technique is useful for direct at-line validation for the fluorescence detection. The advantage of fluorescence detection is a better reproducibility, which yields lower RSDs. Due to the technical limitations of commercially available fluorescence detectors, which do not allow to detect two different pairs of wavelengths simultaneously, it is important to use MS-detection additionally. It enables the parallel detection of two reaction products as well as of the respective reaction educts. Future work could be directed towards the development of a flow system for fluorescence measurements, which allows a real simultaneous determination of at least two fluorophores. Such a detector applied could comprise, e.g., fast (millisecond) filter changing facilities or a CCD camera. Furthermore, the additional use of nanoparticles may increase the number of possible analytes to be determined due to usually narrow emission bands. Investigations regarding the on-line inhibition of parallel enzymatic assays in flow-injection systems could additionally be performed.

By means of LC/APCI-MS investigations and exact mass measurements (ESI-TOF-MS) presented in Chapter 5, 2,3-diaminophenazine could be identified as main product of the POD-catalyzed oxidation of OPD by hydrogen peroxide. Two side products have been identified as an

intermediate in the formation of the main product and as an oxygen-containing species, but not the second literature-discussed product, 2,2´-diaminoazobenzene. The data provide sufficient evidence on the main reaction product to finish the contradictory discussion in literature.

Chapter 6 describes the development and application of a new HPLC/post-column reaction/fluorescence detection system for the activity determination of microperoxidases in proteolytic digests of cytochrome c from bovine heart. Whereas the digestion of cytochrome c with trypsin yielded the expected MP-9, which was detected by means of a fluorescence-based set-up and confirmed by ESI-MS measurements, the digestion with the unspecific protease from *streptomyces griseus* resulted in a microperoxidase, which was characterized as MP-6, a literature-known but not yet analytically used microperoxidase. Due to its high catalytic activity, investigations regarding possible analytical applications of MP-6 are planned for future work.

Chapter 7 describes the development of a GOD-based ELISA and a TFC/LC/APCI-MS/MS set-up for the determination of telmisartan. The limit of quantification for the immunoassay was lower by factor 3 than the LOQ for the LC/MS method. The two new techniques were applied for the pharmacokinetic observation of the telmisartan concentration in blood plasma samples of four test persons. The correlation of both methods was satisfying, although both techniques are based on completely different principles. Therefore, the immunoassay and the on-line-TFC/LC/UV/APCI-MS/MS method allow the cross-validation of the results obtained. Both techniques

enable a fast, sensitive and selective determination of telmisartan. Future work should be directed towards the determination of further drugs in blood plasma samples applying these measurement principles.

Summary

New detection strategies for bioassays based on liquid chromatography, fluorescence spectroscopy and mass spectrometry were developed and are presented within this thesis.

An introductory overview on different labeling strategies in enzymatic and immunoassays is presented. Direct labeling assays as radioimmunoassays, enzyme-labeled measurement techniques as enzyme-linked immunosorbent assays, nanoparticle-labeled assays as well as methods for coupling bioassays with chromatographic methods are introduced.

Fluorescence detection schemes for the determination of two enzymes in parallel were developed for assays that yield fluorescent reaction products with non-overlapping emission bands. The obtained results were compared with those from the individual determination of the respective enzymes. The method was applied to the simultaneous determination of acid phosphatase and glucose oxidase in honey.

An at-line flow-injection system with fluorescence and subsequent MS detection for the simultaneous enzyme assay system was developed. The alkaline phosphatase-catalyzed reaction of 5-FSAP to 5-FSA and the microperoxidase 11-catalyzed reaction of MNBDH to MNBDA were performed individually as well as simultaneously and the reaction progress was monitored.

The reaction product of the POD-catalyzed reaction of o-phenylenediamine with hydrogen peroxide was identified by LC/APCI-MS investigations and exact mass measurements (ESI-TOF-MS). The reaction was carried out under ELISA conditions, and it was found out that 2,3-diaminophenazine is the main reaction product.

A new HPLC/post-column reaction/fluorescence detection system for the activity determination of microperoxidases was developed and applied to proteolytic digests of cytochrome c from bovine heart. Microperoxidase 9 and microperoxidase 6 were identified as products in digests using trypsin and an unspecific protease, respectively. The fluorescence-based results were confirmed by ESI-MS measurements.

Furthermore, two independent methods for the determination of the hypertension drug telmisartan were developed. The GOD-based ELISA and the TFC/LC/APCI-MS/MS set-up were applied to human plasma samples and the results were compared. Both methods showed good correlation.

Samenvatting

Dit proefschrift beschrijft de ontwikkeling van nieuwe detectiestrategieën voor bioassays gebaseerd op vloeistofchromatografie, fluorescentiespectroscopie en massaspectrometrie.

Allereerst wordt een overzicht gepresenteerd van verschillende labeling-technieken. Dit betreft assays die gebruik maken van directe labeling zoals radioimmunoassays, enzym-gelabelde assays zoals ELISA, nanopartikel-gelabelde assays en koppeling van bioassays met chromatografische technieken.

Voor de simultane bepaling van twee enzymen in een assay waarbij fluorescerende reactieproducten worden gevormd is een fluorescentie detectietechniek ontwikkeld. De reactieproducten vertonen geen overlappende emissie lijnen. De resultaten zijn vergeleken met individuele assays van de enzymen. De methode is toegepast op de gelijktijdige bepaling van zure fosfatase en glucose oxidase in honing.

Een at-line flow-injectiesysteem met fluorescentie- en MS-detectie is ontwikkeld voor een simultane enzymassay. De alkalisch fosfatase-gekatalyseerde reactie van 5-FSAP tot 5-FSA en de reactie van MNBDH tot MNBDA m.b.v. microperoxidase 11 katalyse zijn met dit systeem gemeten, beide reacties zowel individueel als gelijktijdig. Hierbij kon het reactieverloop worden gevolgd.

Het reactieproduct van de POD-gekatalyseerde reactie van o-fenyleendiamine met waterstofperoxide is door LC/APCI-MS analyse en exacte-massabepalingen (ESI-TOF-MS) aangetoond. De reactie is uitgevoerd onder ELISA condities en 2,3-diaminophenazine is vervolgens als het hoofdproduct geïdentificeerd.

Een nieuw HPLC/post-kolom reactie/fluorescentie detectie-systeem is in dit onderzoek ontwikkeld voor de bepaling van de activiteit van microperoxidase. Het systeem is toegepast op proteolytische digesten van cytochroom C uit runderhart. De geïdentificeerde producten van de post-kolom reactie waren microperoxidase 9 en microperoxidase 6, waarbij respectievelijk trypsine en een niet-specifieke protease zijn gebruikt. De resultaten zijn bevestigd door middel van ESI-MS metingen.

Tenslotte worden in dit proefschrift twee onafhankelijke methoden beschreven voor de bepaling van de angiotensin II-antagonist telmisartan. Met behulp van de op GOD gebaseerde ELISA methode en de TDC/LC/APCI-MS/MS opzet werden plasmamonsters getest. Vergelijking van beide methoden resulteert in een goede correlatie.

Acknowledgement

The work of this thesis was carried out from April 2002 until July 2005 in the Chemical Analysis Group of Prof. Dr. Uwe Karst at the University of Twente in Enschede, The Netherlands. As the end of my dissertation gets closer, it is time to thank a couple of people for their advice, support, for collaboration and for the nice time within the group.

First, I thank Prof. Dr. Uwe Karst for the interesting research topic, for giving me the opportunity to do my doctorate abroad and for the possibility to attend international conferences as well as for his overall support.

Then, I would like to thank my lab colleagues: Georg Diehl; Sebastian “heilende Hände” Götz, who started with me in Enschede; “my” HBO-student Rob Haselberg; Heiko Hayen, for his helpfulness and several sunny lunch breaks; Hartmut Henneken, for insights in his way to economize; Nicole Jachmann and Rasmus Schulte-Ladbeck, for the nice time in our office; Suze van Leeuwen, my fitness-mate, for the collaboration, which led to Chapter 5; André Liesener, who also started with me in Enschede, for the cooperation for Chapter 4; Tobias Revermann and Bettina Seiwert, my office-mates in the second half of my Ph.D. time; Tanja Steinkamp, for her friendly and warm (non-)analytical support and our “Koopavond” shopping tours and our “Mini-Boss” Martin Vogel, especially for numerous times of proof-reading. My

special and honest thanks goes to all friends and colleagues who gave non-scientific support in difficult times.

Furthermore, I also want to thank our Dutch colleagues who “hartelijk” welcomed us in the Netherlands, for getting to know more about the Dutch way-of-life and traditions: Martijn Heuven, who translated the summary for me into Dutch; Nancy Heijnekamp-Snellens and Marcel de Bruine, who ordered and organized things, also on the short-notice; Annemarie Montanaro-Christenhusz and our two secretaries Susanne van Rijn and Saskia Tekkelenburg-Rompelmann.

Additionally, I thank Dr. Ulrich Kunz and Liane Gläsle-Schwarz from Boehringer Ingelheim Biberach, Germany, for the collaboration and many helpful hints.

Mein Dank gilt ganz besonders meinen Eltern, deren Unterstützung ich mir während meines gesamten Studiums in jeder Hinsicht sicher sein konnte.

Schließlich danke ich Christof für seine Hilfe, Geduld und moralische Unterstützung in allen Lebenslagen.

Christel

Curriculum Vitae

Personal Details

Name:	Christel Maria Hempen
Nationality:	German
Date of Birth:	December 1st, 1977
Born in:	Haren, Germany

Education

1984 – 1988:	Elementary School in Haren-Wesuwe, Germany
1988 - 1997:	Gymnasium Marianum Meppen, Germany Graduation in June 1997 in Meppen, Germany
1997 – 2002:	Studies of Chemistry at the University of Münster, Germany Intermediate exam in October 1999 Graduation (diploma) in April 2002 Thesis: "Investigations regarding the enzyme-catalyzed determination of fluorescent substrates" (practical work at the University of Twente (Enschede, The Netherlands) with Prof. Dr. Uwe Karst)
April 2002:	Begin of dissertation in Analytical Chemistry at the University of Twente (Enschede, The Netherlands) with Prof. Dr. Uwe Karst

List of Publications

Original Papers

---

1. C. Hempen, U. Karst, A dual fluorophore system for simultaneous bioassays, *Analytica Chimica Acta* **2004,** 521, 117-122.

2. C. Hempen, S. M. van Leeuwen, H. Luftmann, U. Karst, Liquid chromatographic/mass spectrometric investigation on the reaction products in the peroxidase-catalyzed oxidation of o-phenylenediamine by hydrogen peroxide, *Analytical and Bioanalytical Chemistry* **2005,** 382, 234-238.

3. C. Hempen, A. Liesener, U. Karst, Fluorescence and mass spectrometric detection schemes for simultaneous enzymatic conversions: method development and comparison, *Analytica Chimica Acta* **2005,** 543, 137-142.

4. C. Hempen, U. Karst, Labeling strategies for bioassays, *Analytical and Bioanalytical Chemistry* (accepted for publication).

5. R. Haselberg, C. Hempen, S. M. van Leeuwen, M. Vogel, U. Karst, Analysis of microperoxidases using liquid chromatography, post-column substrate conversion and fluorescence detection, *Journal of Chromatography B* (submitted for publication 2005).

6. C. Hempen, L. Gläsle-Schwarz, U. Kunz, U. Karst, Immunoassay and liquid chromatography/mass spectrometry methods for the determination of telmisartan in human blood plasma, *Analytical Chemistry* (submitted for publication 2005).

Oral Presentations

1. *Investigations on the Simultaneous Determination of Enzymes by Means of Fluorescence Spectroscopy,* Pittcon 2003, Orlando, USA.

2. *Simultane Bestimmung von Enzymen mittels Fluoreszenz-spektroskopie,* InCom 2003, Düsseldorf, Germany.

3. *Analysis of Microperoxidases Using Liquid Chromatography, Post-Column Substrate Conversion and Fluorescence Detection,* Pittcon 2005, Orlando, USA.